8-15-2014 12:00 AM

Micromechanics Modeling of the Electrical Conductivity of Carbon Nanotude (CNT)- Polymer Nanocomposites

Chuang Feng, *The University of Western Ontario*

Supervisor: Dr. Liying Jiang, *The University of Western Ontario*
A thesis submitted in partial fulfillment of the requirements for the Doctor of Philosophy degree in Mechanical and Materials Engineering
© Chuang Feng 2014

MICROMECHANICS MODELING OF THE ELECTRICAL CONDUCTIVITY OF
CARBON NANOTUBE (CNT)–POLYMER NANOCOMPOSITES

(Thesis format: Integrated Article)

by

Chuang <u>Feng</u>

Graduate Program in Engineering Science
Department of Mechanical and Materials Engineering

A thesis submitted in partial fulfillment
of the requirements for the degree of
Doctor of Philosophy

The School of Graduate and Postdoctoral Studies
The University of Western Ontario
London, Ontario, Canada

Abstract

The addition of carbon nanotubes (CNTs) in polymers to form conductive composites has been attracting great interest from research and industry communities due to their potential applications. Experiments and simulations have demonstrated that the addition of a very small amount of CNTs into polymers can significantly improve the electrical conductivity of the composites. Such significant improvement in the electrical conductivity is attributed to two conductivity mechanisms: nanoscale electron hopping and microscale conductive networks. Understanding and prediction of the overall electrical conductivity of the composites with the incorporation of the conductivity mechanisms that underpin the macroscopic electrical properties are essential for their engineering applications. One of the most promising applications of the conductive composites is for stretchable electronics. For such an application, it is naturally necessary to investigate the stretching effects upon the overall electrical conductivity of the composites. Furthermore, CNTs dispersed in polymers are usually not straight but rather have a certain degree of waviness due to the CNTs' large aspect ratio and low bending stiffness. It has been suggested that the waviness can have considerable effect on the electrical conductivity of the composites. Therefore, the investigation of CNT waviness effect is of great importance for the prediction of the overall electrical conductivity of the composites.

In this thesis, based on the micromechanics theory, a mixed micromechanics model with the incorporation of the nanoscale electron hopping and the microscale conductive networks is first developed to predict the electrical conductivity of the composites. The modeling results successfully predict the trend of existing experimental data. It is found that both the electron hopping and the conductive networks contribute to the electrical conductivity of the composites while conductive networks become dominant to the electrical conductivity of the composites after percolation. It was also indicated that the sizes of CNTs have significant effects on the percolation threshold and the overall electrical conductivity of the nanocomposites. Based on the developed micromechanics model, stretching effects are then investigated by incorporating the stretching induced changes into the micromechanics model. The investigation found that the stretching, including uni-axial and bi-axial stretching, decreases the electrical conductivity of the composites in the stretching direction and the

decrease is more evident for the bi-axial stretching compared to uni-axial stretching. It is also observed that the electrical conductivity is more sensitive to stretching for the composites with lower CNT volume fraction. Finally, we studied the CNT waviness effects upon the electrical conductivity of the composites under a uni-axial stretching. It is demonstrated that the waviness significantly decreases the electrical conductivity of the composites and the electrical conductivity is more sensitive to the waviness for the composites with lower CNT volume fraction and larger stretching strain. Reasons for the observed variations and phenomena are interpreted. The work in this thesis is expected to obtain increased understanding on the overall electrical conductivity of CNT-polymer composites from the theoretical perspective and provide useful guidelines for the design and optimization of the composites.

Keywords

Carbon nanotube, conductive polymer composites, micromechanics model, electrical conductivity, stretching; waviness.

Co-Authorship Statement

Title: Micromechanics modeling of the electrical conductivity of carbon nanotube (CNT)-polymer nanocomposites

Authors: C. Feng and L. Y. Jiang

The preliminary idea of the work was suggested by Dr. Jiang. All formulations and derivations were done by C. Feng. The draft of manuscript on the work was written by C. Feng and Dr. Jiang revised the draft and provided great advices on the structure of the manuscript and on the presentation of the results. This work was published by Composites Part A, 47, 143-149 (2013).

Title: Multi-scale modeling on the electrical conductivity of CNT-polymer composites

Authors: C. Feng and L. Y. Jiang

Dr. L. Y. Jiang proposed the idea of multi-scale modeling. The formulation of the problem was carried out by C. Feng under the supervision of Dr. Jiang. C. Feng drafted the manuscript and Dr. Jiang made revisions on the manuscript. The work was presented in CSME International Congress 2014, Toronto June 1-4 and was published by the Proceedings of CSME International Congress 2014.

Title: Investigation of uni-axial stretching effects on the electrical conductivity of CNT–polymer composites

Authors: C. Feng and L. Y. Jiang

Consideration of the uni-axial stretching effects was jointly proposed by C. Feng and Dr. Jiang after discussion. All the formulation was derived by C. Feng under the supervision of Dr. Jiang, who provided constructive suggestions on presenting and discussing results. The first version of the manuscript was written by C. Feng. Dr. Jiang made the following revisions. This work has been accepted by Journal of Physica D: Applied Physics.

Title: Bi-axial stretching effects on the electrical conductivity of CNT-polymer composites

Authors: C. Feng and L. Y. Jiang

The idea of the work was proposed by Dr. Jiang and the formulation was carried out by C. Feng under the supervision of Dr. Jiang. Dr. Jiang provided invaluable suggestions on

presenting and discussing results. C. Feng wrote the first draft and Dr. Jiang modified the manuscript. This work has been submitted for publication.

Title: Micromechanics modeling of waviness effects on the electrical conductivity of CNT-polymer composites

Authors: C. Feng and L. Y. Jiang

Dr. Jiang suggested the importance of considering waviness effects. The consideration of wavy CNT effects was jointly finished by C. Feng and Dr. Jiang after several discussions. C. Feng carried out the simulation work under the supervision of Dr. Jiang, who made modifications and revisions on the writing of the work. This work has been finished to be submitted for publication.

To my wife Fei and my son Haoyu

For their love, sacrifice and the happiness they brought to my life

To my parents and my sisters

For their continuous support and encouragement

Acknowledgments

Completing my PhD project is like a long journey of climbing a high mountain, filled with both painful and enjoyable experience. As I reached the peak of the mountain enjoying the spectacular view, I realized that one of the joys of this journey is to look back and remember all the support, encouragement, guidance and patience from friends and family, who made this journey meaningful and fruitful.

First of all I would like to express my sincere thanks to my supervisor, Dr. Liying Jiang, an enthusiastic and respected scholar, for her patient and continuous guidance and support during the past four years, without which my thesis would not have been in the current form. Her meticulous supervision will also be a great asset for my future research and professional career.

I would like to thank my committee members, Drs. Andy Sun, Samuel F. Asokanthan and John Dryden, for their constructive and valuable comments and suggestions in my comprehensive exam and in the discussion after my seminar presentations. I would also like to thank my examination board, Drs. Samuel F. Asokanthan, Jun Yang, Zihui Xia and Dazhi Jiang for reviewing my thesis and providing useful suggestions on my work.

I would also like to express my gratitude to my parents and my two sisters for their unreserved support and encouragement during the past years, without which my thesis would not be possible.

Finally, I would like to give great thanks to my wife Fei and my son Haoyu for their companionship and the happiness they brought to my life, which made my study and life at Western so enjoyable and fruitful.

Table of Contents

List of Figures

Nomenclature

d_a	average separation distance between CNTs
d_c	critical separation distance
e	charge of electron
f_c	percolation threshold
f_{CNT}	volume fraction of CNTs
f_{eff}	volume fraction of effective filler
m	mass of electron
r_c	radius of CNT
t	thickness of interphase
$\boldsymbol{A}_{CN}$	concentration tensor corresponded to conductive networks
$\boldsymbol{A}_{EH}$	concentration tensor corresponded to electron hopping
D_{CNT}	diameter of CNT
E	electrical field
L_{CNT}	length of CNT
J	electrical flux
$\boldsymbol{Q}$	transformation matrix
R	electrical resistance
$\boldsymbol{S}$	Eshelby tensor
V_{CNT}	volume of CNT
θ	initial polar angle
θ_s	polar angle after stretching
γ	angel between CNTs
$\boldsymbol{\delta}$	Kronecker delta tensor
ε	stretching strain
λ	potential barrier height between CNTs
$\boldsymbol{\delta}$	Kronecker delta tensor
ε	stretching strain
ρ	orientation distribution function
σ_c	electrical conductivity of CNT
σ_e	effective electrical conductivity of composites

σ_{Int}	electrical conductivity of interphase
σ_{m}	electrical conductivity of polymer
φ	initial azimuth angle
φ_{s}	azimuth angle after stretching
χ	waviness ratio
$\hbar$	Planck constant
$\langle V_{\text{e}} \rangle$	average excluded volume of CNT
$\langle V_{\text{ex}} \rangle$	total average excluded volume of CNT

Chapter 1

1 Introduction

1.1 CNT-polymer nanocomposites

Electrically conductive polymer composites have been attracting interest from academic and industrial communities since 1950s due to their excellent combination of electrical conductivity and beneficial attributes of polymers. The basic idea of producing conductive polymer composites is adding conductive fillers into polymers, which are usually insulators (Narkis *et al*., 1978; Tchoudakov *et al*., 1997; Feller *et al*., 2002). Among conductive fillers, carbon black and metals are two typical conductive fillers which are traditionally used to produce conductive or semi-conductive polymer composites. However, since the discovery of CNTs in 1991 (Iijima, 1991), the excellent mechanical and physical properties as well as high aspect ratio have made CNTs one of the most preferred conductive fillers to develop multi-functional conductive polymer composites during the past decades. Due to the large disparity of electrical conductivity between the polymer matrix and CNTs, i.e., the electrical conductivity of CNTs is several orders of magnitude larger than that of all neat polymers (Ebbesen *et al*., 1996), a very small amount of CNTs added into polymers can remarkably improve the electrical conductivity without significantly reducing the intrinsic properties of the polymers. Compared to traditionally conductive or semi-conductive materials, such as silicon, metal, ceramics etc, CNT-polymer nanocomposites possess desirable conductive properties from conductive fillers while keeping the beneficial attributes of the polymers, such as flexibility, light weight, easy processability and good chemical and biological compatibility (Yu *et al*., 2009; Nambiar and Yeow, 2011; Shang *et al*., 2011). Such unique combination of the excellent electrical conductivity of CNTs and the beneficial features of polymers have made CNT-polymer conductive nanocomposites one of the most promising material candidates for a variety of applications, such as stretchable electronics, conductive coatings, electromagnetic shielding and solar cells (Yang *et al*., 2005; Berson *et al*., 2007 Yu *et al*., 2009; Shang *et al*., 2011), which cannot be achieved by the traditional rigid conductive or semi-conductive materials.

1.2 Electrical behaviors of CNT-polymer nanocomposites

In addition to the as-mentioned features of CNT-polymer nanocomposites, i.e., a very small amount of CNTs added into polymer can significantly improve the overall electrical conductivity of the composites, it has been confirmed by both experiments and simulations that the electrical conductivity demonstrates a percolation-like behavior as shown in Figure 1.1 (Kim *et al*., 2005), i.e., the electrical conductivity of the composites increase abruptly when the CNT volume fraction reaches a certain critical value, which is usually referred as percolation threshold (Kim *et al*., 2005; Gojny *et al*., 2006; Yan *et al*., 2007; Seidel and Lagoudas, 2009; Qunaies *et al*., 2013).
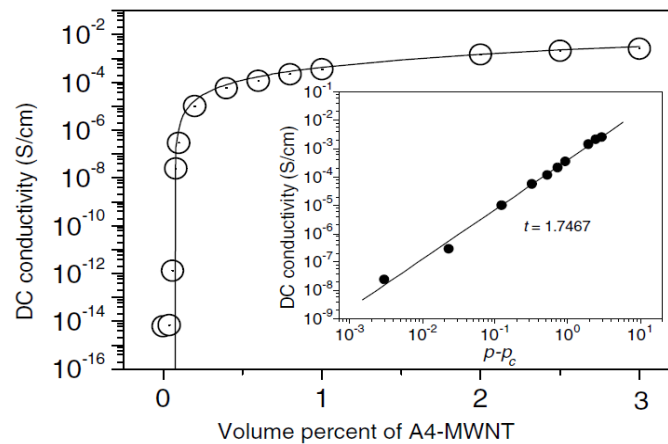
Figure 1.1 Variation of electrical conductivity of CNT-polymer composite with CNT volume fraction (Kim *et al*., 2005).

Explanations for the percolation-like behavior attribute to two conductivity mechanisms: electron hopping (or quantum tunneling) at the nanoscale and conductive networks at the microscale (Ounaies *et al*., 2003; Du *et al*., 2004; Chang *et al*., 2009; Zhang *et al*., 2009). As argued by Deng and Zheng (2008), the contribution of the electron hopping and the conductive networks to the electrical conductivity of the composites depends on the CNT concentration. From the perspective of quantum mechanics, electrons always have the probability of hopping intra-tube or from one CNT to another (as illustrated in Figure 1.2), but the probability is highly dependent on the separation distance between CNTs (Seidel and Lagoudas, 2009). When the CNT concentration in the composite is extremely

low with larger separation distance between CNTs, CNTs are more electrically independent and electron hopping governs the electrical conductivity of the composite. However, when the separation distance between CNTs decreases with the increase of CNT concentration, some adjacent CNTs may be electrically connected resulting in microscale conductive networks/pathways (as illustrated in Figure 1.3).
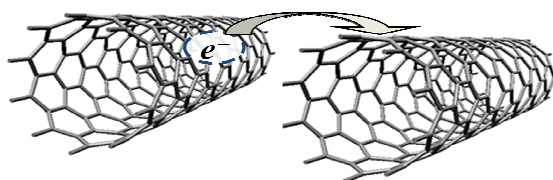
Figure 1.2 Electron hopping between CNTs
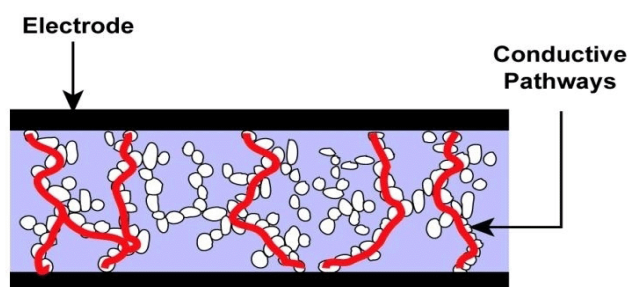
Figure 1.3 Conductive networks (http://www.eetimes.com).

In addition to the dependency of the electrical conductivity of the composites on the CNT concentration and the conductivity mechanisms, it has been demonstrated that stretching can also significantly affect the electrical performance of the CNT-polymer composites (Park *et al*., 2008; Cheng *et al*., 2009; Hu *et al*., 2010; Miao *et al*., 2011; Miao *et al*., 2011; Shang *et al*., 2011; Wang *et al*., 2011; Miao *et al*., 2012; Mayoral *et al*., 2013), which is of great importance for the application of the composites as stretchable electronics. Figure 1.4 (Park *et al*., 2008) shows an example of the stretching effects on the resistance of the composites for different CNT volume fractions. From the figure, it can be seen that the stretching increases the resistance of the composites, especially for lower CNT volume fraction (i.e., MWCNT 0.56 vol%). Therefore, to facilitate the full potential application as stretchable electronics it is naturally necessary to investigate the

stretching effects on the electrical behavior of the composites. Furthermore, due to CNTs' large aspect ratio and low bending stiffness (Li *et al*., 2008), it is well observed and accepted that CNTs dispersed in polymers are usually not straight but rather have a certain degree of waviness. Such wavy feature of the CNTs is suggested to have considerable effects on the electrical behavior of the composites (Yi *et al*., 2004; Li *et al*., 2008; Takeda *et al*., 2011; Yu *et al*., 2013), i.e., increasing waviness of CNTs will decrease the electrical conductivity of the composites. Therefore, the consideration of CNT waviness effects is necessary and essential for the improvement on the prediction of the electrical conductivity of CNT-polymer composites.
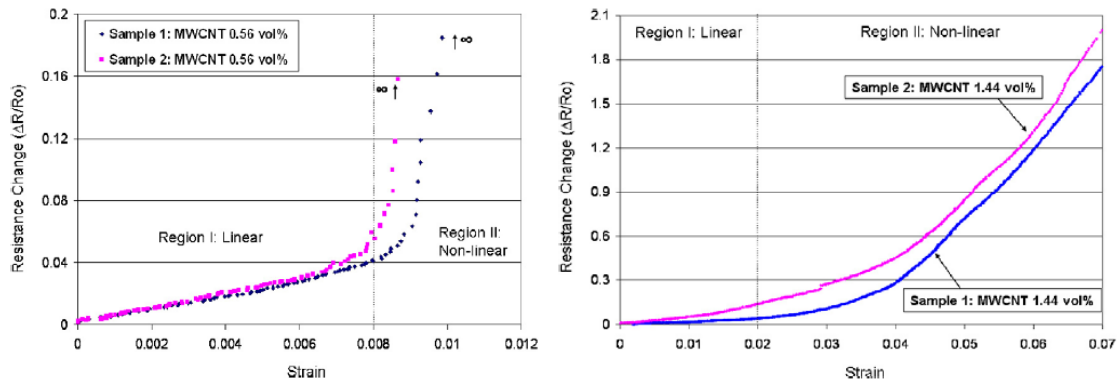
Figure 1.4 Stretching effects on the electrical property of CNT-polymer composites (Park *et al*., 2008).

1.3 Literature review

Although extensive explorations by experiments and simulations have been done on investigating the electrical conductivity of the composites, there is relatively less theoretical work in this topic. Therefore, this thesis will work on the investigation from the perspective of theoretical modeling and make qualitative predictions on the electrical conductivity of the composites. In this literature review section, existing studies on the investigation of the electrical conductivity of the nanocomposites involving the effects of the as-mentioned factors will be presented and discussed in the following sub-sections.

1.3.1 Studies on the electrical conductivity of CNT-polymer composites

For the electrical conductivity of CNT-polymer composites, extensive experimental work has been found to investigate the variation of the electrical conductivity with CNT volume fraction. Sandler *et al.* (1999) dispersed catalytically-grown carbon nanotubes in an epoxy matrix and found that compared to carbon black the use of CNTs reduced the percolation threshold and increased the overall electrical conductivity of the composites. Ramasubramaniam and his co-workers (2003) fabricated homogeneous carbon nanotube/polymer composites and found that very low CNTs loading is required to achieve satisfactory electrical conductivity without compromising the beneficial properties of the polymer. Qunaies *et al.* (2003) and Gojny *et al.* (2006) evaluated the electrical conductivity of CNT reinforced polyimide composites and epoxy resin, respectively. Both of their experiments demonstrated that the electrical conductivity increased with the increase of CNT volume fraction and concluded that the electrical conductivity of the composites could be attributed to the formation of conductive pathways. There are some other experimental work (Barrau *et al.*, 2003; Grunlan *et al.*, 2004; Kim *et al.*, 2005) that had observed the same phenomena, i.e., the addition of a very small amount of CNTs into polymers can significantly increases the electrical conductivity of the composites.

In addition to experimental work, there also exist modeling and simulation work on the investigation of the electrical conductivity of the composites. Regardless of the conductivity mechanisms, percolation theory, in which a power law equation is applied, had been widely adopted to predict the electrical conductivity of the composites after percolation (Kirkpatrick, 1973; Grimmett, 1999; Ramasubramaniam *et al.*, 2003; McLachlan *et al.*, 2005). Comparisons showed that the power law equation successfully predicted the trend of experimental data. However, such proposed power law equation is phenomenological and several parameters in this power law equation need to be fitted from existing experimental data. In addition, the power law equation cannot capture the variation of electrical conductivity prior to percolation and is unable to distinguish the two conductivity mechanisms. In addition to the percolation theory, Monte Carlo (MC)

and Molecular Dynamics (MD) simulations have been considered as effective ways to study the CNT-polymer composites (Ma and Gao, 2008; Zhang and Yi, 2008; Lu et al., 2010). However, MD and MC simulations are numerically expensive for large-scale simulation and impractical to obtain the overall property of the composites. In addition, MC and MD simulations cannot provide any explicit formulation for material design and optimization. Alternatively, some micromechanics theory based models have also been extended to predict the overall electrical conductivity of CNT-polymer nanocomposites. Deng and Zheng (2008) developed a simplified micromechanics model to evaluate the effective electrical conductivity for CNT composites by accounting for the percolation, conductive networks, conductivity anisotropy and non-straightness of CNTs. Based on Deng and Zheng's model, Takeda *et al.* (2011) considered the effect of electron hopping among CNTs to predict the overall electrical conductivity of the composites. However, both Deng and Takeda's work did not involve any prediction of the electrical conductivity before percolation. The influence of electron hopping and the formation of conductive networks on the electrical conductivity of CNT-polymer composites was also investigated by Seidel and Lagoudas (2009) using a Mori-Tanaka micromechanics model. In their work, electron hopping was assessed through an interphase layer surrounding the CNT, while the effect of conductive networks was captured by changing the CNT aspect ratio. The developed micromechanics model was successful in qualitatively identifying the potential causes for the low percolation concentrations. However, large discrepancy was observed between Seidel's predicted results and experimental data after the percolation. It should be mentioned that in Seidel's work (2009), the thickness and the electrical conductivity of the interphase layer were kept constant, and the two electrical conductivity mechanisms were considered separately in the simulations, i.e., either electron hopping or conductive networks solely dominated the electrical conductivity. From a statistical mechanics point of view, it is believed that some of CNTs in the polymer form conductive networks, while others contribute to the effective electrical conductivity of the composites through the electron hopping (Deng *et al.*, 2008). The probability of the formation of conductive networks will increase with the increase of the CNT concentration. In addition, the thickness and the electrical conductivity of the interphase layer accounting for the electron hopping will also vary

with the CNT concentration. In order to more accurately predict the overall electrical conductivity of CNT-polymer composites, all these factors need to be incorporated into a micromechanics model.

1.3.2   Investigation on stretching effects

Although efforts have been devoted to investigating the electrical properties of CNT-polymer nanocomposites through experiments and simulations (Kim *et al*., 2005; Gojny *et al*., 2006; Li *et al*., 2007; Yan *et al*., 2007; Chang *et al*., 2009; Seidel *et al*., 2009; Takeda *et al*., 2011), most of the existing studies were focused on preparing composites with well dispersed conductive fillers or predicting the electrical behavior of the as-received composites without considering stretching effects. However, for the potential application of the composites as stretchable electronics it is necessary to investigate the stretching effects upon the overall electrical conductivity of the composites in order to accurately predict and control the device performance. Existing experiments have demonstrated that stretching may significantly influence the electrical behavior of conductive polymer composites. For example, under a uni-axial stretching, Bao *et al.* (2011) experimentally examined the morphology and the electrical conductivity of carbon nanofibre composites before and after stretching and showed that the mechanical stretching could lead to decrease in the electrical conductivity of the composites due to breakdown of conductive networks. Park *et al*., and Hu *et al*., (2010) demonstrated that an abrupt increase in resistance of CNT-polymer composites subjected to a uni-axial stretching. In addition, Miao and his co-workers (2011a, 2011b and 2012) examined the piezoresistive response of CNT-polymer composites by experiments and percolation theory and indicated that the stretching decreases the electrical conductivity of the composites. There are some other experimental results having the same trend (Das N. C. *et al*., 2002; Dang *et al*., 2007). However, other experimental results (Cheng *et al*., 2009; Shang *et al*., 2011; Wang *et al*., 2011) presented an opposite trend, i.e., stretching increased the electrical conductivity of CNT-polymer composites due to substantial alignment enhancement of CNTs along the stretching direction. In addition to uni-axial stretching, bi-axial stretching is another typical stretching mode for CNT-polymer composites. Shen *et al*. (2012) and Mayoral *et al*. (2013) experimentally investigated the

bi-axial stretching effects on the electrical conductivity of CNT-polymer composites and obtained similar contradictive trends as that for uni-axial stretching. However, both of the work stated that the bi-axial stretching enables the CNTs to re-orientate along the two stretching directions in the polymer matrix. Such a stretching mode is expected to reduce the anisotropy of the electrical properties of the composites in the stretching plane compared to the uni-axial stretching case, altering the electrical behavior of the composites.

In addition to experimental studies, efforts have also been devoted in investigating the stretching effects upon the electrical conductivity of the CNT-polymer composites theoretically and numerically. Taya *et al.* (1998) and Lin *et al*. (2010) applied the fibre percolation model and Monte Carlo method, respectively, to investigate the stretching/compression effects upon the electrical properties of fibre-filled composites and their results showed that the deformation could shift the percolation threshold of the composites. Ghazavizadeh *et al.* (2011) proposed a 3-D Monte Carlo model to evaluate the effect of mechanical loading on the electrical percolation threshold of CNT reinforced polymers and indicated that a percolating nanocomposite became non-percolating under a unidirectional stretching. A recent study by Tallman and Wang (2013) also indicated that stretching could increase the percolation threshold due to the CNTs' re-orientation. Although contradictory stretching effects have been observed in the literature, i.e., some studies found stretching decreases electrical conductivity while others found stretching increases electrical conductivity, it is suggested that there are three major expected changes occurred during the stretching, including composite volume expansion, re-orientation of conductive fillers and change in conductive networks, which may contribute to the variation of the overall electrical properties of the polymer composites.

It should be mentioned that there is limited work on theoretical modeling with the consideration of the stretching induced three changes as mentioned, especially on bi-axial stretching. Therefore, another objective of the thesis is to investigate the effects of the stretching induced volume expansion, CNT re-orientation and conductive network

change on the overall electrical conductivity of the CNT–polymer composites following the previously developed micromechanics modeling work.

1.3.3 Modeling on CNT waviness effects

As cited in previous sub-sections, numerous works have been done on investigating the electrical properties of the composites, including the work on stretching effects. However, most of the work was focusing on the composites with straight conductive fillers. It is well accepted that for CNT dispersed composites, CNTs in the composites are usually not straight but rather have a certain degree of waviness mainly due to their large aspect ratio and low bending stiffness (Shaffer and Windle, 1999; Qian *et al*., 2000; Li *et al*., 2008). The waviness of the CNTs is suggested to have considerable effects on the electrical conductivity of the composites (Yi *et al*., 2004; Li *et al*.; 2008; Takeda *et al*.; 2011; Yu *et al*.; 2013). Therefore, the consideration of the CNT waviness effects is necessary and essential for the improvement on the prediction of the properties of CNT-polymer composites. Due to the difficulty in experimentally characterizing CNT waviness, most of the existing works on investigating the CNT waviness effects were focused on using modeling and simulation techniques. For example, assuming wavy CNTs with a sinusoidal shape, Yi *et al*. (2004), Berhan and Sastry (2007) and Fisher *et al*. (2003) considered the effect of the waviness on the percolation onset of CNT-polymer composites. It was observed that the waviness increases the percolation threshold of the composites. Shi *et al*. (2004) considered CNTs being in a helical shape and investigated the CNT waviness effects on the mechanical properties of the composites. Their investigation found that CNT waviness decreases the elastic modulus of the composites. Approximating wavy CNTs as elongated polygons, Li *et al.'s* (2008) computational simulation on the CNT waviness effects suggested that the waviness could increase the percolation threshold and decrease the electrical conductivity and elastic stiffness of the composites. Recently, assuming wavy CNTs with bow and sinusoidal shapes, respectively, Dastgerdi *et al.* (2013) and Yanase *et al.* (2013) investigated the effects of CNT waviness on the mechanical property of CNT reinforced polymer composites by micromechanics model and demonstrated that the waviness could significantly reduce the stiffening effect of the CNTs on the composites.

From the existing studies on the waviness effects, it can be seen that most of the studies were focusing on the mechanical properties and relatively less theoretical work has been found on the investigation of the CNT waviness effects upon the electrical conductivity of the composites, especially when the composites are under stretching. For complementary understanding on the electrical behavior of the composites, the CNT waviness effects are needed to be taken into account.

1.4   Objectives

Based on the introduction and literature review, it can be seen that developing a micromechanics model incorporating the two conductivity mechanisms, nanoscale electron hopping and microscale conductive networks, the stretching effects and the CNT waviness effects is necessary and essential to better understand and predict the electrical behaviors of the CNT-polymer composites and provide guidelines for the composites based stretchable electronics. Therefore, the objectives of the current work will focus on the following:

1.   Develop a mixed micromechanics model for CNT-polymer composites with the incorporation of the nanoscale electron hopping and the microscale conductive networks.

2.   Investigate the uni-axial stretching effects on the electrical conductivity of the composites by considering stretching induced changes in the composites structures.

3.   Based on the consideration of the uni-axial stretching, extend the investigation to the bi-axial stretching effects upon the electrical conductivity of the composites.

4.   Incorporate CNT waviness effects into the developed micromechanics model under uni-axial stretching.

1.5   Thesis structure

General introduction, literature review, motivation and objectives of the current work are presented in Chapter 1. For the work on specific objectives, detailed introductions are

presented in later Chapters. In Chapter 2, a mixed micromechanics model is developed to predict the overall electrical conductivity of CNT-polymer nanocomposites, in which the two electrical conductivity mechanisms, electron hopping and conductive networks, were incorporated. By incorporating stretching induced changes into the developed mixed micromechanics model, Chapter 3 investigates the uni-axial stretching effects on the electrical conductivity of the composites Based on the work of Chapter 3, the investigation on the stretching effects is extended in Chapter 4 to the bi-axial stretching case. The CNT waviness effects on the electrical conductivity of the composites under a uni-axial stretching are studied in Chapter 5. At last, Chapter 6 summarizes the conclusions of the thesis and proposes future work on the modeling of the electrical behavior of CNT-polymer nanocomposites.

References

Bao, S., Liang, G. and Tjong, S., 2011. Effect of mechanical stretching on electrical conductivity and positive temperature coefficient characteristics of poly (vinylidene fluoride)/carbon nanofiber composites prepared by non-solvent precipitation. Carbon **49**, 1758–1768.

Berhan, L. and Sastry, A. M., 2007. Modeling percolation in high-aspect-ratio fiber systems. II. The effect of waviness on the percolation onset. Phys. Rev. E **75**, 041121.

Barrau, S., Demont, P., Perez, E., Peigney, A., Laurent, C. and Lacabanne, C., 2003. Effect of palmitic acid on the electrical conductivity of carbon nanotube-epoxy resin composites. Macromolecules **36**, 9678–9680.

Chang, L., Friedrich, K., Ye, L. and Toro, P., 2009. Evaluation and visualization of the percolating networks in multi-wall carbon nanotube/epoxy composites. J. Mater. Sci. **44**, 4003–4012.

Cheng, Q., Bao, J., Park, J., Liang, Z., Zhang, C. and Wang, B., 2009. High Mechanical Performance Composite Conductor: Multi-Walled Carbon Nanotube Sheet/Bismaleimide Nanocomposites. Adv. Funct. Mater. **19**, 3219–3225.

Dastgerdi, J. N., Marquis, G. and Salimi, M., 2013. The effect of nanotubes waviness on mechanical properties of CNT/SMP composites. Compos. Sci. Technol. **86**, 164–169.

Deng, F. and Zheng, Q. S., 2008. An analytical model of effective electrical conductivity of carbon nanotube composites. Appl. Phys. Lett. **92**, 071902.

Du, F., Scogna, R. C., Zhou, W., Brand, S., Fischer, J. E. and Winey, K. I., 2004. Nanotube networks in polymer nanocomposites: rheology and electrical conductivity. Macromolecules **37**, 9048–9055.

Ebbesen, T. W., Lezec, H. J., Hiura, H., Bennett, J. W., Ghaemi, H. F. and Thio, T., 1996. Electrical conductivity of individual carbon nanotubes. Nature **382**, 54–56.

Feller, J. F., Linossier, I. and Levesque, G., 2002. Conductive polymer composites (CPCs): comparison of electrical properties of poly (ethylene-co-ethyl Acrylate)-carbon black with Poly (butylene Terephthalate)/poly (ethylene-co-ethyl Acrylate)-carbon balck. Poly. Adv. Technol. **13**, 714–724.

Fisher, F. T., Bradshaw, R. D. and Brinson, L. C., 2003. Fiber waviness in nanotube-reinforced polymer composites-1: Modulus predictions using effective nanotube properties. Compos. Sci. Technol. **63**, 1689–1703.

Gojny, F. H., Wichmann, M. H. G., Fiedler, B., Kinloch, I. A., Bauhofer, W., Windle, A. H. and Schulte, K., 2006. Evaluation and identification of electrical and thermal conduction mechanisms in carbon nanotube/epoxy composites. Polymer **47**, 2036–2045.

Grimmett, G., 1999. Percolation. Springer, Berlin.

Grunlan, J. C., Mehrabi, A. R., Bannon, M. V. and Bahr, J. L., 2004. Water-based single-walled-nanotube-filled polymer composite with an exceptionally low percolation threshold. 2004 Adv. Mater. **16**, 150–153

http://www.eetimes.com

Hu, N., Karube, Y., Arai, M., Watanabe, T., Yan, C., Li, Y., Liu, Y. and Fukunaga, H., 2010. Investigation on sensitivity of a polymer/carbon nanotube composite strain sensor. Carbon **48**, 680–687.

Iijima, S., 1991. Helical Microtubules of Graphitic Carbon. Nature **354**, 56–58.

Kim, Y. J., Shin, T. S., Choi, H. D., Kwon, J. H., Chung, Y. C. and Yoon, H. G., 2005. Electrical conductivity of chemically modified multiwalled carbon nanotube/epoxy composites. Carbon **43**, 23–30.

Kirkpatrick, S., 1973. Percolation and conduction. Rev. Mod. Phys. **45**, 574–588.

Li, C., Thostenson, E. T. and Chou, T. W., 2007. Dominant role of tunneling resistance in the electrical conductivity of carbon nanotube–based composites. Appl. Phys. Lett. **91**, 223114.

Li, C., Thostenson, E. T. and Chou, T. W., 2008. Effect of nanotube waviness on the electrical conductivity of carbon nanotube-based composites. Compos. Sci. Technol. **68**, 1445–1452.

Lin, C., Wang, H. and Yang, W., 2010. Variable percolation threshold of composites with fiber fillers under compression. J. Appl. Phys. **108**, 013509.

Lu, W., Chou, T.-W. and Thostenson, E. T., 2010. A three-dimensional model of electrical percolation thresholds in carbon nanotube-based composites. Appl. Phys. Lett. **96**, 223106.

Ma, H. and Gao, X. L., 2008. A three-dimensional Monte Carlo model for electrically conductive polymer matrix composites filled with curved fibers. Polymer **49**, 4230–4238.

Mayoral, B., Hornsby, P. R., McNally, T., Schiller, T. L., Jack, K. and Martin, D. J., 2013. Quasi-solid state uniaxial and biaxial deformation of PET/MWCNT composites: structural evolution, electrical and mechanical properties. RSC Adv. **3**, 5162–5183.

McLachlan, D. S., Chiteme, C., Park, C., Wise, K. E., Lowther, S. E., Lillehei, P. T., Siochi, E. J. and Harrison, J. S., 2005. AC and DC percolative conductivity of single wall carbon nanotube polymer composites. J. Poly. Sci. Pt. B: Poly. Phys. **43**, 3273–3287.

Miao, Y., Chen, L., Lin, Y., Sammynaiken, R. and Zhang, W., 2011. On finding of high piezoresistive response of carbon nanotube films without surfactants for in-plane strain detection. J. Intell. Mater. Syst. Struct. **22**, 2155–2159.

Miao, Y., Chen, L., Sammynaiken, R., Lin, Y. and Zhang, W., 2011. Note: Optimization of piezoresistive response of pure carbon nanotubes networks as in-plane strain sensors. Rev. Sci. Instrum. **82**, 126104.

Miao, Y., Yang, Q., Chen, L., Sammynaiken, R. and Zhang, W., 2012. Modelling of piezoresistive response of carbon nanotube network based films under in-plane straining by percolation theory. Appl. Phys. Lett. **101**, 063120.

Narkis, M., Ram, A. and Flashner F., 1978. Electrical properties of carbon black filled polyethylene. Poly. Eng. Sci. **18**, 649–653.

Ounaies, Z., Park, C., Wise, K. E., Siochi, E. J. and Harrison, J. S., 2003. Electrical properties of single wall carbon nanotube reinforced polyimide composites. Compos. Sci. Technol. **63**, 1637–1646.

Park, M. and Kim, H., 2006. Evaporation-based method for fabricating conductive MWCNT/PEO composite film and its application as strain sensor. Proc. 12th US-Japan Conf. Compos. Mater. Michigan, US, pp 78–86

Park, M., Kim, H. and Youngblood, J. P., 2008. Strain-dependent electrical resistance of multi-walled carbon nanotube/polymer composite films. Nanotechnology **19**, 055705.

Qian, D., Dickey, E. C., Andrews, R. and Rantell, T., 2000. Load transfer and deformation mechanisms in carbon nanotube-polystyrene composites. Appl. Phys. Lett. **76**, 2868.

Ramasubramaniam, R., Chen, J. and Liu, H., 2003. Homogeneous carbon nanotube/polymer composites for electrical applications. Appl. Phys. Lett. **83**, 2928–2930.

Sandler, J., Shaffer, M. S. P., Prasse, T., Bauhofer, W., Schulte, K. and Windle, A. H., 1999. Development of a dispersion process for carbon nanotubes in an epoxy matrix and the resulting electrical properties. Polymer 40, 5967–5971.

Seidel, G. D. and Lagoudas, D. C., 2009. A Micromechanics Model for the Electrical Conductivity of Nanotube-Polymer Nanocomposites. J. Compos. Mater. **43**, 917–941.

Shaffer, M. S. P. and Windle, A. H., 1999. Fabrication and characterization of carbon nanotube /poly(vinyl alcohol) composites. Adv. Mater. **11**, 937–941.

Shang, S., Zeng, W. and Tao, X. M., 2011. High stretchable MWNTs/polyurethane conductive nanocomposites. J. Mater. Chem. **21**, 7274–7280.

Shen, J., Champagne, M. F., Yang, Z., Yu, Q., Gendron, R. and Guo, S., 2012. The development of a conductive carbon nanotube (CNT) network in CNT/polypropylene composite films during biaxial stretching. Compos. Pt. A: Appl. Sci. Manuf. **43**, 1448–1453.

Shi, D. L., Feng, X. Q., Huang, Y. G. Y., Hwang, K. C. and Gao, H. J., 2004. The effect of nanotube waviness and agglomeration on the elastic property of carbon nanotube-reinforced composites. J. Eng. Mater.-Tran. ASME **126**, 250–257.

Takeda, T., Shindo, Y., Kuronuma, Y. and Narita, F., 2011. Modeling and characterization of the electrical conductivity of carbon nanotube-based polymer composites. Polymer **52**, 3852–3856.

Tallman, T. and Wang, K. W., 2013. An arbitrary strains carbon nanotube composite piezoresistivity model for finite element integration. Appl. Phys. Lett. **102**.

Taya, M., Kim, W. and Ono, K., 1998. Piezoresistivity of a short fiber/elastomer matrix composite. Mech. Mater. **28**, 53–59.

Tchoudakov, R., Breuer, O., Narkis, M. and Siegmann, A., 1997. Conductive polymer blends with low carbon black loading: high impact polystyrene/thermoplastic elastomer (styrene-isoprene-styrene). Poly. Eng. Sci. **37**, 1928–1935.

Wang, X., Bradford, P. D., Liu, W., Zhao, H., Inoue, Y., Maria, J. P., Li, Q., Yuan, F. G. and Zhu, Y., 2011. Mechanical and electrical property improvement in CNT/Nylon composites through drawing and stretching. Compos. Sci. Technol. **71**, 1677–1683.

Yan, K. Y., Xue, Q. Z., Zheng, Q. B. and Hao, L. Z., 2007. The interface effect of the effective electrical conductivity of carbon nanotube composites. Nanotechnology **18**, 255705

Yanase, K., Moriyama, S. and Ju, J. W., 2013. Effects of CNT waviness on the effective elastic responses of CNT-reinforced polymer composites. Acta Mech. **224**, 1351–1364.

Yi, Y., Berhan, L. and Sastry, A., 2004. Statistical geometry of random fibrous networks, revisited: Waviness, dimensionality, and percolation. J. Appl. Phys. **96**, 1318–1327.

Yu, Y., Song, S., Bu, Z., Gu, X., Song, G. and Sun, L., 2013. Influence of filler waviness and aspect ratio on the percolation threshold of carbon nanomaterials reinforced polymer nanocomposites. J. Mater. Sci. **48**, 5727–5732.

Yu, Y., Song, S. Q., Bu, Z. X., Gu, X. F., Song, G. B. and Sun, L., 2013. Influence of filler waviness and aspect ratio on the percolation threshold of carbon nanomaterials reinforced polymer nanocomposites. J. Mater. Sci. **48**, 5727–5732.

Zhang, R., Dowden, A., Deng, H., Baxendale, M. and Peijs, T., 2009. Conductive network formation in the melt of carbon nanotube/thermoplastic polyurethane composite. Compos. Sci. Technol. **69**, 1499–1504.

Zhang, T. and Yi, Y., 2008. Monte Carlo simulations of effective electrical conductivity in short-fiber composites. J. Appl. Phys. **103**, 014910.

Chapter 2

2 Micromechanics modeling on electrical conductivity of CNT-polymer composites[1]

2.1 Introduction

Recently, the addition of carbon nanotubes (CNTs) in compliant polymers to form conductive nanocomposites has stimulated a surge of scientific interests from the research communities due to their potential applications in stretchable electronics (Subramanian *et al*., 2006; Yu *et al*., 2009; Li *et al*., 2010). Such interests stem from CNT's excellent electrical conductivity, which is several orders of magnitude larger than that of all neat polymers (Ebbesen *et al*., 1996). Existing experiments have shown the remarkable improvement of electrical conductivity of polymer medium with the addition of CNTs (Kim *et al*., 2005; Gojny *et al*., 2006; Hu *et al*., 2008). Due to the large disparity of electrical conductivity between the polymer matrix and CNTs, the CNT-polymer composite demonstrates a percolation like behavior, and its electrical conductivity increases abruptly when the CNT concentration reaches a certain threshold. Explanations for this percolation behavior have centered on two conductivity mechanisms: electron hopping (or quantum tunneling) at the nanoscale and conductive networks at the microscale (Qunaies *et al*., 2003; Du *et al*., 2004; Chang *et al*., 2009; Zhang *et al*., 2009). From quantum mechanics, electrons have the probability of hopping intra-tube or from one CNT to another, but the probability is highly dependent on the separation distance between CNTs (Seidel and Lagoudas, 2009). When the CNT concentration in the composite is extremely low with larger separation distance between CNTs, electron hopping governs the electrical conductivity of the composite. However, when the separation distance between CNTs decreases with the increase of CNT concentration, some adjacent CNTs may be electrically connected resulting in microscale conductive

---

[1] A version of this chapter has been published.

Feng C. and Jiang L.Y. (2013) Composites Part A, 47, 143–149

networks. With the CNT concentration getting larger and larger, conductive networks are believed to be dominant over electron hopping. Quantitative prediction on the overall electrical conductivity of CNT-polymer composites which can capture the percolation behavior is essential for the design and optimization of conductive nanocomposites. However, accurate modeling of the electrical conductivity of nanocomposites is challenging due to the multi-scale nature of the problem as indicated by the conductivity mechanisms, i.e., phases of CNT-polymer nanocomposites range from the microscale down to the nanoscale.

Efforts have been devoted to predicting the electrical conductivity of CNT-polymer nanocomposites. Monte Carlo (MC) simulation has commonly been considered as an effective way to predict the electrical conductivity of the nanocomposites (Ma and Gao, 2008; Zhang and Yi, 2008; Lu *et al.*, 2010) by incorporating the nanoscale features of the materials. However, MC simulation is numerically expensive for large-scale systems and does not provide an explicit formulation for materials design and optimization, thus analytical models have naturally been pursued as alternative tools. Regardless of the conductivity mechanisms, a three-parameter power law equation, which is based on classical percolation theory, has been adopted to predict the electrical conductivity of nanocomposites after percolation (Kirkpatrick, 1973; Grimmett, 1999). Comparisons showed that the power law equation successfully predicted the trend of some experimental data (Ramasubramaniam *et al.*, 2003; McLachlan *et al.*, 2005), however, such power law equation is phenomenological and the parameters in this power law equation need to be fitted from experimental data. In addition, the power law equation cannot capture the variation of electrical conductivity prior to percolation and is not able to distinguish the two conductivity mechanisms. Alternatively, some micromechanics theory based models have also been extended to predict the overall electrical conductivity of CNT-polymer nanocomposites. Deng and Zheng (2008) developed a simplified micromechanics model to evaluate the effective electrical conductivity for CNT composites by accounting for the percolation, conductive networks, conductivity anisotropy and non-straightness of CNTs. It was found that the non-straightness of CNTs had significant influence on the effective electrical conductivity of the composites, and

model predictions successfully predicted the trend of some measured experimental data in literature. Based on Deng and Zheng's model, Takeda et al. (Takeda *et al*., 2011) considered the effect of electron hopping among CNTs by taking CNTs as effective fibers to predict the overall electrical conductivity of the composites.

The influence of electron hopping and the formation of conductive networks on the electrical conductivity of CNT-polymer composites has been investigated by Seidel and Lagoudas (2009) using a Mori-Tanaka micromechanics model (Mori and Tanaka, 1973; Hatta and Taya, 1985). In their work, electron hopping was assessed through an interphase layer surrounding the CNT, while the effect of conductive networks was captured by changing the CNT aspect ratio. The developed micromechanics model was successful in qualitatively identifying the potential causes for low percolation concentrations. However, large discrepancy was observed between Seidel and Lagoudas predicted results and experimental data after percolation. It should be mentioned that in Seidel's work (2009) the thickness and the electrical conductivity of the interphase layer were kept constant, and the two electrical conductivity mechanisms were considered separately in the simulations, i.e., either electron hopping or conductive networks solely dominated electrical conductivity. From a statistical mechanics point of view, it is believed that some of CNTs in the polymer form conductive networks, while others contribute to the effective electrical conductivity of the composites through electron hopping (Deng and Zheng, 2008). The probability of the formation of conductive networks will increase with the increase of CNT concentration. In addition, the thickness and the electrical conductivity of the interphase layer accounting for electron hopping will also vary with CNT concentration. In order to more accurately predict the overall electrical conductivity of CNT-polymer composites, all these factors should be incorporated into a micromechanics model.

It is the objective of the current work to develop a mixed micromechanics model for CNT-polymer composites with the incorporation of electron hopping and conductive networks simultaneously. According to the percolation process, electron hopping is believed to be dominant below the percolation threshold. In this model, hollow CNTs

were modeled as effective solid fibers, in which an interphase layer outside the CNT was used to capture nanoscale effects of electron hopping among CNTs as shown in literature. After percolation, the thickness and the electrical conductivity of the interphase layer were defined by considering electric tunneling effect, which vary with CNT concentration. The developed micromechanics model was validated by comparing the prediction results with experimental data.

2.2 Nanoscale composite cylinder model for CNT

As mentioned before, electron hopping exists among CNTs distributed in the polymer matrix, which results in the formation of a continuum interphase layer surrounding the CNT. In order to capture this interphase layer and the hollow nature of CNTs, an effective composite cylinder model well accepted by researchers (Hashin, 1990; Yan *et al*., 2007; Seidel and Lagoudas, 2009), was used to determine the effective electrical conductivity of the CNT together with the surrounding interphase. Such an effective composite cylinder assemblage was further homogenized as an equivalent solid filler based on the application of a set of homogeneous boundary conditions as shown in Figure 2.1. In this way, the composite itself is composed of two phases: the polymer matrix and the effective solid filler. For this two-phase composite, a micromechanics model can further be applied to determine its overall electrical conductivity.
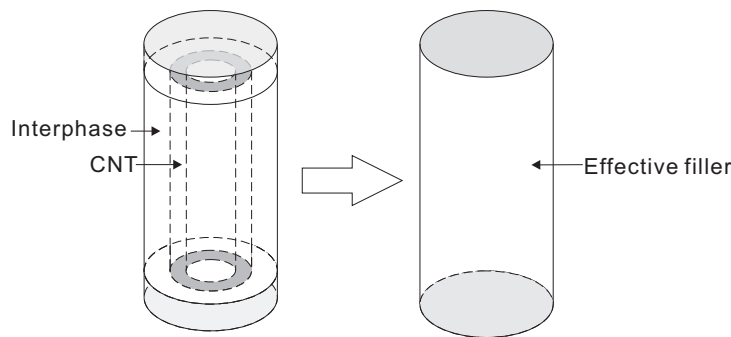
Figure 2.1 Schematic illustration of the composite cylinder and the effective filler.

2.2.1 Effective electrical conductivity of composite cylinder

In order to apply micromechanics theory, the effective electrical conductivity of the solid filler phase needs to be determined first. Figure 2.2 is a sketch of the composite cylinder assemblage (Yan *et al.*, 2007), which consists of a CNT and the surrounding interphase with thickness *t*. A local coordinate system ($\tilde{x}_1, \tilde{x}_2, \tilde{x}_3$) is used to describe the cylinder assemblage, in which the electrical isotropic plane (cross-section) can also be described by a polar coordinate system (*r, β*). Here the CNT is treated as a solid cylinder instead of a hollow tube due to the difficulty of obtaining the actual electrical conductivity of the CNT considering the nanoscale structures (Ebbesen *et al.*, 1996; Takeda *et al.*, 2011). According to the structure shown in Figure 2.2, the composite cylinder can be divided into three parts: isotropic parts 1 and 3 are interphases; transversely isotropic part 2 is a combination of the CNT with the surrounding interphase. Knowing the properties of these three parts, the law-of-mixture rule (Taya, 2005; Yan *et al.*, 2007), which is based on equating the total electric energy of the composite cylinder consisting of three parts to the electric energy of a homogeneous effective solid filler transferred by the same electric field, can be applied to determine the effective longitudinal and transverse electrical conductivity of the effective filler. For part 2, which consists of a CNT (length *L*, radius r_c) and an annual interphase (thickness *t*), the effective longitudinal electrical conductivity, $\tilde{\sigma}_2^L$ in the local coordinate system, is first determined from the law-of-mixture as (Taya, 2005; Yan *et al.*, 2007):
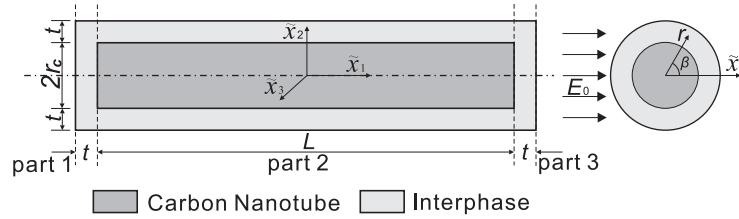
Figure 2.2 Sketch of a composite cylinder.

$$\tilde{\sigma}_2^L = \frac{\sigma_c^L r_c^2 + \sigma_{Int}\left(2 r_c t + t^2\right)}{\left(r_c + t\right)^2} \ , \tag{2.1}$$

where σ_c^L and σ_{Int} are the electrical conductivities of the CNT along the longitudinal direction and the interphase, respectively. The superscript "L" represents the longitudinal direction in the local coordinate system.

Due to the variation of the cylindrical surface area in the transverse direction, the law-of-mixture rule is not applicable for calculating the electrical conductivity in this direction. In order to determine the transverse electrical conductivity $\tilde{\sigma}_2^T$ in the isotropic plane of part 2, Maxwell's equation in the local polar coordinates (r, β) is applied when the system is subjected to an uniform electric field E_0 along $\tilde{x}_3$ at a large distance R sufficiently far away from the CNT (Yan *et al.*, 2007), i.e.,

$$\nabla^2\phi = \frac{1}{r}\frac{\partial}{\partial r}\left(r\frac{\partial\phi}{\partial r}\right) + \frac{1}{r^2}\frac{\partial^2\phi}{\partial\beta^2} = 0 \ , \tag{2.2}$$

where $\phi(r, \beta)$ is the electric potential. Note the (r, β) plane is the isotropic plane and $\tilde{x}_3$ is an arbitrary radial direction along which the electrical conductivity is the same. The boundary conditions for this problem are prescribed as

$$\phi_c\big|_{r=0} = \text{constant}, \qquad E_m\big|_{r=R} = -\frac{\partial\phi_m}{\partial r}\bigg|_{r=R} = E_0$$

$$\phi_c\big|_{r=r_c} = \phi_{Int}\big|_{r=r_c}, \quad -\sigma_c^T\frac{\partial\phi_c}{\partial r}\bigg|_{r=r_c} = -\sigma_{Int}\frac{\partial\phi_{Int}}{\partial r}\bigg|_{r=r_c} \tag{2.3}$$

$$\phi_{Int}\big|_{r=r_c+t} = \phi_m\big|_{r=r_c+t}, \quad -\sigma_{Int}\frac{\partial\phi_{Int}}{\partial r}\bigg|_{r=r_c+t} = -\sigma_m\frac{\partial\phi_m}{\partial r}\bigg|_{r=r_c+t}$$

The subscripts "c", "m" and "Int" represent the CNT, the polymer matrix and the interphase, respectively, while superscript "T" represents the transverse direction in the local coordinate system. Solving Eq. (2.2) with the corresponding boundary conditions from Eq. (2.3), the electric potential distribution can be derived as

$$\phi_c(r,\beta) = 2A\sigma_{Int}E_0 r\cos\beta \quad 0 \le r \le r_c$$

$$\phi_{Int}(r,\beta) = A\left[\sigma_{Int} + \sigma_c^T + \left(\frac{r_c}{r}\right)^2\left(\sigma_{Int} - \sigma_c^T\right)\right]E_0 r\cos\beta \quad r_c < r < r_c + t \tag{2.4}$$

$$\phi_m(r,\beta) = \left\{A\left[\left(\frac{r_c+t}{r}\right)^2\left(\sigma_{Int} + \sigma_c^T\right) + \left(\frac{r_c}{r}\right)^2\left(\sigma_{Int} - \sigma_c^T\right)\right] + \left(\frac{r_c+t}{r}\right)^2 - 1\right\}E_0 r\cos\beta \quad r_c + t \le r = R$$

where

$$A = \frac{2\sigma_m}{\left(\sigma_{Int} - \sigma_c^T\right)\left(\sigma_{Int} - \sigma_m\right)\left(\dfrac{r_c}{r_c+t}\right)^2 - \left(\sigma_{Int} + \sigma_c^T\right)\left(\sigma_{Int} + \sigma_m\right)} \tag{2.5}$$

Correspondingly, the electric field along the $\tilde{x}_3$-axis for the composite assemblage can be determined as

$$E_{c,\tilde{x}_3} = -\frac{\partial\phi_c}{\partial\tilde{x}_3} = -\frac{\partial\phi_c}{\partial r}\frac{\partial r}{\partial\tilde{x}_3} = -\frac{1}{\cos\beta}\frac{\partial\phi_c}{\partial r}$$

$$E_{Int,\tilde{x}_3} = -\frac{\partial\phi_{Int}}{\partial\tilde{x}_3} = -\frac{\partial\phi_{Int}}{\partial r}\frac{\partial r}{\partial\tilde{x}_3} = -\frac{1}{\cos\beta}\frac{\partial\phi_{Int}}{\partial r} \tag{2.6}$$

with the electric current density in the CNT and the interphase being derived as

$$j_{c,\tilde{x}_3} = \sigma_c^T E_{c,\tilde{x}_3} \quad \text{and} \quad j_{Int,\tilde{x}_3} = \sigma_{Int} E_{Int,\tilde{x}_3}. \tag{2.7}$$

From Eqs. (2.4)–(2.7), it can be seen that the electric field and the electric current density of the CNT and the interphase are dependent on the radius. To obtain the equivalent transverse electrical conductivity of part 2, a spatial average expression is introduced as (Yan *et al.*, 2007)

$$\left\langle j_{\tilde{x}_3}\right\rangle = \tilde{\sigma}_2^T\left\langle E_{\tilde{x}_3}\right\rangle, \tag{2.8}$$

where $\langle j_{\tilde{x}_3} \rangle = \dfrac{1}{V} \int_v j_{\tilde{x}_3} dv$ and $\langle E_{\tilde{x}_3} \rangle = \dfrac{1}{V} \int_v E_{\tilde{x}_3} dv$ are the spatial averages of the electric current density and the electric field along the $\tilde{x}_3$-axis, respectively. Combining Eqs. (2.4)–(2.8) the equivalent transverse electrical conductivity of part 2, $\tilde{\sigma}_2^T$ in the local coordinate system, can be derived as

$$\tilde{\sigma}_2^T = \frac{\langle j_{\tilde{x}_3} \rangle}{\langle E_{\tilde{x}_3} \rangle} = \frac{\int_0^{r_c} \sigma_c^T E_{c,\tilde{x}_3} 2\pi r dr + \int_{r_c}^{r_c+t} \sigma_{Int} E_{Int,\tilde{x}_3} 2\pi r dr}{\int_0^{r_c} E_{c,\tilde{x}_3} 2\pi r dr + \int_{r_c}^{r_c+t} E_{Int,\tilde{x}_3} 2\pi r dr} = \frac{2r_c^2 \sigma_c^T \sigma_{Int} + \sigma_{Int}\left(\sigma_{Int} + \sigma_c^T\right)\left(t^2 + 2r_c t\right)}{2r_c^2 \sigma_{Int} + \left(\sigma_{Int} + \sigma_c^T\right)\left(t^2 + 2r_c t\right)}. \quad (2.9)$$

Then by using the law-of-mixture rule again for the composite cylinder composed of parts 1, 2, and 3, the effective electrical conductivity of the solid filler in both the transverse and longitudinal directions in the local coordinate system can be derived as (Yan *et al.*, 2007):

$$\begin{aligned} \tilde{\sigma}^T &= \frac{\sigma_{Int}}{L + 2t}\left[L \frac{2r_c^2 \sigma_c^T + \left(\sigma_c^T + \sigma_{Int}\right)\left(t^2 + 2r_c t\right)}{2r_c^2 \sigma_{Int} + \left(\sigma_c^T + \sigma_{Int}\right)\left(t^2 + 2r_c t\right)} + 2t \right] \\ \tilde{\sigma}^L &= \frac{(L + 2t)\sigma_{Int}\left[\sigma_c^L r_c^2 + \sigma_{Int}\left(2r_c t + t^2\right)\right]}{2\sigma_c^L r_c^2 t + 2\sigma_{Int}\left(2r_c t + t^2\right)t + \sigma_{Int} L\left(r_c + t\right)^2} \end{aligned}. \quad (2.10)$$

2.2.2 Thickness and conductivity of interphase

It is clearly indicated in Eq. (2.10) that the properties of the interphase, i.e., the thickness (t) and the electrical conductivity (σ_{Int}), may also play a significant role in the effective electrical conductivity of the solid filler. In addition, the percolation behavior is governed by two mechanisms as discussed before: nanoscale electron hopping (EH) (or quantum tunneling) and microscale conductive networks (CN). Therefore, definitions of the thickness and the electrical conductivity of the interphase accounting for electron hopping and conductive networks are essential. Figure 2.3 shows an example of an in-plane contact configuration between two adjacent CNTs (Takeda *et al.*, 2011), in which the separation distance naturally decreases with the increase of CNT volume fraction. When the CNT volume fraction reaches the percolation threshold f_c, the formation of

conductive networks starts. In literature, several works have demonstrated that the average separation distance d_a between adjacent CNTs when conductive networks are formed after percolation rate follows a power law description (Allaoui *et al.*, 2008; Deng and Zheng, 2008; Takeda *et al.*, 2011). Here we take the power law relation suggested in (Deng and Zheng, 2008), i.e.,
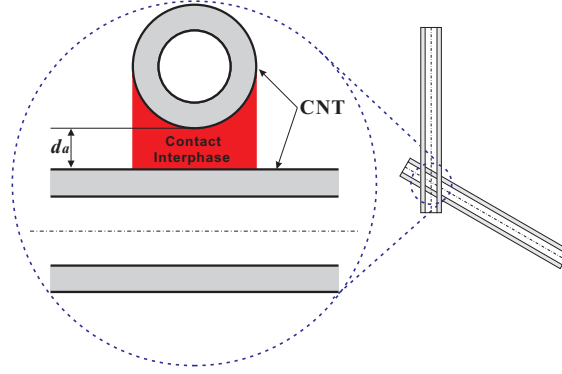
Figure 2.3 Contact configuration between two SWCNTs.

$$d_a = \frac{\alpha}{f^{1/3}}, \tag{2.11}$$

where f is the volume fraction of CNTs and α is a constant to be determined. The upper limit separation distance for CNTs in conductive networks was suggested as $d_c = 1.8$ nm (Li *et al.*, 2007; Takeda *et al.*, 2011), which is the maximum possible thickness of the medium separating two adjacent CNTs that allows the tunneling penetration of electrons. Therefore, α can be approximately determined as

$$\alpha = d_c f_c^{1/3}. \tag{2.12}$$

Electron hopping is highly dependent on the separation distance between CNTs. When the separation distance of CNTs is larger than 1.8 nm with CNT volume fraction less than the percolation threshold f_c, it is regarded that CNTs are more independent rather than electrically connected to each other. Under this situation, electron hopping dominates the electrical conductivity of the composite. When the CNT volume fraction reaches the

percolation threshold f_c, conductive networks start to form and the separate distance between percolated CNTs is taken as 1.8 nm. With the increase of CNT volume fraction after percolation, it is understood that the separation distance of CNTs in conductive networks is getting smaller than 1.8 nm. However, these percolated CNTs are still in electrical contact rather than physical contact due to van der Waals forces. For each CNT forming a conductive network, the thickness of the interphase can be defined as

$$t = \frac{1}{2}d_a = \frac{1}{2}\left(\frac{f_c}{f}\right)^{1/3} d_c .$$
(2.13)

It should be noted that the interphase thickness of part 1 (or 3) and part 2 of the composite cylinder was taken the same as assumed in (Takeda *et al.*, 2011). By using Simmons' derivation for electron tunneling (Simmons, 1963; Takeda *et al.*, 2011), the tunneling-type contact resistance between two CNTs can be expressed as

$$R_{Int}(d_a) = \frac{d_a \hbar^2}{ae^2(2m\lambda)^{1/2}} \exp\left(\frac{4\pi d_a}{\hbar}(2m\lambda)^{1/2}\right),$$
(2.14)

where λ is the potential barrier height, which is approximate 5.0 eV for CNTs dispersed in most polymers (Shiraishi and Ata, 2001; Takeda *et al.*, 2011); m ($9.10938291 \times 10^{-31}$ kg) and e ($-1.602176565 \times 10^{-19}$ C) are the mass and the electric charge of an electron, respectively; a is the contact area of CNTs and $\hbar$ (6.626068×10^{-34} m^2·kg/s) is the Planck constant. The electrical conductivity of the interphase surrounding a CNT in conductive networks can then be obtained correspondingly,

$$\sigma_{Int} = \frac{d_a}{aR_{Int}(d_a)} .$$
(2.15)

Due to the lack of information in literature for estimating the average separation distance between CNTs without electrical contact, an assumption of d_c is given on this quantity in the current work, which is the upper limit separation distance between CNTs allowing

electron to tunnel through. Therefore, the thickness and the electrical conductivity of the interphase surrounding CNTs without forming conductive networks are determined as:

$$t = \frac{1}{2} d_c \tag{2.16}$$

and

$$\sigma_{Int} = \frac{d_c}{a R_{Int}(d_c)}. \tag{2.17}$$

It is obvious that such an assumption on the average separation distance between CNTs may result in an overestimated electrical conductivity of the nanocomposites, particularly for the composite with CNT volume fraction below and around the percolation threshold. For example, when the CNT volume fraction is $f = 0.003\%$ and the CNT aspect ratio is $L/d = 1000$, the electrical conductivity of the interphase was calculated as 8.6776×10^{-14} S/m from Eq. (2.17), which is comparable to the interphase electrical conductivity 9.95×10^{-14} S/m calculated from Eq. (2.15). However, with the increase of CNT volume fraction, the contribution of conductive networks becomes more dominant. For example, when CNT volume fraction f reaches 0.01%, the electrical conductivity for the interphase surrounding CNTs is calculated as 7.922×10^{-8} S/m from Eq. (2.15), which is much larger than the one calculated from Eq. (2.17). Therefore, such an overestimation can be neglected after percolation.

2.3 Mixed micromechanics model

For the purpose of modeling simplicity, CNTs were assumed to be straight, and uniformly and randomly dispersed in the polymer matrix. The CNT volume fraction is denoted as f. As discussed in the previous section, CNTs together with their surrounding interphases can be simulated as equivalent solid fillers due to electron hopping. Therefore, the composite can be considered as a two-phase system with solid fillers dispersed in the polymer matrix. The volume fraction f_{eff} of the effective solid fillers can

be obtained in terms of the volume fraction of CNTs in the polymer according to Figure 2.2 (Seidel and Lagoudas, 2009; Yan *et al*., 2007) as:

$$f_{\text{eff}} = \frac{\left(r_c + t\right)^2 \left(L + 2t\right)}{r_c^2 L} f .$$

(2.18)

To determine the effective electrical conductivity of the composites with two phases, a representative volume element (RVE) containing enough effective fillers with random orientations, which is able to statistically represent overall properties of the material, as shown in Figure 2.4 was chosen in the micromechanics model to study the overall electrical conductivity of the composite. In micromechanics theory, each orientation of a given effective filler in the polymer can be treated as a separate phase, and the effective electrical conductivity of the nanocomposite can be determined by averaging over all possible orientations in the RVE according to the following expression (Odegard *et al*., 2003; Taya, 2005):
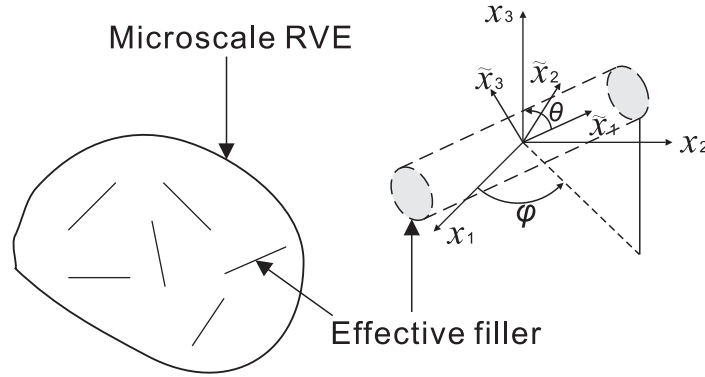
Figure 2.4 Sketch of a microscale RVE containing effective filler.

$$\sigma_{\text{eff}} = \sigma_m + \frac{\int_0^{2\pi} \int_0^{\pi} \rho(\varphi,\theta) f_{\text{eff}} \left(\sigma - \sigma_m\right) A \sin\theta \, \mathrm{d}\theta \, \mathrm{d}\varphi}{\int_0^{2\pi} \int_0^{\pi} \rho(\varphi,\theta) \sin\theta \, \mathrm{d}\theta \, \mathrm{d}\varphi}$$

(2.19)

where φ and θ are Euler angles defining effective filler orientation as shown in Figure 2.4; $\rho(\varphi, \theta)$ is the orientation distribution function, which equals unity for a random

distribution; σ and σ_m are electrical conductivity tensors of the effective filler and the polymer, respectively; and A is the electric field concentration tensor.

Since all quantities in Eq. (2.19) are in the global coordinate system (x_1, x_2, x_3), quantities obtained in the local coordinate system need to be transferred to the global coordinate system through a transformation, i.e.,

$$\boldsymbol{\sigma} = \boldsymbol{Q}^{\mathrm{T}} \tilde{\boldsymbol{\sigma}} \boldsymbol{Q} , \tag{2.20}$$

where $\tilde{\sigma}$ is the electrical conductivity tensor of the effective filler in the local coordinate system, which is given as:

$$\tilde{\boldsymbol{\sigma}} = \begin{bmatrix} \tilde{\sigma}^{\mathrm{L}} & 0 & 0 \\ 0 & \tilde{\sigma}^{\mathrm{T}} & 0 \\ 0 & 0 & \tilde{\sigma}^{\mathrm{T}} \end{bmatrix} , \tag{2.21}$$

with $\tilde{\sigma}^{\mathrm{L}}$ and $\tilde{\sigma}^{\mathrm{T}}$ being the longitudinal and transverse electrical conductivity of the effective filler as obtained in Eq. (2.10), and the transformation matrix is (Seidel and Lagoudas, 2009)

$$\boldsymbol{Q} = \begin{bmatrix} \sin\theta\cos\varphi & -\cos\theta\cos\varphi & \sin\varphi \\ \sin\theta\sin\varphi & -\cos\theta\sin\varphi & -\cos\varphi \\ \cos\theta & \sin\theta & 0 \end{bmatrix} . \tag{2.22}$$

As a case study, the Mori-Tanaka method (Hatta and Taya, 1985; Mori and Tanaka, 1973) was selected as the micromechanics model. Based on the assumption of uniform and random distribution of CNTs, the electric field concentration tensor A in the global coordinate system can be expressed as (Seidel and Lagoudas, 2009; Taya, 2005):

$$\boldsymbol{A} = \boldsymbol{Q}^{\mathrm{T}} \tilde{\boldsymbol{T}} \boldsymbol{Q} \left\{ (1 - f_{\mathrm{eff}}) \boldsymbol{\delta} + \frac{f_{\mathrm{eff}}}{4\pi} \int_0^{2\pi} \int_0^{\pi} \left\{ \boldsymbol{Q}^{\mathrm{T}} \tilde{\boldsymbol{T}} \boldsymbol{Q} \right\} \sin\theta \mathrm{d}\theta \mathrm{d}\varphi \right\}^{-1} , \tag{2.23}$$

where

$$\tilde{T} = \left\{ \delta + S\left(\sigma_m\right)^{-1}\left(\tilde{\sigma} - \sigma_m\right) \right\}^{-1} \tag{2.24}$$

with δ and S being the Kronecker delta tensor and the Eshelby tensor of the effective filler, respectively. The Eshelby tensor of the effective filler is given as

$$S = \begin{bmatrix} S_{11} & 0 & 0 \\ 0 & S_{22} & 0 \\ 0 & 0 & S_{33} \end{bmatrix}, \tag{2.25}$$

where

$$S_{22} = S_{33} = \frac{A_{re}}{2\left(A_{re}^{2}-1\right)^{3/2}}\left[A_{re}\left(A_{re}^{2}-1\right)^{1/2} - \cosh^{-1} A_{re} \right] \tag{2.26}$$

with A_{re} being the aspect ratio of the effective filler, i.e., $A_{re}=(L+2t)/(2r_c+2t)$, and $S_{11}=1-S_{22}$, respectively (Taya, 2005; Seidel and Lagoudas, 2009).

As mentioned before, several experiments and simulations have demonstrated that CNT-polymer nanocomposites have a percolation-like behavior displaying a sharp increase in electrical conductivity after the CNT volume fraction reaches a certain threshold. For a two-phase nanocomposite with a uniformly random distribution of CNTs, the percolation threshold, f_c, is approximately determined by the following analytical formulation (Gao and Li, 2003; Deng and Zheng, 2008)

$$f_c\left(H\right) = \frac{9H\left(1-H\right)}{2+15H-9H^{2}} \, , \tag{2.27}$$

where $H\left(A_r\right) = \dfrac{1}{A_r^{2}-1}\left[\dfrac{A_r}{\sqrt{A_r^{2}-1}}\ln\left(A_r+\sqrt{A_r^{2}-1}\right)-1 \right]$ and A_r is the aspect ratio of the CNT,

i.e., $A_r = L/2r_c$. Here it should be noted that the percolation threshold defined in Eq. (2.27)

is the critical CNT volume fraction denoting the onset of the percolation process (a process of forming conductive networks). As argued by Deng and Zheng (2008), the percolation process of CNT composites would last for a volume fraction range due to the random distribution nature of CNTs. Before the CNT volume fraction reaches the percolation threshold, i.e., $f < f_c$, no CNTs are percolated due to the very small CNT concentration and large separation distance between CNTs. Under this condition, only electron hopping is believed to contribute to the electrical conductivity of the nanocomposite. However, once percolation starts ($f > f_c$), certain amount of CNTs are percolated to form conductive networks, i.e., a percentage ξ of CNTs are percolated while $(1-\xi)$ are not. Therefore, in the percolation process, both electron hopping and conductive networks contribute to the overall electrical conductivity of the composite. It is obvious that with the CNT volume fraction increasing from f_c to 1 (a limiting case for material consisting of CNTs only), the percentage of percolated CNTs, ξ, will change from 0 to 1. According to Deng and Zheng (2008), the percentage of percolated CNTs, ξ, can be approximately estimated as

$$\xi = \frac{f^{1/3} - f_c^{1/3}}{1 - f_c^{1/3}}, \quad \left(f_c \leq f < 1 \right). \tag{2.28}$$

From the above analysis, it is concluded that both electron hopping and conductive networks govern the electrical conductivity of the composite after percolation, while only electron hopping contributes to the electrical conductivity of the composite prior to percolation. Therefore, the overall electrical conductivity of CNT-polymer nanocomposites can be determined in a mixed form from the general micromechanics formulation of Eq. (2.19), i.e.,

$$\boldsymbol{\sigma}_{\text{eff}} = \begin{cases} \boldsymbol{\sigma}_{\text{m}} + \dfrac{1}{4\pi}\displaystyle\int_0^{2\pi}\int_0^{\pi}\left\{ f_{\text{eff}}\left(\boldsymbol{\sigma}_{\text{EH}} - \boldsymbol{\sigma}_{\text{m}}\right)\boldsymbol{A}_{\text{EH}}\right\}\sin\theta\, \mathrm{d}\theta\mathrm{d}\varphi, \ f < f_c \\[2ex] \boldsymbol{\sigma}_{\text{m}} + \left(1-\xi\right)\dfrac{1}{4\pi}\displaystyle\int_0^{2\pi}\int_0^{\pi}\left\{ f_{\text{eff}}\left(\boldsymbol{\sigma}_{\text{EH}} - \boldsymbol{\sigma}_{\text{m}}\right)\boldsymbol{A}_{\text{EH}}\right\}\sin\theta\, \mathrm{d}\theta\mathrm{d}\varphi \\[2ex] \quad + \xi\dfrac{1}{4\pi}\displaystyle\int_0^{2\pi}\int_0^{\pi}\left\{ f_{\text{eff}}\left(\boldsymbol{\sigma}_{\text{CN}} - \boldsymbol{\sigma}_{\text{m}}\right)\boldsymbol{A}_{\text{CN}}\right\}\sin\theta\, \mathrm{d}\theta\mathrm{d}\varphi, \ \ f \geq f_c \end{cases}, \tag{2.29}$$

where σ_{EH} and σ_{CN} denote the electrical conductivity tensors of the effective filler contributed by electron hopping and conductive networks, respectively. These two tensors in the global coordinate system are determined from Eq. (2.20) with $\tilde{\sigma}_{\text{EH}}$ and $\tilde{\sigma}_{\text{CN}}$ being derived by Eqs. (2.10) and (2.21). For electron hopping, the interphase thickness and electrical conductivity are determined from Eqs. (2.16) and (2.17), while for conductive networks, these quantities are determined from Eqs. (2.13) and (2.15). A_{EH} and A_{CN} are the corresponding electric field concentration tensors determined from Eq. (2.23) with the Eshelby tensor given in Eq. (2.25). For conductive networks, several CNTs will be electrically connected to each other (not in physical contact because of van der Waals forces between CNTs), and the effective aspect ratio of formed networks can thus be taken as infinite due to the large aspect ratio of the CNTs (Seidel and Lagoudas, 2009). Therefore, the quantities associated with the electron hopping corresponds to the real CNTs aspect ratio, while the quantities related to conductive networks corresponds to an infinite aspect ratio.

This mixed micromechanics model with considering electron hopping and conductive networks was employed to predict the effective electrical conductivity of CNT-polymer nanocomposites.

2.4   Results and discussion

To validate the micromechanics model developed in the current work, the modeling results were compared with the experimental data for a single walled carbon nanotube (SWCNT)-epoxy nanocomposite (Gojny *et al*., 2006) and a multiple walled carbon nanotube (MWCNT)-epoxy nanocomposite (Kim *et al*., 2005), respectively. In these experimental works the electrical conductivities of the nanocomposites were measured by means of a dielectric spectroscopy analyzer. It should be noted that for the current theoretical modeling, CNTs were assumed to be uniformly dispersed in the polymer. Conventionally, it is accepted that such a perfect dispersion without any agglomeration of CNTs is desirable to enhance the electrical properties of composites as validated in experiments (Song and Youn, 2008; Golosova *et al*., 2012). However, some other experiments showed that a less than perfect dispersion with CNT agglomerations could

favor the formation of conductive networks in composites (Martin *et al.*, 2004; Li *et al.*, 2007). In order to get a better uniform dispersion of CNTs in the polymer, in Gojny's (2006) experiments SWCNTs were dispersed in the epoxy matrix by a three-roll mill (with roller speeds 20, 30 180 rpm, respectively). The suspensions were fully mixed before hardening and then cured for 48 hours to reduce agglomerations. For the MWCNT-epoxy nanocomposite in (Kim *et al.*, 2005), surfaces of MWCNTs were chemically treated by acetone/surfactant solution and sonication to reduce van der Waals interactions among MWCNTs. MWCNTs were dispersed and fully mixed with epoxy matrix by a two-roll mill. After approximate five hour's cure, it was observed that MWCNTs were well dispersed in the epoxy. Figure 2.5 shows the comparison between the analytical results from the current micromechanics model and the experimental data for the SWCNT-epoxy nanocomposite (Gojny *et al.*, 2006), in which the SWCNTs were dispersed in a modified DGEBA-based epoxy resin. In this work, the length and diameter of the CNTs and the electrical conductivity of the epoxy were selected as $L = 2$ µm, $d = 2$ nm and $\sigma_m = 9 \times 10^{-9}$ S/m, respectively. The electrical conductivity of the CNT was taken as 5×10^4 S/m from (Ebbesen *et al.*, 1996). By comparison, it was observed that the analytical result derived from the mixed micromechanics model of Eq. (2.29) successfully predicts the trend of the experimental data. Without considering conductive networks, the micromechanics modeling result was also provided in this figure for comparison. It was noticed that when the volume fraction is small, little discrepancy exists between the modeling results considering conductive networks and the results without considering conductive networks. However, with the increase of CNT volume fraction, a significant discrepancy appears between these two modeling results. It can be concluded that both electron hopping and conductive networks contribute to the overall electrical conductivity of the composite, while conductive networks become dominant conductivity mechanism for the composite with higher CNT volume fraction. Therefore, the overestimation of electron hopping caused by definitions in Eqs. (2.16) and (2.17) as mentioned in section 2 can be neglected after percolation due to the dominant contribution of conductive networks to the overall electrical conductivity of the nanocomposites. The same conclusion can be obtained for the MWCNT case as shown in Figure 2.6.
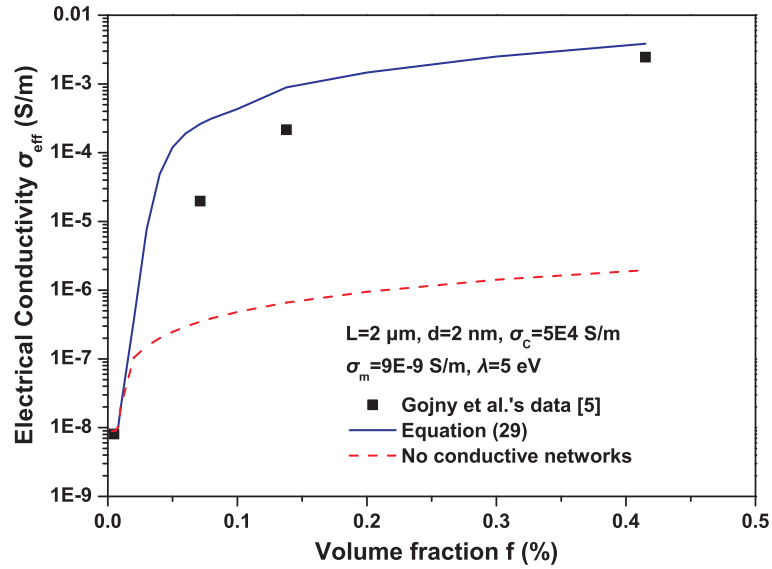
Figure 2.5 Comparison between modeling results and experimental data of a SWCNT–epoxy nanocomposite.

Figure 2.6 shows another comparison between the micromechanics results and the experimental data of a MWCNT-epoxy nanocomposite. In simulation, the length and diameter of the CNTs and the electrical conductivity of the epoxy were selected as $L = 20$ µm, $d = 20$ nm and $\sigma_m = 1 \times 10^{-13}$ S/m, respectively (Kim $et\ al.$, 2005). According to literature Deng's work (2008), the electrical conductivity of MWCNTs ranges from 10 S/m to 10000 S/m, which will be used in the simulation for comparison. It was found that the analytical results successfully predict the trend of the experimental data when the electrical conductivity of the CNT was set between 100 S/m and 1000 S/m. It was also observed that for MWCNTs with the same aspect ratio the increasing in electrical conductivity of the CNT significantly enhances the overall electrical conductivity of the nanocomposite. It was also found that the overall electrical conductivity of the nanocomposite increases with the increase of CNT volume fraction. Without considering conductive networks in the micromechanics model, significant discrepancy from the experimental data was observed in Figure 2.6. Therefore, the formation of conductive networks is a significant factor in governing the percolation behavior of nanocomposites, and a micromechanics model without considering conductive networks may lead to significant error in predicting the overall electrical conductivity of CNT-polymer
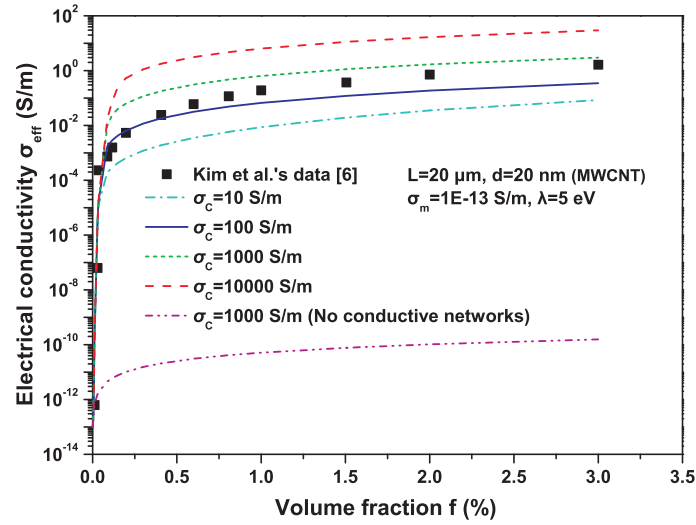
composites.

Figure 2.6 Comparison between modeling results and experimental data for a MWCNT–epoxy nanocomposite.

Figure 2.7 and Figure 2.8 demonstrate the effects of CNT sizes, i.e. length and diameter, on the overall electrical conductivity of MWCNT-epoxy nanocomposites. It was found that CNT sizes have a significant effect on the percolation rate of the composite, while having a moderate effect on the overall electrical conductivity after percolation. For the same CNT volume fraction, the overall electrical conductivity increases with the increase in CNT length or the decrease in CNT diameter. These results suggest that the electrical conductivity of CNT-polymer nanocomposite can be improved by increasing the CNT aspect ratio. Such a phenomenon on the improved electrical conductivity can be explained by the existence of more conductive networks for CNTs with larger aspect ratio at the same CNT concentration. Moreover, the percolation rate was found to decrease with the increase of CNT length, while increasing with the increase of CNT diameter. Similar trends of the aspect ratio effect on the percolation rate have also been observed in existing literature (Yan *et al.*, 2007).
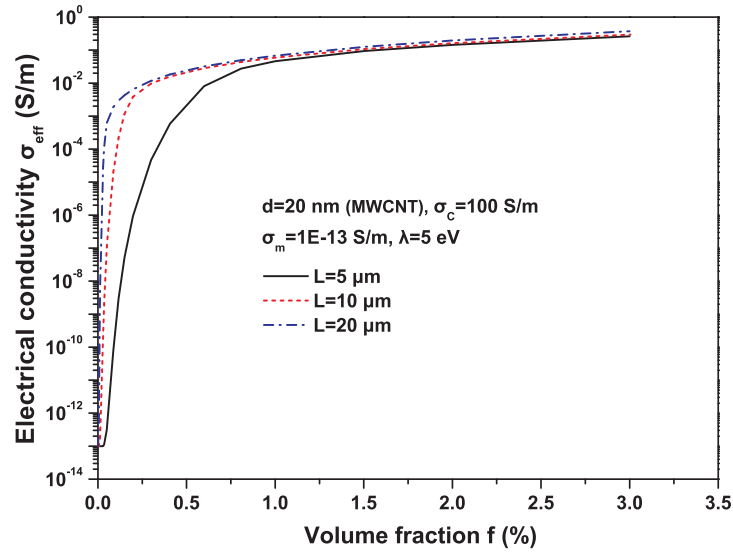
Figure 2.7 Effect of the CNT length on the electrical conductivity of the MWCNT–epoxy nanocomposite.
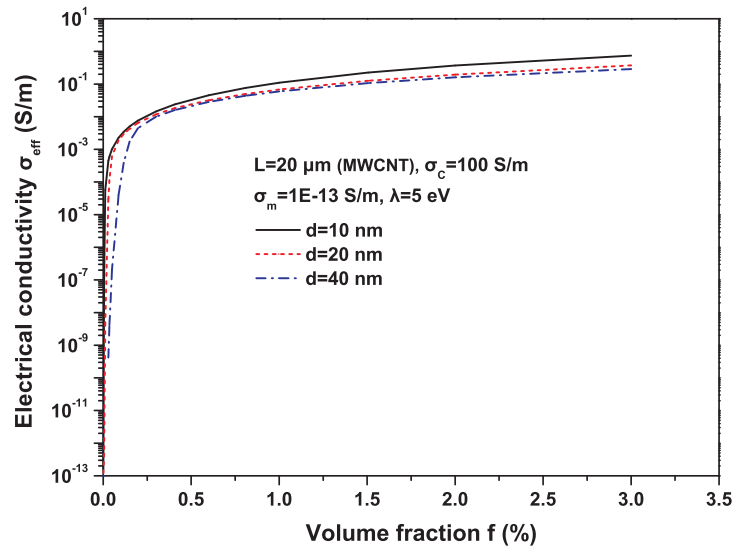
Figure 2.8 Effect of the CNT diameter on the electrical conductivity of the MWCNT–epoxy nanocomposite.

It should be mentioned that the mixed micromechanics model in the current work was developed based on the assumption of uniformly random distribution of straight CNTs in polymers. However, due to the large aspect ratio of CNTs and van der Waals forces among CNTs, CNTs distributed in polymer media usually exist in agglomerates and in a

curved state. A more accurate model with the consideration of the effects of curvature and agglomerates should be further developed to analyze the electrical properties of nanocomposites, which is our future research concentration.

2.5 Conclusions

In this work, two conductivity mechanisms, electron hopping and conductive networks, have been considered to develop a mixed micromechanics model to predict the overall electrical conductivity of CNT-polymer nanocomposites. An interphase surrounding the CNT was introduced to capture the electron hopping effect, and its properties such as thickness and conductivity, were defined through electron hopping theory. By comparison with experimental data, the mixed micromechanics model was validated to provide accurate quantitative predictions on the overall electrical conductivity of the nanocomposite. It was found that both electron hopping and conductive networks contribute to the electrical conductivity of the nanocomposite, while conductive networks become dominant after percolation. Meanwhile, effects of CNT sizes on the electrical conductivity were also investigated. It was observed that both CNT length and diameter significantly affect the percolation concentration of nanocomposites, while having moderate effects on the overall electrical conductivity of the nanocomposites after percolation. This work with quantitative prediction on the electrical conductivity of CNT-polymer composites is envisaged to be helpful for the design and optimization of the CNT-polymer nanocomposites with desirable electrical properties.

References

Allaoui, A., Hoa, S. V. and Pugh, M. D., 2008. The electronic transport properties and microstructure of carbon nanofiber/epoxy composites. Compos. Sci. Technol. **68**, 410–416.

Chang, L., Friedrich, K., Ye, L. and Toro, P., 2009. Evaluation and visualization of the percolating networks in multi-wall carbon nanotube/epoxy composites. J. Mater. Sci. **44**, 4003–4012.

Deng, F. and Zheng, Q. S., 2008. An analytical model of effective electrical conductivity of carbon nanotube composites. Appl. Phys. Lett. **92**, 071902.

Du, F. M., Scogna, R. C., Zhou, W., Brand, S., Fischer, J. E. and Winey, K. I., 2004. Nanotube networks in polymer nanocomposites: Rheology and electrical conductivity. Macromolecules **37**, 9048–9055.

Ebbesen, T. W., Lezec, H. J., Hiura, H., Bennett, J. W., Ghaemi, H. F. and Thio, T., 1996. Electrical conductivity of individual carbon nanotubes. Nature **382**, 54–56.

Gao, L. and Li, Z., 2003. Effective medium approximation for two-component nonlinear composites with shape distribution. J. Phys.: Condens. Matter **15**, 4397–4409.

Ghazavizadeh, A., Baniassadi, M., Safdari, M., Atai, A. A., Ahzi, S., Patlazhan, S. A., Gracio, J. and Ruch, D., 2011. Evaluating the effect of mechanical loading on the electrical percolation threshold of carbon nanotube reinforced polymers: a 3D Monte-Carlo study. J. Comput. Theor. Nanosci. **8**, 2087–2099.

Gojny, F. H., Wichmann, M. H. G., Fiedler, B., Kinloch, I. A., Bauhofer, W., Windle, A. H. et al., 2006. Evaluation and identification of electrical and thermal conduction mechanisms in carbon nanotube/epoxy composites. Polymer **47**, 2036–2045.

Golosova, A. A., Adelsberger, J., Sepe, A., Niedermeier, M. A., Lindner, P., Funari, S. S. et al., 2012. Dispersions of Polymer-Modified Carbon Nanotubes: A Small-Angle Scattering Investigation. J. Phys. Chem. C **116**,15765−15774

Grimmett, G., 1999. Percolation. Springer Verlag, Berlin.

Hashin, Z., 1990. Thermoelastic properties and conductivity of carbon/carbon fiber composites. Mech. Mater. **8**, 293–308.

Hatta, H. and Taya, M., 1985. Effective Thermal-Conductivity of a Misoriented Short Fiber Composite. J. Appl. Phys. **58**, 2478–2486.

Hu, N., Masuda, Z., Yan, C., Yamamoto, G., Fukunaga, H. and Hashida, T., 2008. The electrical properties of polymer nanocomposites with carbon nanotube fillers. Nanotechnology **19**, 215701.

Kim, Y. J., Shin, T. S., Choi, H. D., Kwon, J. H., Chung, Y. C. and Yoon, H. G., 2005. Electrical conductivity of chemically modified multiwalled carbon nanotube/epoxy composites. Carbon **43**, 23–30.

Kirkpatrick, S., 1973. Percolation and conduction. Rev. Mod. Phys. **45**, 574–588.

Li, X., Rong, J. P. and Wei, B.Q., 2010. Electrochemical Behavior of Single-Walled Carbon Nanotube Supercapacitors under Compressive Stress. Acs Nano **4**, 6039–6049.

Li, C. Y., Thostenson, E. T. and Chou, T. W., 2007. Dominant role of tunneling resistance in the electrical conductivity of carbon nanotube-based composites. Appl. Phys. Lett. **91**, 223114.

Li, J., Ma, P. C., Chow, W. S., To, C. K., Tang, B. Z. and Kim. J. K., 2007. Correlations between percolation threshold, dispersion state, and aspect ratio of carbon nanotubes. Adv. Funct. Mater. **17**, 3207–3215.

Lu, W. B., Chou, T. W. and Thostenson, E. T., 2010. A three-dimensional model of electrical percolation thresholds in carbon nanotube-based composites. Appl. Phys. Lett. **96**, 223106.

Ma, H. M. and Gao. X. L., 2008. A three-dimensional Monte Carlo model for electrically conductive polymer matrix composites filled with curved fibers. Polymer **49**, 4230–4238.

Martin, C., Sandler, J. K. W., Shaffer, M. S. P., Schwarz, M-K., Bauhofer, W., Schulte, K. et al., 2004.   Formation of percolating networks in multi-wall carbon-nanotube-epoxy composites. Compos. Sci. Technol. **64**, 2309–2316.

McLachlan, D. S., Chiteme, C., Park, C., Wise, K. E., Lowther, S. E., Lillehei, P. T. et al., 2005. AC and DC percolative conductivity of single wall carbon nanotube polymer composites. J. Polym. Sci. Pol. Phys. **43**, 3273–3287.

Mori, T. and Tanaka, K., 1973. Average Stress in Matrix and Average Elastic Energy of Materials with Misfitting Inclusions. Acta Metall. Mater. **21**, 571–574.

Odegard, G. M., Gates, T., Wise, K. E., Park, C. and Siochi, E., 2003. Constitutive modeling of nanotube-reinforced polymer composites. Compos. Sci. Technol. **63**,1671–1687.

Ounaies, Z., Park, C., Wise, K. E., Siochi, E. J. and Harrison, J. S., 2003. Electrical properties of single wall carbon nanotube reinforced polyimide composites. Compos. Sci. Technol. **63**,1637–1646.

Ramasubramaniam, R., Chen, J. and Liu, H. Y., 2003. Homogeneous carbon nanotube/polymer composites for electrical applications. Appl. Phys. Lett. **83**, 2928–2930.

Seidel, G. D. and Lagoudas, D. C., 2009. A Micromechanics Model for the Electrical Conductivity of Nanotube-Polymer Nanocomposites. J. Compos. Mater. **43**, 917–941.

Shiraishi, M. and Ata, M., 2001. Work function of carbon nanotubes. Carbon **39**,1913–1917.

Simmons, J. G., 1963. Generalized formula for the electric tunnel effect between similar electrodes separated by a thin insulating film. J. Appl. Phys. **34**,1793–1803.

Song, Y. S. and Youn, J. R., 2005. Influence of dispersion states of carbon nanotubes on physical properties of epoxy nanocomposites. Carbon **43**, 1378–1385

Subramanian, V., Zhu, H. and Wei, B., 2006. Synthesis and electrochemical characterizations of amorphous manganese oxide and single walled carbon nanotube composites as supercapacitor electrode materials. Electrochem. Commun. **8**, 827–832.

Takeda, T., Shindo, Y., Kuronuma, Y. and Narita, F., 2011. Modeling and characterization of the electrical conductivity of carbon nanotube-based polymer composites. Polymer **52**, 3852–3856.

Taya, M., 2005. Electronic composites. Cambridge University Press, Cambridge.

Yan, K. Y., Xue, Q. Z., Zheng, Q. B. and Hao, L. Z., 2007. The interface effect of the effective electrical conductivity of carbon nanotube composites. Nanotechnology **18**, 255705.

Yu, C. J., Masarapu, C., Rong, J. P., Wei, B. Q. and Jiang, H. Q., 2009. Stretchable Supercapacitors Based on Buckled Single-Walled Carbon Nanotube Macrofilms. Adv. Mater. **21**, 4793–1797.

Zhang, R., Dowden, A., Deng, H., Baxendale, M. and Peijs, T., 2009. Conductive network formation in the melt of carbon nanotube/thermoplastic polyurethane composite. Compos. Sci. Technol. **69**, 1499–1504.

Zhang, T. and Yi, Y. B., 2008. Monte Carlo simulations of effective electrical conductivity in short-fiber composites. J. Appl. Phys. **103**, 014910.

Chapter 3

3 Uni-axial stretching effects on electrical conductivity of CNT-polymer composites[2]

3.1 Introduction

In recent years, conductive polymer composites have been attracting extensive interests from scientific and industrial communities due to their unique features, such as high stretchability, low cost, easy processability and good compatibility (Yu *et al*., 2009; Nambiar and Yeow, 2011; Shang *et al*., 2011). Compared with traditional conductive or semi-conductive materials, such as metals or silicon, conductive polymer composites possess conductive properties from the filler materials while keeping the intrinsic flexibility of the polymers. Thus, the unique combination of conductivity and flexibility enables conductive polymer composites the most promising materials in a variety of applications including flexible and stretchable electronics, conductive coatings, electromagnetic shielding, solar cells, etc, which cannot be achieved by traditional rigid conductive materials (Yang et al., 2005; Berson et al., 2007; Yu *et al*., 2009; Shang *et al*., 2011).

Due to their extraordinary physical properties, particularly electrical properties, carbon nanotubes (CNTs) are widely adopted as promising candidates of conducting fillers in soft polymers for the potential fabrication of conductive polymer composites. Experiments have shown that the addition of a very small amount of CNTs into polymers can remarkably improve the electrical conductivity of the composites with a percolation-like behavior (Ounaies *et al*., 2003; Kim *et al*., 2005; Gojny *et al*., 2006). Interpretation on the conductivity of these CNT–polymer composites is attributed to two mechanisms: nanoscale electron hopping (or quantum tunneling) and microscale conductive networking (Chang *et al*., 2009; Zhang *et al*., 2009; Lu *et al*., 2010). It is well explained

---

[2] A version of this chapter has been accepted by Journal of Physics D: Applied Physics.

in literature (Deng and Zheng, 2008; Seidel and Lagoudas, 2009; Takeda *et al*., 2011) that the contribution of the electron hopping and conductive networking depends on the CNT concentration, such that, with increasing CNT concentration, conductive networks are formed and believed to be dominant over the electron hopping, while electrons always have the probability of hopping intra-tube or among different CNTs, which governs the overall electrical conductivity of the composites particularly with extremely low CNT concentration.

Understanding on the overall electrical conductivity of CNT–polymer composites is essential for their design and full potential applications. In literature, efforts have been devoted to investigating the electrical properties of these composites through experiments, numerical simulations and theoretical modeling (Chang *et al*., 2009; Feng and Jiang, 2013; Gojny *et al*., 2006; Kim *et al*., 2005; Li *et al*., 2007; Seidel and Lagoudas, 2009; Takeda *et al*., 2011; Yan *et al*., 2007). However, most of these studies were focused on preparing composites with well dispersed conductive fillers or predicting the electrical behavior of the as-received composites without considering stretching effects. For the potential application of conductive polymer composites as stretchable electronics, it is necessary to investigate the stretching effects upon the overall electrical conductivity of the composites in order to accurately predict and control the device performance. Existing studies have demonstrated that stretching may significantly influence the electrical behavior of conductive polymer composites. For example, Bao *et al*. (2011) experimentally examined the morphology and the electrical conductivity of carbon nanofibre composites before and after mechanical stretching. Their results showed that mechanical stretching could lead to a sharp decrease in the electrical conductivity of the composites due to the breakdown of conductive networks. Miao and his co-workers (2011a, 2011b and 2012) examined the piezoresistive response of CNT–polymer composites by experiments and percolation theory and their results indicated that stretching decreases the electrical conductivity of the composites. In addition, Park *et al.* (2008) and Hu *et al.*'s (2010) works demonstrated an abrupt increase in resistance of CNT–polymer composites when subjected to stretching. However, other experimental results (Cheng *et al*., 2009; Shang *et al*., 2011; Wang *et al*., 2011) showed an opposite

trend, i.e., stretching increased the electrical conductivity of CNT–polymer composites. This phenomenon was explained as resulting from the substantial alignment enhancement of conductive fillers along the stretching direction of the composites. From the aspect of numerical simulations, Taya *et al.* (1998) and Lin *et al.* (2010) applied the fibre percolation model and Monte Carlo method, respectively, to investigate the stretching/compression effects upon the electrical properties of fibre-filled composites and their results showed that the deformation could shift the percolation threshold of the composites. A recent study by Tallman and Wang (2013) also indicated that stretching could alter the percolation threshold due to the CNTs' re-orientation. Despite the fact that different results have been observed in literature, it is suggested that there are three major expected changes occurred during the stretching, including composite volume expansion, re-orientation of conductive fillers and change in conductive networks, which may contribute to the variation of the overall electrical properties of the polymer composites.

Traditional compressible materials expand when subjected to stretching. Since CNTs are much stiffer than polymers in the CNT–polymer composites, the stretching deformation is mainly sustained by the polymer matrix. As a result, the concentration of the conductive fillers decreases due to the very low concentration and the nearly unchanged volume of conductive CNTs. Consequently, the electrical conductivity of the composites will be altered by the decrease in CNT concentration. Some researchers argued that such effect of volume expansion of the CNT–polymer composites could be neglected for small deformation due to their limited compressibility Taya (1998). After stretching, experiments have shown that CNTs tend to be more re-aligned along the stretching direction rather than randomly distributed as observed before stretching (Cheng *et al*., 2009; Wang *et al*., 2011). Due to the highly anisotropic properties of CNTs, the electrical properties of the CNT–polymer composites strongly depend upon the orientation of the CNTs, which has been demonstrated by several experiments (Du *et al*., 2005; Cheng *et al*., 2009; Wang *et al*., 2011). Conductive networking is one of the conductivity mechanisms in conductive composites as discussed before. Researchers have argued that due to the re-alignment of CNTs certain existing conductive networks may break down causing an increase in the percolation threshold, which is believed to be responsible for

the observed decrease in the electrical conductivity of composites (Taya *et al*., 1998; Du *et al*., 2005; Bao *et al*., 2011). In addition, some simulations and analytical studies (Taya *et al*, 1998; Lin *et al*., 2010; Tallman and Wang, 2013;) also showed that stretching/compression could change the percolation threshold, a critical concentration of conductive fillers identifying the formation of conductive networks.

Despite the fact that efforts have been made to investigate the stretching effects on the electrical conductivity of CNT–polymer composites experimentally and numerically, there is limited work on theoretical modeling with the consideration of the three expected changes mentioned before. Therefore, the objective of the current work is to investigate the effects of the stretching induced volume expansion, CNT re-orientation and conductive network change on the overall electrical conductivity of the CNT–polymer composites following our previous work (Feng and Jiang, 2013).

3.2   Micromechanics model for CNT-polymer composites

For a two-phase composite, in which conductive fillers with volume fraction *f* are assumed as straight and uniformly dispersed in the polymer matrix, micromechanics model is commonly adopted by researchers to quantitatively predict the overall effective physical properties of the composite, i.e., mechanical and electrical properties (Entchev and Lagoudas, 2002; Seidel and Lagoudas, 2009). Following the routine procedure of the micromechanics theory, a representative volume element (RVE) containing enough fillers with random orientations as shown in Figure 3.1 (Seidel and Lagoudas, 2009; Feng and Jiang, 2013) is chosen to study the overall electrical conductivity of the composite in the current work. In the RVE, ($\tilde{x}_1, \tilde{x}_2, \tilde{x}_3$) is selected as the local coordinate system describing the position of an individual filler and φ and θ are Euler angles identifying its orientation with respect to the global coordinate system (X_1, X_2, X_3). Based on the micromechanics theory, the effective electrical conductivity of this two-phase composite can be determined in terms of the electrical conductivity of the fillers and the polymer by averaging the contribution of the fillers from all possible orientations in the RVE (Taya, 1995; Entchev and Lagoudas, 2002; Odegard *et al*., 2003; Taya, 2005; Seidel and Lagoudas, 2009), i.e.,
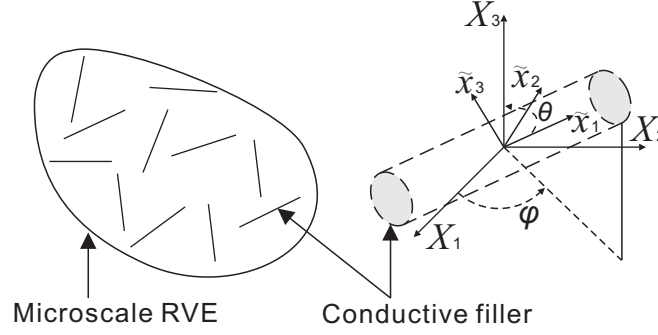
Figure 3.1 Sketch of a RVE containing conductive fillers.

$$\boldsymbol{\sigma}_{\text{eff}} = \boldsymbol{\sigma}_{\text{m}} + \frac{\int_0^{2\pi}\int_0^{\pi} \rho(\varphi,\theta) f(\boldsymbol{\sigma}-\boldsymbol{\sigma}_{\text{m}}) A \sin\theta \, \mathrm{d}\theta \mathrm{d}\varphi}{\int_0^{2\pi}\int_0^{\pi} \rho(\varphi,\theta)\sin\theta \, \mathrm{d}\theta \mathrm{d}\varphi} \quad , \tag{3.1}$$

where A is the electric field concentration tensor, which will be defined later, σ and σ_{m} are the electrical conductivity tensors of the fillers and the polymer, respectively and $\rho(\varphi,\theta)$ is the orientation distribution function (ODF) representing the probability density of the distribution of the fillers with a given orientation, particularly $\rho(\varphi,\theta)$ equals unity for a random distribution of fillers.

In CNT–polymer composites, electron hopping among CNTs results in the formation of a continuum interphase layer surrounding a CNT. In order to capture the effect of this interphase layer and the hollow nature of the CNT, a well-accepted effective composite cylinder model (Yan *et al*., 2007; Seidel and Lagoudas, 2009; Feng and Jiang, 2013) as shown in Figure 3.2, which consists of a CNT (length L, radius r_c) and a surrounding interphase layer (thickness t), is adopted in the current work to determine the effective electrical conductivity of the CNT with the consideration of the electron hopping effect. Knowing the electrical conductivity of the interphase (σ_{Int}) and the CNT (σ_c) and the interphase thickness (t), the effective longitudinal and transverse electrical conductivity of the effective solid filler in its own local coordinate system was determined by applying the law-of-mixture rule as (Taya, 2005; Yan *et al*., 2007; Feng and Jiang, 2013):
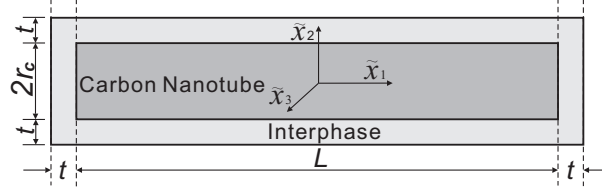
Figure 3.2 Sketch of an effective composite cylinder.

$$\tilde{\sigma}^{L} = \frac{(L+2t)\sigma_{Int}\left[\sigma_{c}^{L}r_{c}^{2} + \sigma_{Int}\left(2r_{c}t + t^{2}\right)\right]}{2\sigma_{c}^{L}r_{c}^{2}t + 2\sigma_{Int}\left(2r_{c}t + t^{2}\right)t + \sigma_{Int}L(r_{c}+t)^{2}},$$

$$\tilde{\sigma}^{T} = \frac{\sigma_{Int}}{L+2t}\left[L\frac{2r_{c}^{2}\sigma_{c}^{T} + \left(\sigma_{c}^{T} + \sigma_{Int}\right)\left(t^{2} + 2r_{c}t\right)}{2r_{c}^{2}\sigma_{Int} + \left(\sigma_{c}^{T} + \sigma_{Int}\right)\left(t^{2} + 2r_{c}t\right)} + 2t\right]$$

(3.2)

where superscripts "L" and "T" denote the longitudinal and the transverse directions in the local coordinate system. Thus, the electrical conductivity tensor of the effective cylinder assembly in its local coordinate system can be written as:

$$\tilde{\boldsymbol{\sigma}} = \begin{bmatrix} \tilde{\sigma}^{L} & & \\ & \tilde{\sigma}^{T} & \\ & & \tilde{\sigma}^{T} \end{bmatrix}.$$

(3.3)

It should be mentioned that the electrical conductivity tensor σ in Eq. (3.1) is the one in the global coordinate system, which can be obtained from its counterpart $\tilde{\sigma}$ in the local coordinate system through a transformation (Seidel and Lagoudas, 2009), i.e.,

$$\sigma = \boldsymbol{Q}\tilde{\sigma}\boldsymbol{Q}^{T}$$

(3.4)

with the transformation matrix Q being given in terms of the Euler angles (φ, θ) as (Entcheve and Lagoudas, 2002):

$$\boldsymbol{Q} = \begin{bmatrix} \sin\theta\cos\varphi & -\cos\theta\cos\varphi & \sin\varphi \\ \sin\theta\sin\varphi & -\cos\theta\sin\varphi & -\cos\varphi \\ \cos\theta & \sin\theta & 0 \end{bmatrix}.$$

(3.5)

For the CNT–polymer composite with an initial volume fraction f_{CNT} of hollow CNTs before stretching, the homogenization of the solid filler from the CNT with the consideration of the interphase results in the change of the filler volume fraction, i.e., the volume fraction of the effective solid fillers is re-defined as (Yan $et\ al.$, 2007; Seidel and Lagoudas, 2009):

$$f_{eff} = \frac{(r_c + t)^2 (L + 2t)}{r_c^2 L} f_{CNT}.$$ (3.6)

From the above analysis, it is obvious that the properties of the interphase, i.e., the electrical conductivity (σ_{Int}) and the thickness (t), must be defined for determining the electrical conductivity tensor and the volume fraction of the effective solid filler. Since the electrical behavior of the CNT–polymer composite is governed by both the electron hopping and the conductive networks, it is naturally believed that the interphase properties are correlated to these two conductivity mechanisms. When the CNT concentration is small, CNTs are more independent rather than electrically connected to each other with electron hopping dominating the conductivity. However, when CNT concentration reaches a critical value f_c, i.e., the percolation threshold, the formation of conductive networks starts. According to existing experiments and simulations (Li $et\ al.$, 2007; Allaoui $et\ al.$, 2008; Takeda $et\ al.$, 2011), the upper limit of the critical separation distance between adjacent CNTs for the formation of conductive networks is suggested as $d_c = 1.8$ nm, which is the maximum possible thickness of the separating medium between adjacent CNTs allowing the tunneling penetration of electrons. Obviously, such a separation distance varies with the CNT concentration, which was suggested by some studies (Allaoui $et\ al.$, 2007; Deng and Zheng, 2008; Takeda $et\ al.$, 2011) to follow a power law relation after percolation. Accordingly, in our previous work (Feng and Jiang, 2013), the separation distance between the adjacent CNTs in the conductive networks was defined as:

$$d_a = \left(\frac{f_c}{f_{CNT}} \right)^{1/3} d_c.$$ (3.7)

In contrast, when the CNT concentration is under the threshold, the separation distance between adjacent CNTs should be larger than d_c. Under this situation, CNTs are more independent without the formation of conductive networks. Due to the difficulty of estimating the average separation distance between independent CNTs before the percolation, the separation distance was assumed as a constant, i.e., $d_a = d_c$ (Feng and Jiang, 2013). The thickness of the interphase for each CNT was taken as half of the separation distance between the adjacent CNTs, i.e., $t = d_a/2$ (Feng and Jiang, 2013).

As discussed above, the electrical conductance between adjacent CNTs is governed by the tunneling penetration of electrons. Accounting for such electrical tunneling effect, Simmons (1963) has derived a formula for the tunneling-type resistance for the separation interphase between CNTs, i.e., $R_{\mathrm{Int}}(d_a) = \dfrac{d_a \hbar^2}{ae^2(2m\lambda)^{1/2}} \exp\left(\dfrac{4\pi d_a}{\hbar}(2m\lambda)^{1/2}\right)$.

Accordingly, the electrical conductivity of the interphase was derived by the tunneling-type contact resistance R_{Int} as (Takeda *et al*., 2011):

$$\sigma_{\mathrm{Int}} = \frac{d_a}{aR_{\mathrm{Int}}(d_a)} \qquad (3.8)$$

$\lambda = 5.0$ eV is the potential barrier height for CNTs dispersed in most polymers (Celzard *et al*., 1996; Takeda *et al*., 2011); $m = 9.10938291\times10^{-31}$ kg and $e = -1.602176565\times10^{-19}$ C are mass and electric charge of an electron, respectively; a is the contact area of CNTs and $\hbar = 6.626068\times10^{-34}$ m^2 kg/s is the Planck constant.

As argued by Deng and Zheng (2008), before percolation, i.e., $f_{\mathrm{CNT}} < f_c$, no CNTs are percolated and only electron hopping is believed to contribute to the overall electrical conductivity of the composites. However, once the percolation starts, i.e., $f_{\mathrm{CNT}} > f_c$, both electron hopping and conductive networks contribute to the conductivity. In literature, there were several approximations on this critical concentration (percolation threshold) of conductive CNTs. In order to consider the stretching induced CNT re-orientation effect on the percolation threshold or the formation of conducting networks, the excluded volume method (Balberg *et al*., 1984; Shiraishi and Ata, 2001; Tallman and Wang, 2013),

which accounts for fillers' orientation through an averaging expression in terms of the angles between fillers, is adopted in the current work in which the percolation threshold was defined as:

$$f_c = 1 - \exp\left(\frac{-\langle V_{ex} \rangle V_{CNT}}{\langle V_e \rangle} \right), \tag{3.9}$$

where $\langle V_e \rangle = \frac{4\pi}{3} D^3 + 2\pi D^2 L + 2 \cdot D \cdot L^2 \langle \sin\gamma \rangle_\mu$ is the average excluded volume of CNT with D being the diameter of the CNT, $\langle V_{ex} \rangle$ is a dimensionless parameter denoting the total average excluded volume of CNT, which particularly equals 1.4 and 2.8 for randomly oriented CNTs and perfectly aligned CNTs, respectively; V_{CNT} is the volume of the spherocylinder CNT. The term $\langle \sin\gamma \rangle_\mu$ in the expression of $\langle V_e \rangle$ is an averaging term accounting for the filler orientation, with γ being the angle between the ith and the jth CNTs. The detailed interpretation of the parameters in Eq. (3.9) will be discussed later. Obviously, with CNT concentration increasing from f_c to 1, the percentage of the percolated CNTs, ξ, will change from 0 to 1. Deng and Zheng (2008) estimated this percentage of percolated CNTs as:

$$\xi = \frac{f_{CNT}^{1/3} - f_c^{1/3}}{1 - f_c^{1/3}}, \quad \left(f_c \leq f_{CNT} < 1 \right). \tag{3.10}$$

According to the percolation process with the involvement of both the electron hopping and conductive networking, a mixed form of micromechanics model was developed in our previous work (Feng and Jiang, 2013) to determine the overall electrical conductivity of CNT–polymer composites, which was modified from the general formulation (3.1) as:

$$\boldsymbol{\sigma}_{\text{eff}} = \begin{cases} \boldsymbol{\sigma}_{\text{m}} + \dfrac{\int_0^{2\pi}\int_0^{\pi}\left\{f_{\text{eff}}\left(\boldsymbol{\sigma}_{\text{EH}} - \boldsymbol{\sigma}_{\text{m}}\right)\boldsymbol{A}_{\text{EH}}\right\}\rho(\varphi,\theta)\sin\theta \,\mathrm{d}\theta \,\mathrm{d}\varphi}{\int_0^{2\pi}\int_0^{\pi}\rho(\varphi,\theta)\sin\theta \,\mathrm{d}\theta \,\mathrm{d}\varphi}, \quad f_{\text{CNT}} < f_{\text{c}} \\[2em] \boldsymbol{\sigma}_{\text{m}} + \left(1-\xi\right)\dfrac{\int_0^{2\pi}\int_0^{\pi}\left\{f_{\text{eff}}\left(\boldsymbol{\sigma}_{\text{EH}} - \boldsymbol{\sigma}_{\text{m}}\right)\boldsymbol{A}_{\text{EH}}\right\}\rho(\varphi,\theta)\sin\theta \,\mathrm{d}\theta \,\mathrm{d}\varphi}{\int_0^{2\pi}\int_0^{\pi}\rho(\varphi,\theta)\sin\theta \,\mathrm{d}\theta \,\mathrm{d}\varphi} \\[2em] \quad + \xi\dfrac{\int_0^{2\pi}\int_0^{\pi}\left\{f_{\text{eff}}\left(\boldsymbol{\sigma}_{\text{CN}} - \boldsymbol{\sigma}_{\text{m}}\right)\boldsymbol{A}_{\text{CN}}\right\}\rho(\varphi,\theta)\sin\theta \,\mathrm{d}\theta \,\mathrm{d}\varphi}{\int_0^{2\pi}\int_0^{\pi}\rho(\varphi,\theta)\sin\theta \,\mathrm{d}\theta \,\mathrm{d}\varphi}, \quad f_{\text{CNT}} \geq f_{\text{c}} \end{cases} \quad (3.11)$$

where the subscripts "EH" and "CN" denote the terms that are associated with electron hopping and conductive networking, respectively.

3.3   Uni-axial stretching induced changes

As discussed in the introduction of this paper, a mechanical stretching may induce volume expansion of the composites, re-orientation of CNTs and change in conductive networks. Accordingly, certain parameters in Eq. (3.11) should be re-defined, for example, the volume fraction f, Euler angles φ and θ, the orientation distribution function $\rho(\varphi,\theta)$, the percolation threshold, the electrical conductivity tensors $\boldsymbol{\sigma}_{\text{EH}}$ and $\boldsymbol{\sigma}_{\text{CN}}$ in the global coordinate system, and the electric field concentration tensors $\boldsymbol{A}_{\text{EH}}$ and $\boldsymbol{A}_{\text{CN}}$. In the following, the three stretching induced changes are investigated and incorporated into the micromechanics model.

3.3.1   Volume expansion and re-orientation of CNTs

Following the fiber re-orientation model in literature (Kuhn and Grün, 1942; Taya *et al.*, 1998), a cell containing an effective solid filler before and after uni-axial stretching as shown in Figure 3.3 is used here to describe the change of volume expansion and re-orientation of CNTs. The original lengths of the cell in the X_1, X_2 and X_3 directions are h_0, w_0 and l_0, respectively. With any stretching strain ε in the X_3 direction, the lengths of the cell after stretching can be determined by the following general formula:
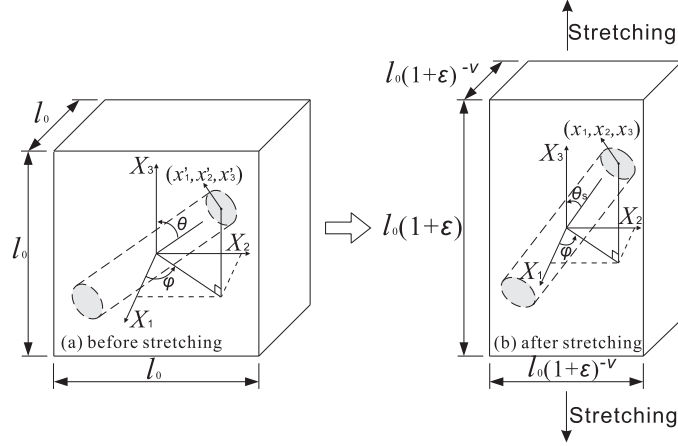
Figure 3.3 Orientation description of a conductive filler in a cell (a) before stretching; (b) after stretching.

$$l = l_0 \left(1 + \varepsilon\right), \ w = w_0 \left(1 + \varepsilon\right)^{-v} \text{ and } h = h_0 \left(1 + \varepsilon\right)^{-v}, \tag{3.12}$$

where v is the Poisson's ratio of the composite. For small deformation, the width and height of the cell defined in Eq. (3.12) can be reduced to $w = w_0(1-v\varepsilon)$ and $h = h_0(1-v\varepsilon)$, respectively. Due to the much larger stiffness of CNTs in comparison to the polymer, the deformation of the composite is mainly sustained by the polymer. Therefore, the volume fraction of the effective solid fillers after the uni-axial stretching can be approximately estimated by neglecting the volume change of the CNTs, i.e.,

$$f_{\text{update}} = \frac{V_0 f_{\text{eff}}}{V} = \frac{f_{\text{eff}}}{\left(1 + \varepsilon\right)^{1-2v}}, \tag{3.13}$$

where V_0 and V are the volumes of the cell in Figure 3.3 before and after stretching, respectively. Particularly, there is no change for the CNT volume fraction after stretching if the composite is incompressible, i.e., $v = 0.5$.

In addition to the volume expansion, after stretching the filler in the cell as shown in Figure 3.3 also tends to re-align along the stretching direction, which results in the decrease of the polar angle from θ to θ_s. However, the change of the azimuth angle, φ, can be neglected for this uni-axial stretching condition (Kuhn and Grün, 1942). After the

stretching of strain ε along the X_3 direction, the new polar angle θ_s can be found in terms of the initial polar angle θ as (Kuhn and Grün, 1942):

$$\tan\theta_s = \left(1+\varepsilon\right)^{-(1+\nu)} \cdot \tan\theta .\tag{3.14}$$

Such a variation of the polar angle will change the orientation distribution function (ODF) from $\rho(\varphi, \theta)$ to $\rho(\varphi, \theta_s)$. It should be mentioned that the ODF which describes the orientation distribution of fillers, always satisfies the following conditions (Perez *et al.*, 2008; Vangurp, 1995):

$$\rho(\varphi,\theta)\geq 0 \text{ and } \frac{1}{4\pi}\int_0^{2\pi}\int_0^{\pi}\rho(\varphi,\theta)\sin\theta\,\mathrm{d}\theta\,\mathrm{d}\varphi = 1 .\tag{3.15}$$

Before stretching, CNTs are assumed as uniformly distributed in the polymer matrix. Thus, the ODF is a constant, exhibiting a uniform distribution of CNTs along any orientation. However, after stretching, the decrease of the polar angle θ of any individual filler means that these fillers are no longer randomly distributed and tend to be more aligned along the stretching direction. In order to determine this new ODF, it is assumed that there are G fillers distributed in the RVE of the micromechanics model. Following Eq. (3.15), the total number of fillers falling in the ranges of $(\theta, \theta+\mathrm{d}\theta)$ and $(\varphi, \varphi+\mathrm{d}\varphi)$ in the RVE can be determined as (Kuhn and Grün, 1942):

$$\mathrm{d}N_{\substack{\theta,\theta+\mathrm{d}\theta \\ \varphi,\varphi+\mathrm{d}\varphi}} = \frac{1}{4\pi}G\rho(\varphi,\theta)\sin\theta\,\mathrm{d}\theta\,\mathrm{d}\varphi .\tag{3.16}$$

These fillers will be re-oriented within the ranges of $(\theta_s, \theta_s+\mathrm{d}\theta_s)$ and $(\varphi, \varphi+\mathrm{d}\varphi)$ after a stretching, i.e.,

$$\mathrm{d}N_{\substack{\theta_s,\theta_s+\mathrm{d}\theta_s \\ \varphi,\varphi+\mathrm{d}\varphi}} = \frac{1}{4\pi}G\rho(\varphi,\theta_s)\sin\theta_s\,\mathrm{d}\theta_s\,\mathrm{d}\varphi = \mathrm{d}N_{\substack{\theta,\theta+\mathrm{d}\theta \\ \varphi,\varphi+\mathrm{d}\varphi}} .\tag{3.17}$$

Substituting Eq. (3.14) into Eq. (3.17), the ODF $\rho(\varphi, \theta_s)$ after stretching is determined as:

$$\rho(\varphi,\theta_s) = \frac{(1+\varepsilon)^{\frac{1+\nu}{2}}}{\left[(1+\varepsilon)^{-(1+\nu)}\cos^2\theta_s + (1+\varepsilon)^{1+\nu}\sin^2\theta_s\right]^{3/2}} \qquad (3.18)$$

Without stretching, i.e., $\varepsilon = 0$, the ODF ρ (φ, θ_s) is reduced to unity for a random distribution as expected. Figure 3.4 demonstrates an example of the variation of the ODF with the strain and the polar angle θ_s. From Figure 3.4 (a), it is observed that with the increase of strain, more conductive fillers tend to be re-aligned along the stretching direction ($\theta_s = 0°$ and $180°$). Figure 3.4(b) suggests that stretching has a more significant effect on the re-alignment of the conductive fillers for the composites with larger Poisson's ratio than that with smaller Poisson's ratio, i.e., with the increase of Poisson's ratio, more CNTs tend to be re-aligned along the stretching direction. Here it should be noted that due to the re-alignment of the CNTs, the Poisson's ratio of the composite is theoretically dependent on the ODF instead of a fixed value. However, according to the evaluation in (Pan, 1996) the variation of the Poisson's ratio due to the re-orientation of fillers can be neglected. From the derived formula in that work, it is calculated that for a CNT composite with volume fraction of 3%, $\nu = 0.46$ for a random CNT distribution while $\nu \approx 0.45$ for a perfectly aligned distribution. Therefore, in the current work the dependency of the Poisson's ratio on the re-orientation of the fillers due to the stretching is neglected and the value of Poisson's ratio is taken as constant regardless of strain.
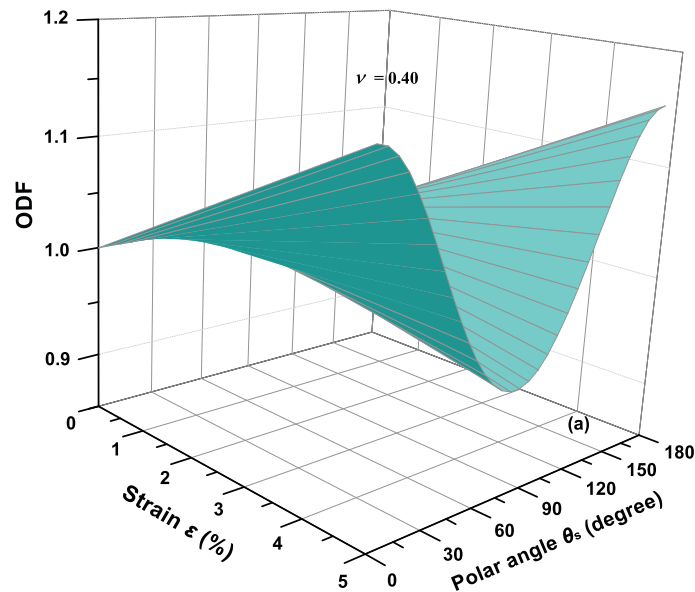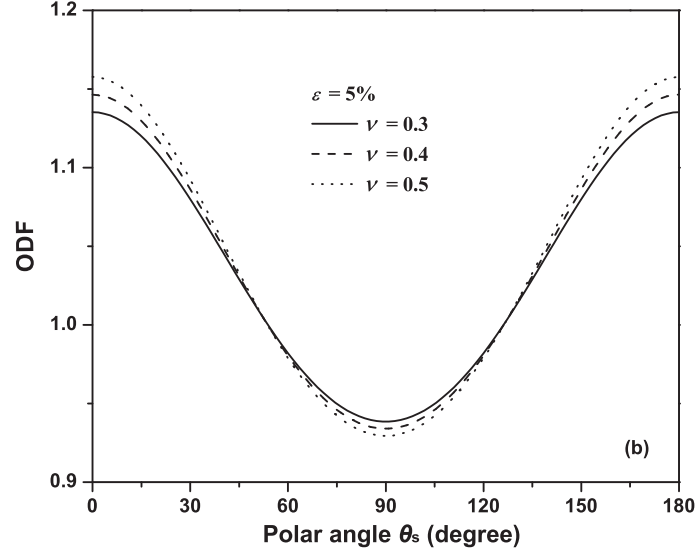
Figure 3.4 Variation of ODF with strain and polar angle θ_s (a) $v = 0.4$; (b) $\varepsilon = 5\%$.

3.3.2 Change in conductive networks

In addition to composite volume expansion and CNT re-orientation, stretching also induces change in the conductive networks, i.e., stretching can induce an increase in the percolation threshold (Tallman and Wang, 2013). As demonstrated in Figure 3.1, the orientation of the CNT is identified by the orientation angles φ and θ. The azimuth angle φ ranges from 0 to 2π while the polar angle ranges from 0 to π for the composites with random CNT distribution. As discussed before, CNTs re-align in a manner which favors the direction of the uni-axial stretching. As a result, the randomness of the CNT distribution decreases with the increase of the stretching strain. Such an assumption on the randomness of the distribution of CNTs can be verified from Figure 3.4, i.e., with the increase of the stretching strain, CNTs tend to more re-align along the X_3 direction. It was understood from (Tallman and Wang, 2013) that more CNTs would concentrate within the range of $[0, \theta_\mu]$ and $[\pi-\theta_\mu, \pi]$ in which θ_μ was related to the strain as $\theta_\mu = \arcsin[(1+\varepsilon)^{-1-v}]$ to represent the randomness of the distribution of the CNTs. According to the fitting from Monte Carlo simulation in (Tallman and Wang, 2013), the term $\langle \sin\gamma \rangle_\mu$ in Eq. (3.9), which accounts for the CNTs' orientation, can be related to θ_μ as:

$$\langle \sin\gamma \rangle_\mu = 0.018\theta_\mu^5 + 0.021\theta_\mu^4 - 0.234\theta_\mu^3 - 0.015\theta_\mu^2 + 0.909\theta_\mu. \tag{3.19}$$

In addition, Tallman and Wang (2013) also proposed a linear relation between $\langle V_{\mathrm{ex}} \rangle$ in Eq. (3.9) and $\langle \sin \gamma \rangle_{\mu}$ as:

$$\langle V_{\mathrm{ex}} \rangle = 2.8 - 5.6 \frac{\langle \sin \gamma \rangle_{\mu}}{\pi}. \tag{3.20}$$

Then with the consideration of the stretching effect the percolation threshold defined in Eq. (3.9) is modified and simplified as:

$$f_{\mathrm{c}} = 1 - \exp\left[-\frac{\left(2.1\pi - 4.2\langle \sin \gamma \rangle_{\mu}\right)p}{4\pi + 6\pi p + 6p^{2}\langle \sin \gamma \rangle_{\mu}} \right], \tag{3.21}$$

where $p = L/D$ is the aspect ratio of the CNTs. It should be noted here that due to the variation of the percolation threshold, the separation distance defined in equation (3.7) changes with the stretching strain, which would result in significant variation of the contact conductivity of the interphase due to its exponential dependency on the separation distance. In addition, the percentage of the percolated CNTs defined in Eq. (3.10) varies with the stretching strain due to the variation of the percolation threshold. Figure 3.5 plots the variations of the normalized percentage $\xi_{\mathrm{N}} = \xi_{\mathrm{s}}/\xi_{0}$ of the percolated CNTs for a composite with the stretching strain for different CNT volume fractions and Poisson's ratios, where ξ_{0} and ξ_{s} denote the percentages of the percolated CNTs before and after stretching, respectively. From Figure 3.5(a), it is found that the percentage of the percolated CNTs decreases with the increase of the stretching strain. It is also indicated that the percentage of the percolated CNTs is more sensitive to the stretching for the composites with lower volume fraction. Figure 3.5(b) informs us that the stretching induced re-alignment of CNTs with larger Poisson's ratio decreases the percentage of the percolated CNTs more significantly than that with smaller Poisson's ratio. It should be noted that in addition to the reduced percentage of percolated CNTs, the separation distance defined in Eq. (3.7) also varies with the strain, resulting in the change of interphase thickness and conductivity.
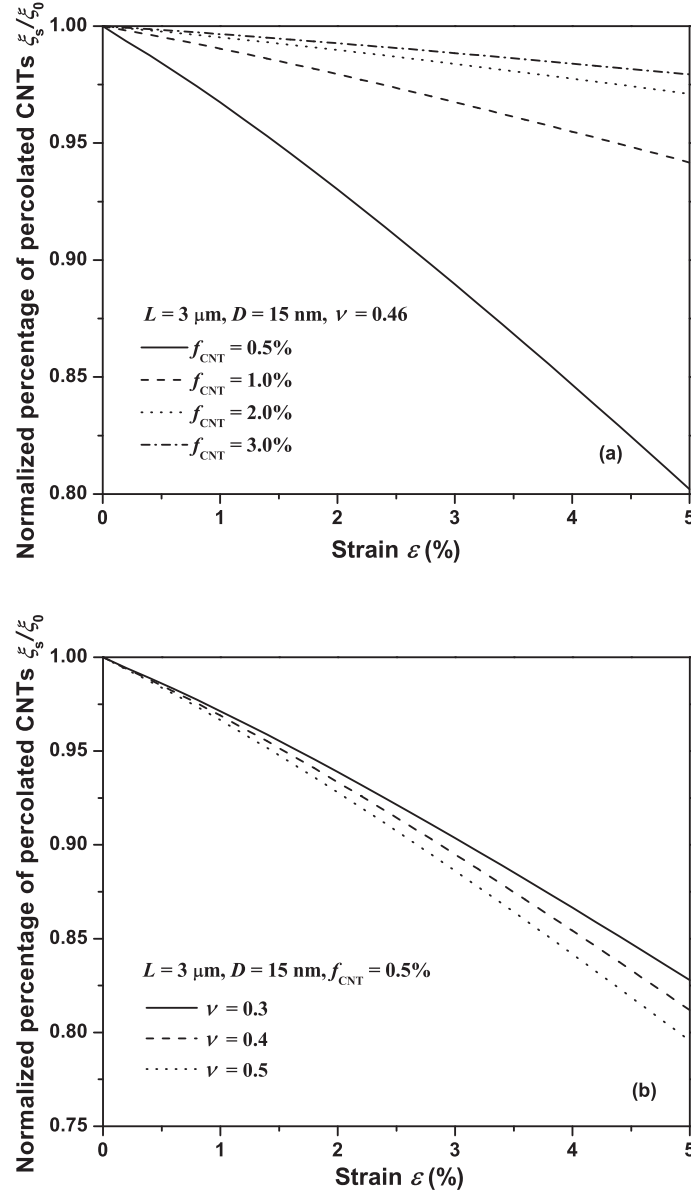
Figure 3.5 Variation of normalized percentage of percolated CNTs with strain (a) $v = 0.46$; (b) $f_{CNT} = 0.5\%$.

In the current work, the Mori-Tanaka method (Taya, 2005; Mori and Tanaka, 1973), which accounts for interactions between dispersed inhomogeneities, is chosen as the micromechanics model. Accounting for the effect of the stretching, the electric field concentration tensor A in Eq. (3.1) is defined as (Taya, 1995; Entchev and Lagoudas, 2002; Odegard *et al.*, 2003):

$$A = QA^{\text{dil}}Q^{\text{T}} \left\{ (1 - f_{\text{update}})\delta + f_{\text{update}} \frac{\int_0^{2\pi}\int_0^{\pi} f_{\text{update}}\left\{QA^{\text{dil}}Q^{\text{T}}\right\}\rho(\varphi,\theta_s)\sin\theta_s \mathrm{d}\theta_s \mathrm{d}\varphi}{\int_0^{2\pi}\int_0^{\pi}\rho(\varphi,\theta_s)\sin\theta_s \mathrm{d}\theta_s \mathrm{d}\varphi} \right\}^{-1}, \qquad (3.22)$$

where the transformation matrix Q is determined by replacing θ with θ_s and A^{dil} is defined as:

$$A^{\text{dil}} = \left\{\delta + S\left(\sigma_{\text{m}}\right)^{-1}\left(\tilde{\sigma} - \sigma_{\text{m}}\right)\right\}^{-1} \qquad (3.23)$$

with δ being the Kronecker delta tensor. S is the Eshelby tensor of the effective filler, which is given by:

$$S = \begin{bmatrix} S_{11} & 0 & 0 \\ 0 & S_{22} & 0 \\ 0 & 0 & S_{33} \end{bmatrix}, \qquad (3.24)$$

where

$$S_{22} = S_{33} = \frac{A_{\text{re}}}{2\left(A_{\text{re}}^2 - 1\right)^{3/2}}\left[A_{\text{re}}\left(A_{\text{re}}^2 - 1\right)^{1/2} - \cosh^{-1}A_{\text{re}}\right] \qquad (3.25)$$

with A_{re} being the aspect ratio of the effective filler, i.e., $A_{\text{re}} = (L+2t)/(D+2t)$, and $S_{11} = 1 - 2S_{22}$. When conductive networks are formed, several CNTs will be electrically connected to each other while not in physical contact due to van der Waals forces between CNTs. Thus, the effective aspect ratio of the formed networks can be taken as infinite due to the large aspect ratio of CNTs. However, quantities associated with the electron hopping correspond to the real effective filler aspect ratio as defined. Correspondingly, A_{EH} and A_{CN} in Eq. (3.11) can be determined from Eq. (3.22) by using different aspect ratios for CNTs. In the following Section, the mixed micromechanics model with the consideration of the uni-axial stretching effects will be employed to predict the effective electrical conductivity of a CNT–polymer nanocomposite through case study.

3.4 Results and discussion

To study the uni-axial stretching effects on the electrical conductivity of the CNT–polymer composites, a MWCNT/PEO (Polyethylene Oxide) composite under stretching in (Park and Kim, 2006; Park *et al*., 2008) is chosen as the example material. The length and diameter of the CNTs range from 1μm to 5μm and 10 nm to 20 nm, respectively. For the purpose of theoretically predicting the electrical conductivity of stretched composites in our simulation, the length and the diameter of the CNTs are taken as constants, i.e., $L = 3$ μm and $D = 15$ nm, respectively. According to the mechanical and physical properties of PEO, the Poisson's ratio and the electrical conductivity of the PEO are approximately set as $v = 0.46$ and $\sigma_m = 1 \times 10^{-13}$ S/m, respectively. While the electrical conductivity of the MWCNTs was not provided in this reference, other references suggest $\sigma_{CNT} = 100$ S/m as the effective conductivity of the MWCNTs (Deng and Zheng, 2008; Feng and Jiang, 2013). In the experiment of (Park and Kim, 2006; Park *et al*., 2008), MWCNTs were surface functionalized and well dispersed in the PEO matrix by stirring and sonication before stretching. Then the MWCNT/PEO composite strip was bonded to a gage section and stretched using a uni-axial test machine. A laser extensometer and a precision multimeter were used simultaneously to record strain and resistance of the composite. Two representative CNT volume fractions, 0.56% (near the percolation threshold before stretching) and 1.44% (away from the percolation threshold before stretching), were tested to investigate the stretching effect on the electrical resistance of the MWCNT/PEO composites. In order to compare the analytical predictions with the experimental results, the relative resistance change of the composite is expressed in terms of the stretching and the electrical conductivity of the composite as:

$$\frac{\Delta R}{R_0} = \frac{\sigma_{eff}^0}{\sigma_{eff}^L}\left(1+\varepsilon\right)^{1+2v} - 1 , \tag{3.26}$$

where σ_{eff}^0 and σ_{eff}^L are electrical conductivities of the composite before and after stretching in the stretching direction, respectively. Figure 3.6 shows the comparison between the analytical results and experimental results for the MWCNT/PEO composite. It is observed that the analytical prediction successfully predicts better the trend of the

experimental result for the composite with higher volume fraction (f_{CNT} = 1.44%) and the variation trend of the resistance change is captured by the current model. However, a large discrepancy between the analytical prediction and the experimental results still exists which may be attributed to the assumption on the electrical conductivity of CNTs, the fixed length and diameter of the CNTs, etc. For the composite with lower volume fraction (f_{CNT} = 0.56%), the sharp increase of the resistance change corresponding to a percolation behavior is not captured by the current model, which could be explained by the adoption of the excluded volume method for predicting the percolation threshold in Eq. (3.21). It is found that with the considered range of the strain, the change of the percolation threshold is negligible, which is always below 0.56% and thus no percolation is observed after stretching. Such a small change in the percolation threshold due to the stretching is also evidenced by the Monte Carlo simulation by Lin *et al.* (2010). However, it should be mentioned that the stretching effect on the percentage of the percolated CNTs is more significant for the composites with smaller volume fraction (see Figure 3.5(a)), which means that the stretching may significantly change the overall electrical conductivity of the composites. Due to the above mentioned limitation of the current model, this work can be claimed to provide a theoretical prediction on the trend of the stretching effect upon the electrical conductivity of the CNT-polymer composites. A more accurate model with the assistance of statistics on the distribution of the CNT size needs to be further pursued.
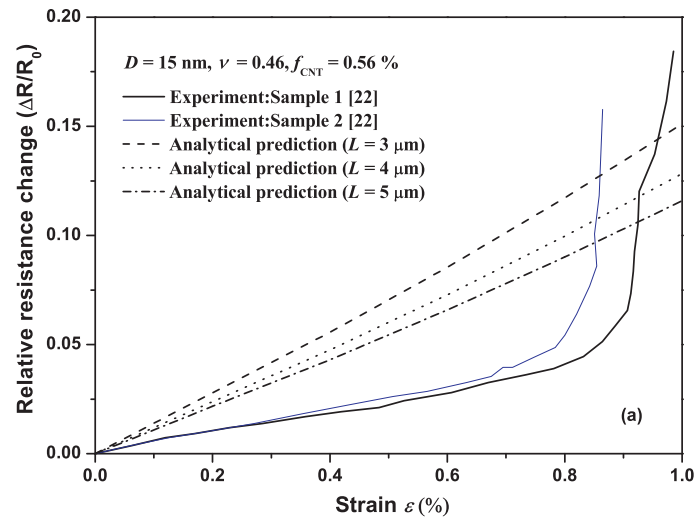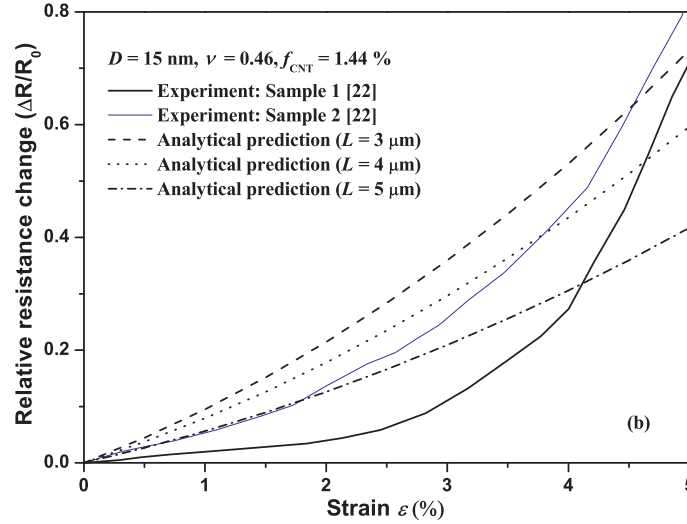
Figure 3.6 Comparisons between experimental results and analytical predictions (a) f_{CNT} = 0.56% ; (b) f_{CNT} = 1.44%.

From equations (3.7) and (3.8), it can be seen that the tunneling-type electrical conductivity of the interphase highly denpends on the critical separation distance d_c, which was suggested by Monte Carlo simulation and experiments (Li *et al*., 2007; Allaoui *et al*., Takeda *et al*., 2011) that this critical separation distance might vary within a small range. In order to see the sensitivity of the overall electrical conductivity on the value of the critical separation distance, Figure 3.7 plots the variation of the electrical conductivity of the composite with the CNT volume fraction for different critical separation distances when the composite is under no stretching. From this figure, it can be seen that for the composite with lower CNT volume fraction, the electrical conductivity is very sensitive to the critical separtion distance, i.e., the increase of the critical separation distance significantly decreases the electrical conductivity. Such high sensitivity of the electrical conductivity to the critical separation distance may partly explain the large discrepancy between the modeling results and the experimental results for lower CNT volume fraction (f_{CNT} = 0.56%). However, the sensitivity decreases as the CNT volume fraction increases.
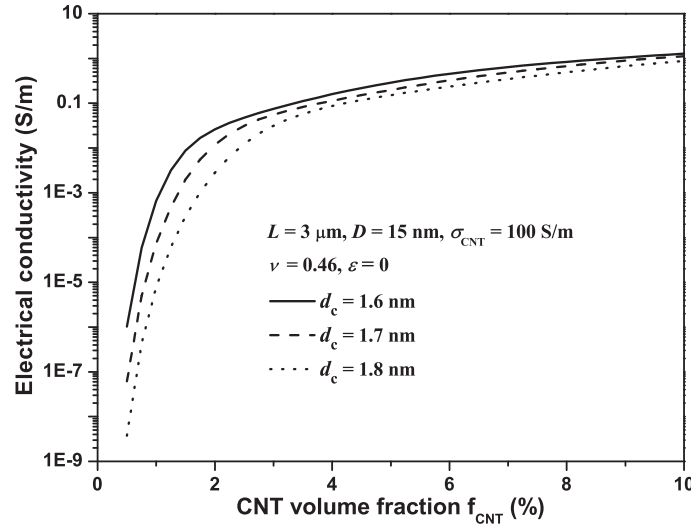
Figure 3.7 Variation of electrical conductivity with CNT volume fraction for different critical separtion distances.

Variation of the electrical conductivity with the CNT volume fraction for different stretching strains is plotted in Figure 3.8. It is observed that the electrical conductivity of the composite in both the longitudinal (along the stretching direction) and the transverse (perpendicular to the stretching direction) directions increases with the increase of CNT volume fractions as expected. In addition, for the composite with a fixed volume fraction of CNTs, stretching decreases the electrical conductivity in both the longitudinal and the transverse directions. Such a decrease can be attributed to the volume expansion and the conductive network change, i.e., increased percolation threshold due to the stretching.

The chart shows:
- Y-axis: Transverse conductivity σ_{eff}^{T} (S/m), values 1, 0.01, 1E-4, 1E-6, 1E-8
- X-axis: CNT volume fraction f_{CNT} (%), values 0, 2, 4, 6, 8, 10
- $L = 3\ \mu m$, $D = 15\ nm$, $\sigma_{CNT} = 100\ S/m$
- $d_c = 1.8\ nm$, $\nu = 0.46$
- —— $\varepsilon = 0$
- - - - $\varepsilon = 5.0\%$
- (b)
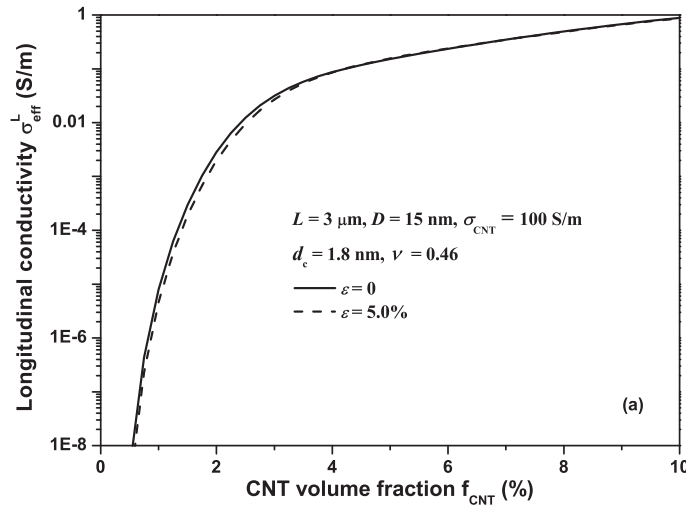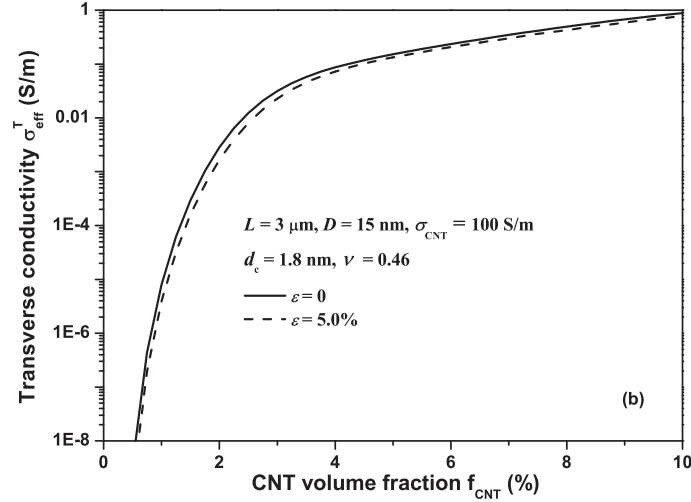
Figure 3.8 Variation of electrical conductivity with CNT volume fraction for different strains (a) Longitudinal direction; (b) Transverse direction.

Figure 3.9 shows the variation of the normalized electrical conductivity $\sigma_N = \sigma_{eff} / \sigma_{eff}^{0}$ with the stretching strain for different CNT volume fractions, where the quantities with the superscript "0" denotes the ones before stretching. It is again demonstrated in this figure that the stretching decreases the electrical conductivity and the stretching effect on the electrical conductivity along both directions is more significant for the composite with lower CNT concentration. This phenomenon can be interpreted by the effect of CNT volume fraction on the normalized percentage of the percolated CNTs (see Figure 3.5(a)), which was also commented by Jiang *et al.* (2007), i.e., for composites with lower filler concentration above the percolation threshold, only a few conductive networks are formed, so any small change in the networks, i.e., the separation distance between CNTs and re-alignment of CNTs, affects the magnitude of the electrical conductivity significantly. In contrast, a large number of conductive networks exist in the composites with higher filler concentration, for which any change in the networks has relatively limited effects on the electrical properties of the composites. The results in this figure suggest that the sensitivity of the electrical conductivity on stretching depends on the CNT volume fraction of the composites.

Figure 3.9 Variation of normalized electrical conductivity with strain for different CNT volume fractions (a) Longitudinal direction; (b) Transverse direction.

As indicated in the previous formulation and Figure 3.4(b), stretching effects also depend on the Poisson's ratio. In order to see the Poisson's ratio effect from a theoretical prediction perspective, the variation of the normalized electrical conductivity along the longitudinal and the transverse directions with the strain is plotted in Figure 3.10 for the composite with a fixed initial CNT volume fraction ($f_{CNT} = 2\%$) but different Poisson's ratios. It is observed that the normalized electrical conductivity decreases with the increase of the strain and the decreasing rate is enhanced by the increase of the Poisson's

ratio. Such an enhancement of the decreasing rate can be explained by the combined effects of the Poisson's ratio on the electrical conductivity. For example, from Eq. (3.13) it is easily understood that with the increase of the Poisson's ratio volume expansion induced decrease in the electrical conductivity becomes more and more limited. From Figure 3.4(b), it is indicated that the increase of the Poisson's ratio enables CNTs to be more aligned along the stretching direction, which increases the electrical conductivity in the longitudinal direction while decreases the electrical conductivity in the transverse direction when the change in conductive networks is not taken into account. However, Eqs. (3.19)–(3.21) with the expression of θ_μ remind us that the re-alignment of the CNTs in the composites with larger Poisson's ratio would always lead to a more significant increase in the percolation threshold and a decrease in the percentage of the percolated CNT (see Figure 3.5(b)), which could result in a more significant decrease in the electrical conductivity along the two directions. The observation of the combined effects of Poisson's ratio on the overall electrical conductivity of the composites suggests that the conductive network change dominates the variation of electrical conductivity during the stretching over the re-alignment of the CNTs along the stretching direction.
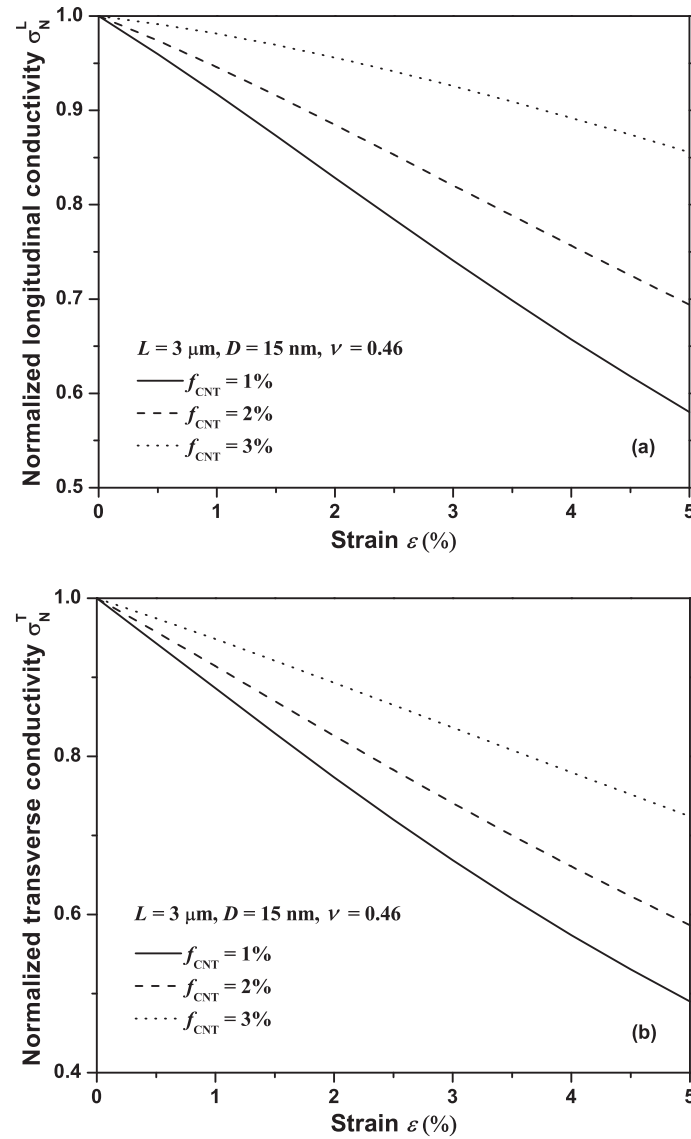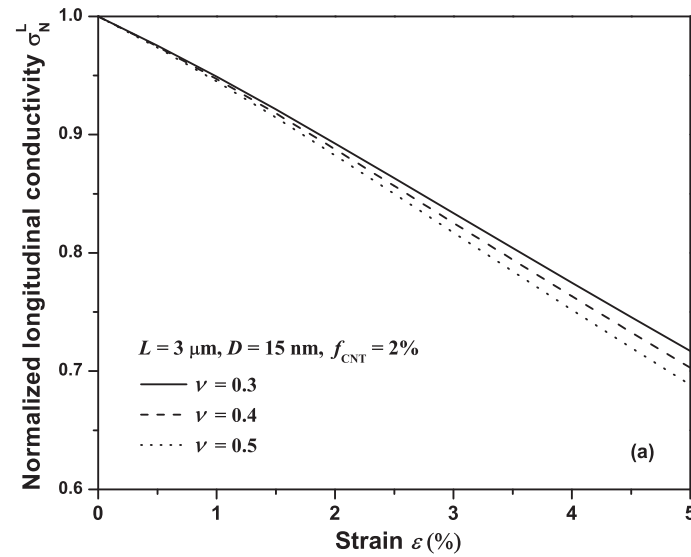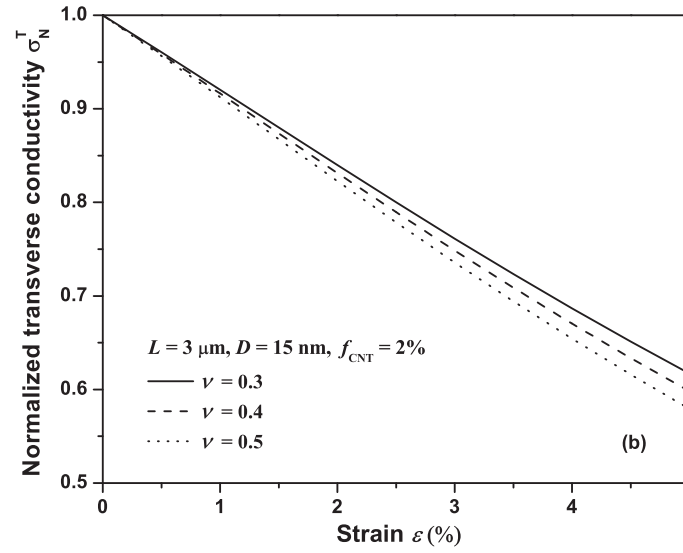
Figure 3.10 Variation of normalized electrical conductivity with strain for different Poisson's ratios (a) Longitudinal direction; (b) Transverse direction.

Another appromixmation made in the current work is to fix the electrical conductivity of the CNTs in the simulation. However, it was suggested that the electrical conductivity of MWCNTs might vary within a big range (Deng and Zheng, 2008), i.e., from 10 S/m to 10000 S/m. Here we also test the sensitivity of the overall electrical conductivity of the composite to the electrical conductivity of the the CNTs in figure 11. From this figure, it can be seen that the electrical conductivity of the composite decreases more significantly with the stretching strain for CNTs with larger electrical conductivity. However, for the CNTs with sufficient large electrical conducitivy, $\sigma_{CNT} = 100$ S/m in the previous simulation for example, the selection value of the electrical conductivity of the CNTs will have slight influence on predicting the stretching effect upon the overall electrical conductivity of the composite.
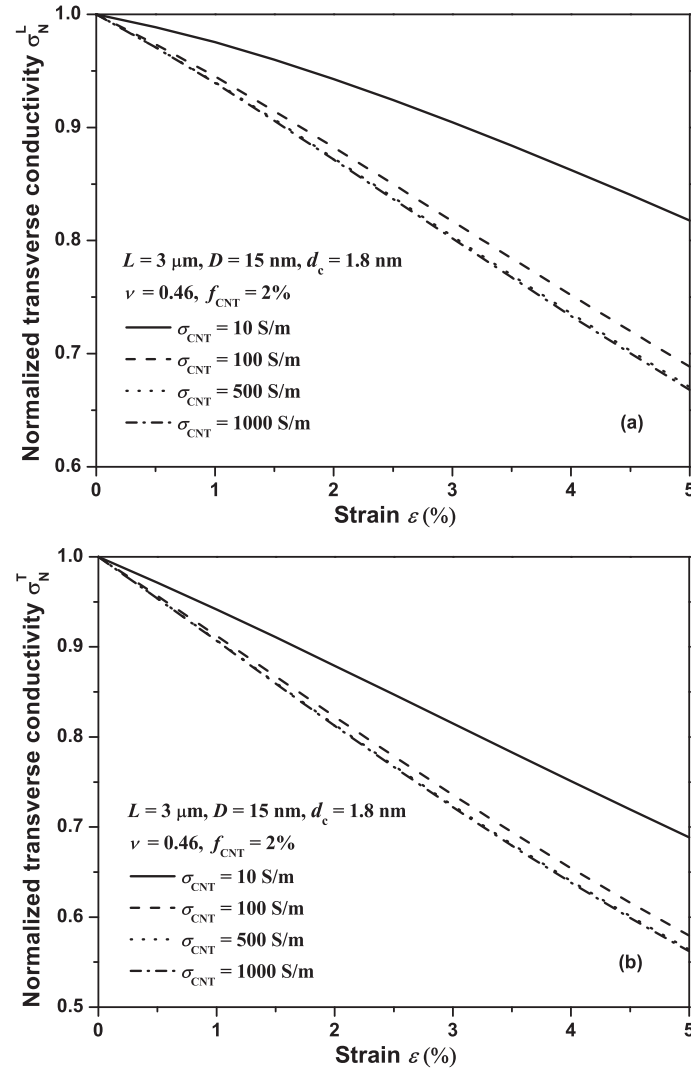
Figure 3.11 Variation of normalized electrical conductivity with strain for different electrical conductivity of CNTs (a) Longitudinal direction; (b) Transverse direction.

It should be mentioned that the modeling results in the current work could theoretically predict the stretching effects on the variation of the electrical conductivity of composites as reported in experiments to some extent (Park *et al*., 2008; Hu *et al*., 2010; Bao *et al*., 2011; Miao *et al*., 2011a, 2011b, 2012). However, the micromechanics model in the current work is based on small strain formulation. For certain CNT–polymer composites, such as CNT–rubber composites, which can undergo large deformation, linear kinematics assumed for micromechanics model with small deformation may be violated. In addition, the change of the azimuth angle φ and elongation of CNT length neglected in this paper

may become significant under large deformation. Therefore, a more comprehensive micromechanics model based on finite deformation formulation with the consideration of the change of all Euler angles and the elongation of CNTs needs to be developed to predict the stretching effects on the electrical properties of conductive polymer composites.

3.5 Conclusions

In the current work, three expected changes induced by a uni-axial stretching, volume expansion, re-orientation of CNTs and change in conductive networks, have been considered and incorporated into a mixed micromechanics model to predict the stretching effects upon the overall electrical conductivity of CNT–polymer composites. Modeling results show that stretching decreases the electrical conductivity in both the longitudinal and transverse directions. It is found that the electrical conductivity of the composites highly depends on the critical separation distance. Also it is shown that the electrical conductivity of the composites is more sensitive to the stretching for composites with lower CNT concentration and shorter CNTs. Simulation results also indicate that the stretching induced change in conductive networks plays a dominant role for the variation of the electrical conductivity along the stretching direction. To some extent, the developed model in the current work is envisaged to be helpful in qualitatively understanding the trend of the stretching effects on the overall electrical conductivity of CNT–polymer composites.

References

Allaoui, A., Hoa, S. V. and Pugh, M. D., 2008. The electronic transport properties and microstructure of carbon nanofiber/epoxy composites. Compos. Sci. Technol. **68**, 410–416.

Balberg, I., Anderson, C. H., Alexander, S. and Wagner, N., 1984. Excluded volume and its relation to the onset of percolation. Phys. Rev. B 30, 3933–3943.

Bao, S. P., Liang, G. D. and Tjong, S. C., 2011. Effect of mechanical stretching on electrical conductivity and positive temperature coefficient characteristics of

poly(vinylidene fluoride)/carbon nanofiber composites prepared by non-solvent precipitation. Carbon 49, 1758–1768.

Berson, S., de Bettignies, R., Bailly, S., Guillerez, S. and Jousselme, B., 2007. Elaboration of P3HT/CNT/PCBM composites for organic photovoltaic cells. Adv. Funct. Mater. 17, 3363–3370.

Chang, L., Friedrich, K., Ye, L. and Toro, P., 2009. Evaluation and visualization of the percolating networks in multi-wall carbon nanotube/epoxy composites. J. Mater. Sci. 44 4003–4012.

Celzard, A., McRae, E., Deleuze, C., Dufort, M., Furdin, G. and Mareche, J. F., 1996. Critical concentration in percolating systems containing a high-aspect-ratio filler Phys. Rev. B 53, 6209–6214.

Cheng, Q. F., Bao, J. W., Park, J., Liang, Z. Y., Zhang, C. and Wang, B., 2009. High mechanical performance composite conductor: multi-Walled carbon nanotube sheet/bismaleimide nanocomposites. Adv. Funct. Mater. 19, 3219–3225.

Dang, Z. M., Yao, S. H. And Xu, H. P., 2007. Effect of tensile strain on morphology and dielectric property in nanotube/polymer nanocomposites. Appl. Phys. Letter. **90**, 012907.

Das, N. C., Chaki, T. K. And Khastgir, D., 2002. Effect of axial stretching on electrical resistitivty of short carbon fibre and carbon black filled conductive rubber composites. Polym. Int. **51**, 156–163.

Deng, F. and Zheng, Q. S., 2008. An analytical model of effective electrical conductivity of carbon nanotube composites. Appl. Phys. Lett. 92, 071902.

Du, F. M., Fischer, J. E. and Winey, K. I., 2005. Effect of nanotube alignment on percolation conductivity in carbon nanotube/polymer composites. Phys. Rev. B 72, 121404.

Entchev, P. B. and Lagoudas, D. C., 2002. Modeling porous shape memory alloys using micromechanical averaging techniques. Mech. Mater. 34, 1–24.

Feng, C. and Jiang, L. Y., 2013. Micromechanics modeling of the electrical conductivity of carbon nanotube (CNT)–polymer nanocomposites. Compos. Pt. A-Appl. Sci. Manuf. 47, 143–149.

Gojny, F. H., Wichmann, M. H. G., Fiedler, B., Kinloch, I. A., Bauhofer, W., Windle, A. H. et al., 2006. Evaluation and identification of electrical and thermal conduction mechanisms in carbon nanotube/epoxy composites. Polymer 47, 2036–2045.

Hu, N., Karube, Y., Arai, M., Watanabe, T., Yan, C., Li, Y., et al., 2010. Investigation on sensitivity of a polymer/carbon nanotube composite strain sensor. Carbon 48, 680–687.

Jiang, M. J., Dang, Z. M. and Xu, H. P., 2007. Giant dielectric constant and resistance-pressure sensitivity in carbon nanotubes/rubber nanocomposites with low percolation threshold. Appl. Phys. Lett. 90, 042914.

Kim, Y. J., Shin, T. S., Choi, H. D., Kwon, J. H., Chung, Y. C. and Yoon, H. G., 2005. Electrical conductivity of chemically modified multiwalled carbon nanotube/epoxy composites. Carbon 43, 23–30.

Kuhn, W. and Grün, F., 1942. Beziehungen zwischen elastischen Konstanten und Dehnungsdoppelbrechung hochelastischer Stoffe. Colloid Polym. Sci. 101, 248–271.

Li, C. Y., Thostenson, E. T., and Chou, T. W., 2007. Dominant role of tunneling resistance in the electrical conductivity of carbon nanotube-based composites. Appl. Phys. Lett. 91, 223114.

Lin, C. A., Wang, H. T. and Yang, W., 2010. Variable percolation threshold of composites with fiber fillers under compression. J. Appl. Phys. 108, 013509.

Lu, W. B., Chou, T. W. and Thostenson, E. T., 2010. A three-dimensional model of electrical percolation thresholds in carbon nanotube-based composites. Appl. Phys. Lett. 96, 223106.

Miao, Y., Chen, L., Lin, Y. Z., Sammynaiken, R., Zhang, W. J., 2011. On finding of high piezoresistive response of CNT films without surfactants for in-plane strain detection. J. Intell. Mater. Syst. Struct. 22, 2155–2159.

Miao, Y., Chen, L., Sammynaiken, R., Lin, Y. and Zhang, W. J., 2011. Optimization of Piezoresistive Response of Pure CNT Networks as In-plane Strain Sensors. Rev. Sci. Instru. 82, 126104.

Miao, Y., Yang, Q., Chen, L., Sammynaiken, R. and Zhang, W. J., 2012. Modeling of piezoresistive response of carbon nanotube network based films under in-plane straining by percolation theory. Appl. Phys. Lett. 101, 063120.

Mori, T. and Tanaka, K., 1973. Average Stress in Matrix and Average Elastic Energy of Materials with Misfitting Inclusions. Acta. Metall. Mater. 21, 571–574.

Nambiar, S. and Yeow, J. T. W., 2011. Conductive polymer-based sensors for biomedical applications. Biosens. Bioelectron. 26, 1825–1832.

Odegard, G. M., Gates, T. S., Wise, K. E., Park, C. and Siochi, E. J., 2003. Constitutive modeling of nanotube-reinforced polymer composites. Compos. Sci. Technol. 63, 1671–1687.

Ounaies, Z., Park, C., Wise, K. E., Siochi, E. J. and Harrison, J. S., 2003. Electrical properties of single wall carbon nanotube reinforced polyimide composites. Compos. Sci. Technol. 63, 1637–1646.

Pan, N., 1996. The elastic constants of randomly oriented fiber composites: A new approach to prediction. Sci. Eng. Compos. Mater. 5, 63–72.

Park, M., Kim, H. and Youngblood, J. P., 2008. Strain-dependent electrical resistance of multi-walled carbon nanotube/polymer composite films. Nanotechnology 19, 055705.

Park, M. and Kim, H., 2006. Evaporation-based method for fabricating conductive MWCNT/PEO composite film and its application as strain sensor. Proc. 12th US-Japan Conf. Compos. Mater. Michigan: University of Michigan, pp 78–86.

Perez, R., Banda, S. and Ounaies, Z., 2008. Determination of the orientation distribution function in aligned single wall nanotube polymer nanocomposites by polarized Raman spectroscopy. J. Appl. Phys. 103, 074302.

Seidel, G. D. and Lagoudas, D. C., 2009. A micromechanics model for the electrical conductivity of nanotube-polymer nanocomposites. J. Compos. Mater. 43, 917–941.

Shang, S. M., Zeng, W. and Tao, X. M., 2011. High stretchable MWNTs/polyurethane conductive nanocomposites. J. Mater. Chem. 21, 7274–7280.

Shiraishi, M. and Ata, M., 2001. Work function of carbon nanotubes. Carbon 39, 1913–1917.

Simmons, J. G., 1963. Generalized formula for the electric tunnel effect between similar electrodes separated by a thin insulating film. J. Appl. Phys. 34, 1793–1803.

Takeda, T., Shindo, Y., Kuronuma, Y. and Narita, F., 2011. Modeling and characterization of the electrical conductivity of carbon nanotube-based polymer composites. Polymer 52, 3852–3856.

Tallman, T. and Wang, K. W., 2013. An arbitrary strains carbon nanotube composite piezoresistivity model for finite element integration. Appl. Phys. Lett. 102, 011909.

Taya, M., 1995. Micromechanics modeling of electronic composites. J. Eng. Mater-Tran. ASME 117, 462–469.

Taya, M. 2005. Electronic composites: modeling, characterization, processing, and MEMS applications. Cambridge: Cambridge University Press.

Taya, M., Kim, W. J. and Ono, K., 1998. Piezoresistivity of a short fiber/elastomer matrix composite. Mech. Mater. 28, 53–59.

Vangurp, M., 1995. The Use of Rotation Matrices in the Mathematical-Description of Molecular Orientations in Polymers. Colloid Polym. Sci. 273, 607–625.

Wang, X., Bradford, P. D., Liu, W., Zhao, H. B., Inoue, Y., Maria, J. P. et al., 2011. Mechanical and electrical property improvement in CNT/Nylon composites through drawing and stretching. Compos. Sci. Technol. 71, 1677–1683.

Yan, K. Y., Xue, Q. Z., Zheng, Q. B. and Hao, L. Z., 2007. The interface effect of the effective electrical conductivity of carbon nanotube composites. Nanotechnology 18, 255705.

Yang, Y., Gupta, M. C., Dudley, K. L. and Lawrence, R. W., 2005. Novel carbon nanotube-polystyrene foam composites for electromagnetic interference shielding. Nano Lett. 5, 2131–2134.

Yu, C. J., Masarapu, C., Rong, J. P., Wei, B. Q. and Jiang, H. Q., 2009. Stretchable supercapacitors based on buckled single-walled carbon nanotube macrofilms. Adv. Mater. 21, 4793–4797.

Zhang, R., Dowden, A., Deng, H., Baxendale, M. and Peijs, T., 2009. Conductive network formation in the melt of carbon nanotube/thermoplastic polyurethane composite. Compos. Sci. Technol. 69, 1499–1504.

Chapter 4

4 Bi-axial stretching effects on electrical conductivity of CNT-polymer composites[3]

4.1 Introduction

Due to their broad spectrum of potential applications, conductive polymer composites have been attracting extensive interests over the past decades. In addition to the attribute of electrical conductivity as owned by traditional conductive or semi-conductive materials, such as metals or silicon, conductive polymer composites also possess a combined performance of flexibility, low cost, easy processability and good chemical and biological compatibility (Yu *et al.*, 2009; Nambiar and Yeow, 2011; Shang *et al.*, 2011), which makes them as promising material candidates for stretchable electronics, conductive coatings, electromagnetic shielding, solar cells, etc (Yang *et al.*, 2005; Berson *et al.*, 2007; Yu *et al.*, 2009; Shang *et al.*, 2011). Most traditional polymers are electrical insulators, while the desired electrical conductivity is commonly achieved by adding conductive fillers into compliant insulating polymers. Among different conductive fillers, CNTs have been widely adopted as doping materials due to their high aspect ratio and excellent intrinsic electrical conductivity. Some experiments (Qunaies *et al.*, 2003; Kim *et al.*, 2005; Gojny *et al.*, 2006) have verified that the addition of a very small amount of CNTs into polymers can significantly improve the electrical conductivity of the nanocomposites, which demonstrate a percolation-like behavior with very low percolation threshold. Such a low percolation threshold is highly beneficial for conductive nanocomposite applications as the desired electrical conductivity could be achieved without any significant loss of the other inherent merits of the polymer matrix. It is well discussed in the literature that the electrical conductivity of the CNT-polymer composites attributes to two conductivity mechanisms, i.e., electron hopping at the nanoscale and conductive networks at the microscale (Chang *et al.*, 2009; Zhang *et al.*, 2009; Lu *et al.*, 2010). As explained by Deng and Zheng (2008), the contribution of the

---

[3] A version of this chapter has been submitted for publication.

electron hopping and the conductive networks depends on the CNT concentration. When the CNT concentration is below the percolation threshold, the electron hopping intra-tube or among different CNTs governs the electrical conductivity of the composites. However, when the CNT concentration exceeds the percolation threshold, some CNTs start to form conductive networks, which contribute to the electrical conductivity of the composites more significantly.

To fulfill the potential applications of CNT-polymer composites, understanding of the fundamental physics governing their overall electrical properties is of essential importance. Up to date, some efforts have been devoted to interpreting the electrical conductivity mechanisms and investigating how the overall electrical properties of the composites vary with their constituent features from both the theoretical and experimental perspectives (Kim *et al.*, 2005; Gojny *et al.*, 2006; Li *et al.*, 2007; Yan *et al.*, 2007; Chang *et al.*, 2009; Seidel and Lagoudas, 2009; Takeda *et al.*, 2011). It should be mentioned that most studies in the literature focused on investigating the electrical properties of the as-received composites without considering the stretching effects. However, for the particular applications of CNT-polymer composites in stretchable electronics, strain sensors (Park and Kim, 2006; Hu *et al.*, 2010) for example, it is natural to investigate how the stretching influences the electrical behavior of the composites, which could particularly offer advice on the better design of the strain sensors. Under a uni-axial stretching, experimental data (Park *et al.*, 2008; Hu *et al.*, 2010; Bao *et al.*, 2011) have demonstrated that such a stretching could lead to a sharp decrease/increase in the electrical conductivity/resistivity of the composites due to the breakdown of conductive networks. Meanwhile, an opposite trend was also observed (Cheng *et al.*, 2009; Shang *et al.*, 2011; Wang *et al.*, 2011), i.e., the electrical conductivity of CNT-polymer composites increases with the increase of the stretching. Such a contrary observation was attributed to the fact that the CNT re-alignment along the stretching direction dominates over the breakdown of the conductive networks. By conducting numerial simulation, Taya *et al.* (1998) and Lin *et al.* (2010) investigated the stretching/compression effects upon the electrical conductivity of fibre-polymer composites and their results indicated that the deformation could increase the percolation threshold. A similar conclusion for the

stretching effects on the percolation threshold was also captured by Tallman and Wang (2013) through applying excluded volume method.

Compared to the extensive explorations in studying the electrical properties of CNT-polymer nanocomposites and the uni-axial stretching effects, limited work has been found in investigating the bi-axial stretching effects on the electrical conductivity of the CNT-polymer composites in the literature. Nevertheless, bi-axial stretching is another typical stretching mode for CNT-polymer composites (Shen *et al.*, 2012; Mayoral *et al.*, 2013), which enables the CNTs to re-orientate along the two stretching directions in the polymer matrix. Such a stretching mode is expected to reduce the anisotropy of the electrical properties of the composites in the stretching plane compared to the uni-axial stretching case in which the CNTs are prone to get parallel along the uni-axial stretching direction. To complement the theoretical modeling of the uni-axial stretching effects upon the electrical conductivity of the CNT-polymer composites, the current work aims to investigate the bi-axial stretching effects on the electrical conductivity of the CNT-polymer composites with the incorporation of possible stretching-induced changes in a mixed micromechanics model.

4.2   Nanoscale and micromechanics modeling on electrical conductivity

Before applying the micromechanics modeling on the overall electrical behavior of the CNT-polymer composite, the nanoscale electrical conductivity mechanism, i.e., the electron hopping, is first considered. It was well-accepted in the literature (Yan *et al.*, 2007; Seidel and Lagoudas, 2009; Feng and Jiang, 2013) that the electron hopping among CNTs results in the formation of an interphase layer surrounding the CNTs. Accordingly, an effective composite cylinder was developed in these studies to capture such a nanoscale electron hopping effect, which consists of a CNT with length L and diameter D and an interphase layer with thickness t. The effective volume fraction f_{eff} of the cylinder is re-defined in terms of the CNT concentration f_{CNT} as (Yan *et al.*, 2007; Seidel and Lagoudas, 2009):

$$f_{\text{eff}} = \frac{(D+2t)^2(L+2t)}{D^2L} f_{\text{CNT}} .$$

(4.1)

Provided the electrical conductivity of the CNT (σ_{CNT}) and the interphase (σ_{Int}), the effective longitudinal and transverse electrical conductivity of the cylinder can be obtained by applying the law-of-mixture rule as (Taya, 2005; Yan *et al.*, 2007; Feng and Jiang, 2013):

$$\tilde{\sigma}^{\text{L}} = \frac{(L+2t)\sigma_{\text{Int}}\left[\sigma_{\text{CNT}}D^2 + 4\sigma_{\text{Int}}\left(Dt+t^2\right)\right]}{2\sigma_{\text{CNT}}D^2t + 8\sigma_{\text{Int}}\left(Dt+t^2\right)t + \sigma_{\text{Int}}L(D+2t)^2} ,$$

$$\tilde{\sigma}^{\text{T}} = \frac{\sigma_{\text{Int}}}{L+2t}\left[L\frac{D^2\sigma_{\text{CNT}} + 2(\sigma_{\text{CNT}}+\sigma_{\text{Int}})\left(t^2+Dt\right)}{D^2\sigma_{\text{Int}} + 2(\sigma_{\text{CNT}}+\sigma_{\text{Int}})\left(t^2+Dt\right)} + 2t\right]$$

(4.2)

where the superscripts "L" and "T" represent the longitudinal and the transverse directions, respectively. Thus the electrical conductivity tensor of the effective cylinder in its local coordinate system can be expressed as $\tilde{\sigma} = \text{diag}\left(\tilde{\sigma}^{\text{L}}, \tilde{\sigma}^{\text{T}}, \tilde{\sigma}^{\text{T}}\right)$. Obviously, the interphase features, i.e., the electrical conductivity (σ_{Int}) and the thickness (*t*), are essential for determining the electrical property of the effective cylinder.

According to the literature (Deng and Zheng, 2008; Seidel and Lagoudas, 2009; Takeda *et al.*, 2011; Feng and Jiang, 2013), the electrical conductivity of the composites relies on the two mentioned conductivity mechanisms depending on the CNT concentration as mentioned in the Introduction Section. For example, when the CNT concentration is below the percolation threshold f_{c}, CNT fillers are more electrically independent and the electron hopping dominates the electrical property of the composite; when the CNT concentration is greater than the percolation threshold, some CNTs start to form conductive networks which govern the electrical conductivity over the electron hopping. For CNTs forming conductive networks, quite a few works suggested that the average separation distance between CNTs follows a power law relation with the CNT concentration (Allaoui *et al.*, 2008; Deng and Zheng, 2008; Takeda *et al.*, 2011). Here we adopt the following expression to determine the average separation distance between CNTs (Feng and Jiang, 2013):

$$d_a = \left(\frac{f_c}{f_{CNT}}\right)^{1/3} d_c, \tag{4.3}$$

where d_c = 1.8 nm is the critical separation distance between two adjacent CNTs that allows the tunneling penetration of electrons. It is easily understood that for the electrically independent CNTs without forming any conductive networks, the separation distance between the CNTs should be greater than d_c. Due to the lack of work on estimating the average separation distance between such CNTs, we assume the average separation distance between CNTs without forming conductive networks as the critical separation distance, i.e., $d_a = d_c$. It should be noted that such an assumption overestimates the electrical conductivity of the composite before the percolation. However, the overestimation in the electrical conductivity after the percolation can be neglected due to the fact that the conductive networks dominate over the electron hopping as argued in our previous work (Feng and Jiang, 2013). The thickness of the interphase was taken as half of the corresponding average separation distance between the CNTs, i.e., $t = d_a/2$ (Feng and Jiang, 2013).

Following Simmons' formulation for electron tunneling (Simmons, 1963; Takeda et al., 2011), the electrical conductivity of the interphase was derived as:

$$\sigma_{Int} = \frac{d_a}{aR_{Int}(d_a)}, \tag{4.4}$$

where $R_{Int}(d_a) = \frac{d_a \hbar^2}{ae^2(2m\lambda)^{1/2}}\exp\left(\frac{4\pi d_a}{\hbar}(2m\lambda)^{1/2}\right)$ is the tunneling-type contact resistance between two CNTs with a being the contact area of CNTs; λ = 5.0 eV is the potential barrier height for CNTs dispersed in most polymers (Shiraishi and Ata, 2001; Takeda et al., 2011), m = 9.10938291×10^{-31} kg and e = −1.602176565×10^{-19} C are mass and electric charge of an electron, respectively, and $\hbar$ = 6.626068×10^{-34} m^2·kg/s is the Planck constant.

With the nanoscale modeling of electron hopping as discussed above, the CNTs are modeled equivalently as solid cylinder fillers. These solid fillers are assumed as straight and uniformly dispersed in the polymer matrix. For such a two-phase composite, the overall effective electrical conductivity of the composite can be theoretically predicted by applying the micromechanics model as performed in the literature (Taya, 1995; Entchev and Lagoudas, 2002; Odegard *et al.*, 2003; Taya, 2005; Seidel and Lagoudas 2009; Feng and Jiang, 2013). The routine procedure in these studies is that the overall electrical conductivity of the composite is derived by averaging the contribution of the fillers from all possible orientations in the representative volume element (RVE) as shown in Figure 4.1, i.e.,
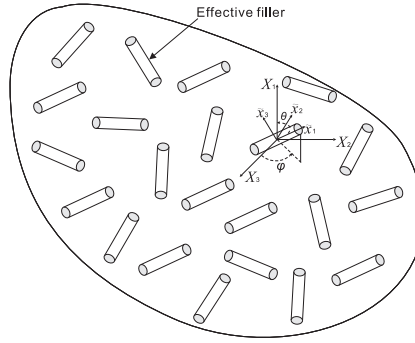
Figure 4.1 RVE containing effective fillers.

$$\sigma_{eff} = \sigma_m + \frac{\int_0^{2\pi} \int_0^{\pi} \rho(\varphi,\theta) f_{eff} (\sigma - \sigma_m) A \sin\theta \mathrm{d}\theta \mathrm{d}\varphi}{\int_0^{2\pi} \int_0^{\pi} \rho(\varphi,\theta) \sin\theta \mathrm{d}\theta \mathrm{d}\varphi},$$ (4.5)

where φ and θ are the Euler angles identifying the orientation of the fillers; $\rho(\varphi,\theta)$ is the orientation distribution function (ODF) of the fillers; A is the electric field concentration tensor; σ_m is the electrical conductivity tensor of the polymer and σ is the electrical conductivity tensor of the effective filler in the global coordinates system (X_1, X_2, X_3) of the composites, which can be determined from the conductivity tensor $\tilde{\sigma}$ of the filler in its local coordinates system $(\tilde{x}_1, \tilde{x}_2, \tilde{x}_3)$ as:

$$\sigma = Q^T \tilde{\sigma} Q,$$ (4.6)

with Q being the transformation matrix given as (Entchev and Lagoudas, 2002):

$$Q = \begin{bmatrix} \sin\theta\cos\varphi & -\cos\theta\cos\varphi & \sin\varphi \\ \sin\theta\sin\varphi & -\cos\theta\sin\varphi & -\cos\varphi \\ \cos\theta & \sin\theta & 0 \end{bmatrix}. \tag{4.7}$$

Following the percolation process proposed by Deng and Zheng (2008), it is understood that the overall electrical conductivity of the composite attributes to the electron hopping and the conductive networks depending on the CNT concentration. For example, only electron hopping contributes to the electrical behavior of the composite prior to the percolation. However, after CNT concentration reaches the percolation threshold f_c, certain percentage ξ of CNTs start to form conductive networks, which was estimated by Deng and Zheng (2008) as:

$$\xi = \frac{f_{CNT}^{1/3} - f_c^{1/3}}{1 - f_c^{1/3}} \quad (f_c \le f_{CNT} < 1). \tag{4.8}$$

It is obvious from this expression that with the increase of the CNT concentration from f_c to 1, the percentage of the CNTs forming conductive networks increases from 0 to 1. With the consideration of this percolation process, it is natural to incorporate both the electron hopping and the conductive networking mechanisms in the micromechanics modeling. Therefore, a mixed micromechanics model was developed in our previous work (Feng and Jiang, 2013) in which the effective electrical conductivity of the composite was derived from Eq. (2.5) in the following form:

$$\sigma_{eff} = \begin{cases} \boldsymbol{\sigma}_m + \dfrac{\int_0^{2\pi}\int_0^{\pi} \{f_{eff}(\boldsymbol{\sigma}_{EH} - \boldsymbol{\sigma}_m)\boldsymbol{A}_{EH}\}\rho(\varphi,\theta)\sin\theta\,\mathrm{d}\theta\,\mathrm{d}\varphi}{\int_0^{2\pi}\int_0^{\pi}\rho(\varphi,\theta)\sin\theta\,\mathrm{d}\theta\,\mathrm{d}\varphi}, \quad f_{CNT} < f_c \\[3em] \boldsymbol{\sigma}_m + (1-\xi)\dfrac{\int_0^{2\pi}\int_0^{\pi} \{f_{eff}(\boldsymbol{\sigma}_{EH} - \boldsymbol{\sigma}_m)\boldsymbol{A}_{EH}\}\rho(\varphi,\theta)\sin\theta\,\mathrm{d}\theta\,\mathrm{d}\varphi}{\int_0^{2\pi}\int_0^{\pi}\rho(\varphi,\theta)\sin\theta\,\mathrm{d}\theta\,\mathrm{d}\varphi} \\[3em] \quad + \xi\dfrac{\int_0^{2\pi}\int_0^{\pi} \{f_{eff}(\boldsymbol{\sigma}_{CN} - \boldsymbol{\sigma}_m)\boldsymbol{A}_{CN}\}\rho(\varphi,\theta)\sin\theta\,\mathrm{d}\theta\,\mathrm{d}\varphi}{\int_0^{2\pi}\int_0^{\pi}\rho(\varphi,\theta)\sin\theta\,\mathrm{d}\theta\,\mathrm{d}\varphi}, \quad f_{CNT} \ge f_c \end{cases} \tag{4.9}$$

where the subscripts "EH" and "CN" denote terms contributed by electron hopping and conductive networks, respectively.

Here we adopt the Mori-Tanaka micromechanics model (Mori and Tanaka, 1973; Taya, 2005), for which the concentration tensor in Eq. (2.5) can be determined as (Taya, 1995; Entchev and Lagoudas, 2002; Odegard *et al.*, 2003):

$$A = QA^{\text{dil}}Q^{\text{T}} \left\{ (1 - f_{\text{eff}})\delta + f_{\text{eff}} \frac{\int_0^{2\pi} \int_0^{\pi} f_{\text{eff}} \left\{ QA^{\text{dil}}Q^{\text{T}} \right\} \rho(\varphi,\theta) \sin\theta \, \mathrm{d}\theta \mathrm{d}\varphi}{\int_0^{2\pi} \int_0^{\pi} \rho(\varphi,\theta) \sin\theta \, \mathrm{d}\theta \mathrm{d}\varphi} \right\}^{-1} \tag{4.10}$$

where $A^{\text{dil}} = \left\{ \delta + S(\sigma_{\text{m}})^{-1}(\tilde{\sigma} - \sigma_{\text{m}}) \right\}^{-1}$ with δ being the Kronecker delta tensor. The parameter S in the expression of A^{dil} is the Eshelby tensor of the effective filler, which is a function of the effective aspect ratio of the filler (Taya, 2005; Seidel and Lagoudas, 2009; Feng and Jiang, 2013). For CNTs in conductive networks, the effective aspect ratio is taken as infinite due to the formed electrically conductive chains across the sample. In contrast, for CNTs associated with electron hopping, the effective aspect ratio is the real effective aspect ratio of single filler. Correspondingly, A_{EH} and A_{CN} in Eq. (2.9) can be calculated from Eq. (2.10) by using the associated aspect ratios.

4.3   Stretching induced changes

When the composite with effective fillers is subjected to a stretching, it is suggested in the literature (Taya *et al.*, 1998; Taya 2005; Feng and Jiang, 2014) that three major changes are expected to occur: volume expansion of the composite, re-orientation of the fillers and the change in conductive networks. In the following, we will characterize these stretching induced changes and illustrate how such stretching effects are incorporated into the micromechanics model developed in the previous Section.

4.3.1   Volume expansion and re-orientation

When subjected to a stretching, the fillers in the composites tend to re-orientate along the stretching direction. Following the fiber re-orientation model in references (Kuhn and

Grün, 1942; Taya et al., 1998; Feng and Jiang, 2014), Figure 4.2 shows the orientation change of a filler in a cell before and after a bi-axial stretching. The original lengths of the cell in the X_1, X_2 and X_3 directions are l_0, w_0 and h_0, respectively. After the bi-axial stretching, the lengths of the cell become:
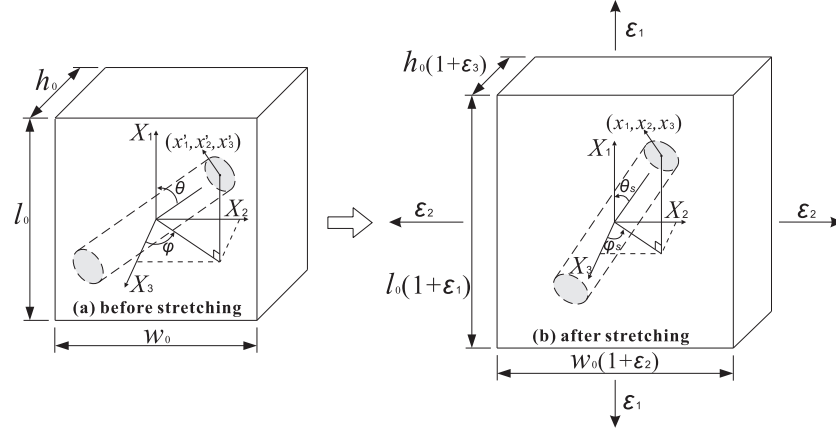
Figure 4.2 Sketch of orientation change of a filler due to bi-axial stretching.

$$l = l_0\left(1+\varepsilon_1\right), \ w = w_0\left(1+\varepsilon_2\right) \text{ and } h = h_0\left(1+\varepsilon_3\right), \tag{4.11}$$

where ε_1, ε_2 and ε_3 are the three principle strains along the X_1, X_2 and X_3 directions in the global coordinate system, respectively, which are assumed to satisfy $\varepsilon_1 \geq \varepsilon_2 \geq \varepsilon_3$. For any bi-axial stretching strains ε_1 and ε_2 under deformation, the stretching strain in the X_3 direction is derived as:

$$\varepsilon_3 = \left[\left(1+\varepsilon_1\right)\left(1+\varepsilon_2\right)\right]^{-\frac{v}{1-v}} - 1. \tag{4.12}$$

Due to the fact that the stiffness of the polymer is usually much lower than that of the CNT filler, the change of the filler's volume can be neglected since the deformation is mainly sustained by the polymer. Accordingly, the effective volume fraction of the fillers in the composite after the stretching can be approximated as:

$$f = \frac{V_0 f_{\text{eff}}}{V} = = \frac{f_{\text{eff}}}{\left[(1+\varepsilon_1)(1+\varepsilon_2)\right]^{\frac{1-2\nu}{1-\nu}}} \quad , \qquad (4.13)$$

where V_0 and V are the volumes of the cell before and after stretching, respectively. Obviously, for compressible materials, the bi-axial stretching induces a volume expansion, resulting in the decrease of the filler concentration. Therefore, the filler volume fraction in Eq. (2.9) needs to be replaced by the volume fraction defined in Eq. (3.3) when considering the bi-axial stretching.

As demonstrated in Figure 4.2, the re-orientation of the filler in the cell results in the variation of the two Euler angles, i.e., the polar angle changes from θ to θ_s and the azimuth angle changes from φ to φ_s. Correspondingly, the coordinates of the upper end of the filler in the cell before the bi-axial stretching are determined in terms of the Euler angles as (Taya et al., 1998):

$$x_1^{'} = \frac{u^{'}}{2}\cos\theta, \ x_2^{'} = \frac{u^{'}}{2}\sin\theta\sin\varphi, \ x_3^{'} = \frac{u^{'}}{2}\sin\theta\cos\varphi, \qquad (4.14)$$

and after stretching as:

$$x_1 = \frac{u}{2}\cos\theta_s, \ x_2 = \frac{u}{2}\sin\theta_s\sin\varphi_s, \ x_3 = \frac{u}{2}\sin\theta_s\cos\varphi_s, \qquad (4.15)$$

where u' and u are the lengths of the filler before and after stretching. Ignoring the change of the filler length, u' = u. From Eqs. (3.4) and (3.5), we have the following expressions:

$$\begin{cases} \dfrac{x_1}{x_1^{'}} = \dfrac{u\cos\theta_s}{u'\cos\theta} = 1+\varepsilon_1 \\[2mm] \dfrac{x_2}{x_2^{'}} = \dfrac{u\sin\theta_s\sin\varphi_s}{u'\sin\theta\sin\varphi} = 1+\varepsilon_2 \\[2mm] \dfrac{x_3}{x_3^{'}} = \dfrac{u\sin\theta_s\cos\varphi_s}{u'\sin\theta\cos\varphi} = \left[(1+\varepsilon_1)(1+\varepsilon_2)\right]^{-\frac{\nu}{1-\nu}} \end{cases} . \qquad (4.16)$$

Based on Eq. (3.6), the two Euler angles of the filler after the bi-axial stretching, φ_s and θ_s, can be determined in terms of the initial Euler angles φ and θ as:

$$\begin{cases} \tan\varphi_s = \left(1+\varepsilon_1\right)^{\frac{\nu}{1-\nu}}\left(1+\varepsilon_2\right)^{\frac{1}{1-\nu}}\tan\varphi \\ \tan\theta_s = \dfrac{1+\varepsilon_2}{1+\varepsilon_1}\cdot\dfrac{\sin\varphi}{\sin\varphi_s}\tan\theta \end{cases}. \tag{4.17}$$

From Eq. (3.7), it is revealed that the two Euler angles denoting the orientation of the filler vary with the stretching strains, which disrupts the randomness of the filler distribution in the composite. To quantify the stretching effects upon the re-orientation of the fillers, the ODF, $\rho(\varphi, \theta)$, is introduced to characterize the distribution of the fillers, which satisfies the following conditions (Gurp, 1995; Pérez et al., 2008):

$$\rho(\varphi,\theta)\geq 0 \text{ and } \frac{1}{4\pi}\int_0^{2\pi}\int_0^{\pi}\rho(\varphi,\theta)\sin\theta\mathrm{d}\theta\mathrm{d}\varphi = 1. \tag{4.18}$$

When fillers are randomly distributed in the polymer matrix before the stretching, the ODF equals unity, indicating a uniform distribution of fillers along any orientation. However, after a stretching, the two Euler angles vary with the stretching strains indicating the re-orientation of the fillers and thus the variation of the ODF. In order to determine the new ODF after the stretching, we assume there are a number of G fillers randomly distributed in the RVE of the micromechanics model before the stretching (as shown in Figure 4.1). Following Eq. (3.8), the total number of the fillers falling in the ranges of $(\theta, \theta+\mathrm{d}\theta)$ and $(\varphi, \varphi+\mathrm{d}\varphi)$ in the RVE can be determined as (Kuhn and Grün, 1942):

$$\mathrm{d}N_{\substack{\theta,\theta+\mathrm{d}\theta \\ \varphi,\varphi+\mathrm{d}\varphi}} = \frac{1}{4\pi}G\rho(\varphi,\theta)\sin\theta\mathrm{d}\theta\mathrm{d}\varphi. \tag{4.19}$$

After a bi-axial stretching, the G fillers will be re-oriented within the ranges of $(\varphi_s, \varphi_s+\mathrm{d}\varphi_s)$ and $(\theta_s, \theta_s+\mathrm{d}\theta_s)$, i.e.,

$$\mathrm{d}N_{\substack{\theta_s,\theta_s+\mathrm{d}\theta_s \\ \varphi_s,\varphi_s+\mathrm{d}\varphi_s}} = \frac{1}{4\pi}G\rho(\varphi_s,\theta_s)\sin\theta_s\mathrm{d}\theta_s\mathrm{d}\varphi_s = \mathrm{d}N_{\substack{\theta,\theta+\mathrm{d}\theta \\ \varphi,\varphi+\mathrm{d}\varphi}}, \tag{4.20}$$

where $\rho(\varphi_s, \theta_s)$ is the new ODF after the stretching. Combining Eq. (3.7) and Eq. (3.10), the new ODF after the bi-axial stretching is derived as:

$$\rho(\varphi_s, \theta_s) = \frac{\dfrac{\left(\dfrac{1+\varepsilon_1}{1+\varepsilon_2} \cdot \dfrac{\sin\varphi_s}{\sin\varphi}\right)^{\frac{1}{2}}}{\left(1+\varepsilon_1\right)^{\frac{v}{1-v}}\left(1+\varepsilon_2\right)^{\frac{1}{1-v}}\cos^2\varphi_s + \dfrac{1}{\left(1+\varepsilon_1\right)^{\frac{v}{1-v}}\left(1+\varepsilon_2\right)^{\frac{1}{1-v}}}\sin^2\varphi_s}}{\left[\left(\dfrac{1+\varepsilon_1}{1+\varepsilon_2}\right)^{-1} \cdot \left(\dfrac{\sin\varphi_s}{\sin\varphi}\right)^{-1}\cos^2\theta_s + \dfrac{1+\varepsilon_1}{1+\varepsilon_2}\cdot\dfrac{\sin\varphi_s}{\sin\varphi}\sin^2\theta_s\right]^{\frac{3}{2}}} . \qquad (4.21)$$

It should be noted here that with the consideration of the bi-axial stretching, the Euler angles and the ODF in Eq. (2.9) should be replaced by the new Euler angles and the ODF determined by Eqs. (3.7) and (3.11), respectively.

Without any stretching, i.e., $\varepsilon_1 = \varepsilon_2 = \varepsilon_3 = 0$, the ODF defined in Eq. (3.11) reduces to unity for a random distribution as expected. Figure 4.3 plots the ODF profile with two Euler angles. From these figures, it can be seen that the stretching tends to re-align the fillers along the stretching directions ($\varphi_s = 90°$ and $\theta_s = 0°$ and $180°$), which was also commented by Mayoral et al. (2013). Comparing the ODF in Figure 4.3(a) and Figure 4.3(b), it is indicated that increasing the stretching strain in a particular direction, the X_2 direction for example, enhances the re-alignment of fillers along that direction.
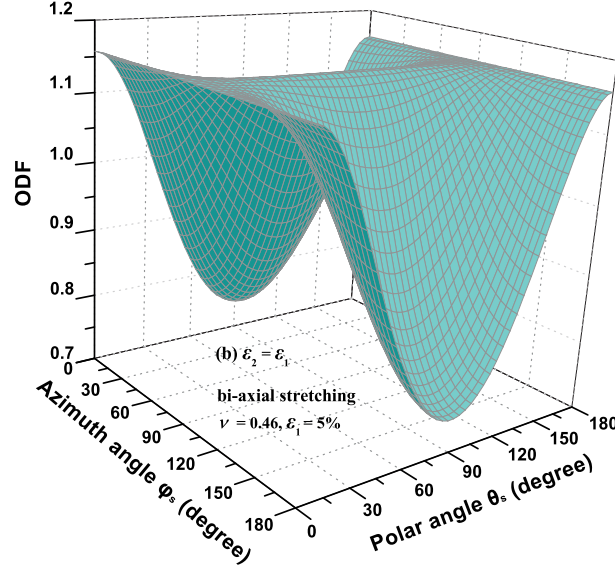

(a) $\varepsilon_2 = 0.25\varepsilon_1$

bi-axial stretching

$v = 0.46$, $\varepsilon_1 = 5\%$
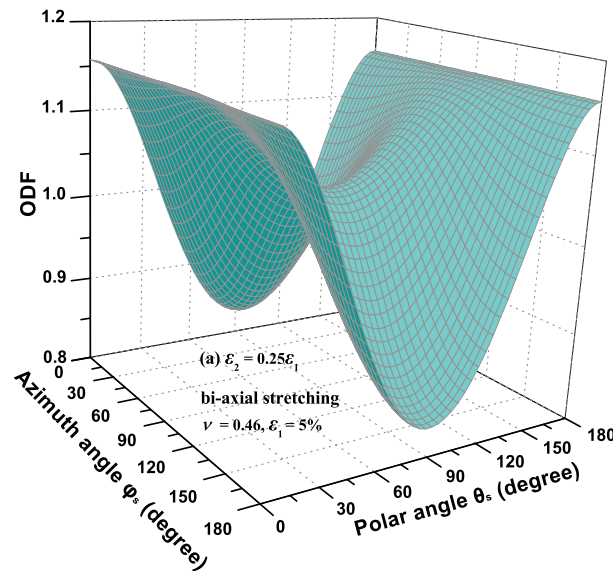
Figure 4.3 Variation of ODF with Euler angles (a) $\varepsilon_2 = 0.25\varepsilon_1$; (b) $\varepsilon_2 = \varepsilon_1$.

4.3.2 Change in conductive networks

As discussed in the literature (Deng and Zheng; 2008; Seidel *et al.*, 2008), when the CNT concentration reaches a certain value (the percolation threshold), the electrical conductivity of the CNT-polymer composite increases abruptly denoting the onset of the formation of conductive networks. According to the fitting from Monte Carlo simulation by Tallman and Wang (2013), it was found that the stretching increases the percolation threshold which influences the conductive networks in the composite. Here we adopt the excluded volume method (Balberg *et al.*, 1984; Celzard *et al.*, 1996; Tallman and Wang, 2013) to incorporate the stretching effects into the percolation threshold, which was given as:

$$f_c = 1 - \exp\left(\frac{-\langle V_{ex} \rangle V_{CNT}}{\langle V_e \rangle}\right), \tag{4.22}$$

where

$$\langle V_e \rangle = \frac{4\pi}{3}D^3 + 2\pi D^2 L + 2 \cdot D \cdot L^2 \langle \sin\gamma \rangle_\mu \tag{4.23}$$

is the average excluded volume of the CNT, $\langle V_{ex} \rangle$ is the total average excluded volume of the CNT and V_{CNT} is the volume of the CNT. The term $\langle \sin\gamma \rangle_\mu$ in Eq. (3.13) is an

averaging term accounting for the CNT orientation, with γ being the angle between the ith and the jth CNTs.

As indicated in Figure 4.3, stretching induces the re-alignment of CNTs favoring the stretching directions. Such a re-alignment disrupts the randomness of the CNT distribution. For example, CNTs uniformly distribute in the ranges of the polar angle ($0 \leq \theta \leq 2\pi$) and the azimuth angle ($0 \leq \varphi \leq \pi$) before the stretching. However, it was understood from the work of Tallman and Wang (2013) that after the stretching more CNTs will concentrate within certain ranges, i.e., within the polar angle ranges of $[0, \theta_\mu]$ and $[\pi-\theta_\mu, \pi]$, in which θ_μ was determined as:

$$\theta_\mu = \arcsin\left[\left(1+\varepsilon_3\right)/\left(1+\varepsilon_1\right)\right], \tag{4.24}$$

where ε_1 and ε_3 are the first and the third principle strains. Based on the fitting data from Monte Carlo simulation, the term $\langle \sin\gamma \rangle_\mu$ in Eq. (3.13) was determined in terms of θ_μ as (Tallman and Wang, 2013):

$$\langle \sin\gamma \rangle_\mu = 0.018\theta_\mu^5 + 0.021\theta_\mu^4 - 0.234\theta_\mu^3 - 0.015\theta_\mu^2 + 0.909\theta_\mu. \tag{4.25}$$

In addition, a linear relation between $\langle V_{\text{ex}} \rangle$ and $\langle \sin\gamma \rangle_\mu$ was also given by Tallman and Wang (2013] as:

$$\langle V_{\text{ex}} \rangle = 2.8 - 5.6\frac{\langle \sin\gamma \rangle_\mu}{\pi}. \tag{4.26}$$

Combining Eqs. (3.12)–(3.16), the percolation threshold with the consideration of the stretching effects was derived as (Feng and Jiang, 2014):

$$f_{\text{c}} = 1 - \exp\left[-\frac{\left(2.1\pi - 4.2\langle \sin\gamma \rangle_\mu\right)p}{4\pi + 6\pi p + 6p^2 \langle \sin\gamma \rangle_\mu}\right], \tag{4.27}$$

where $p = L/D$ is the aspect ratio of the CNTs. Obviously, the stretching induced re-orientation of the CNTs will influence the percolation threshold, which results in the change of the average separation distance among CNTs and the percentage of the percolated CNTs as indicated by Eqs. (2.3) and (2.8), respectively.

In order to see the stretching effects on the conductive networks, Figure 4.4 plots the variation of the normalized percentage $\xi_N = \xi_s/\xi_0$ of the percolated CNTs for a composite under bi-axial stretching, where ξ_0 and ξ_s denote the percentage of the percolated CNTs before and after stretching, respectively. From this figure, it is observed that with a fixed stretching strain in the X_1 direction, the stretching strain in the X_2 direction decreases the percentage of percolated CNTs as compared to the uni-axial stretching case. It is thus concluded that bi-axial stretching induces more breakdown of conductive networks. It is also found that the decreasing rate of the percolated CNTs is more sensitive to the stretching strain in the X_2 direction for the composite with lower CNT concentration than that with higher CNT concentration. Furthermore, the percentage of percolated CNTs of the composite with the same CNT concentration but different aspect ratio (fixed diameter but different length) is also provided in this figure for comparison. It is concluded that the composites with shorter CNTs are more susceptible to the breakdown of conductive networks.
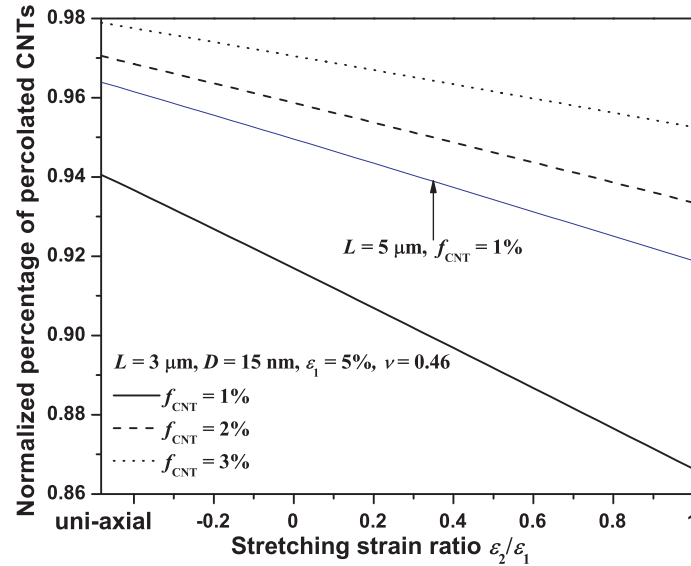

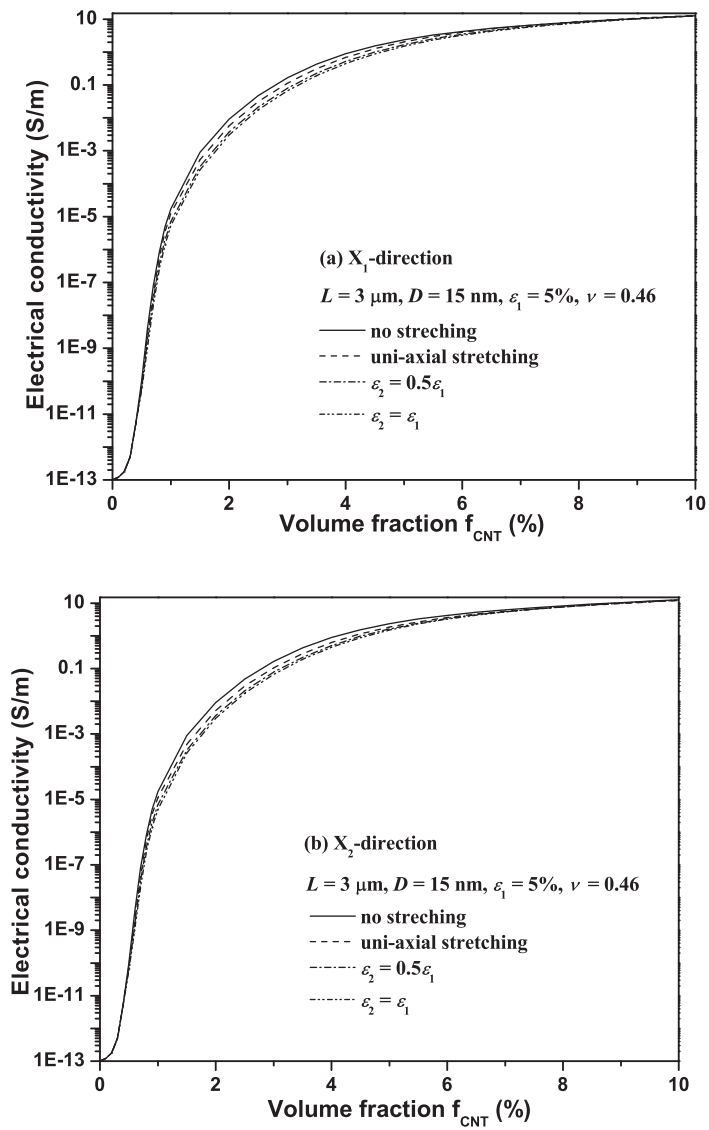Figure 4.4 Variation of normalized percentage of percolated CNTs with stretching strain ratio.

4.4 Results and discussions

To investigate the bi-axial stretching effects on the electrical conductivity of the CNT-polymer composites, a MWCNT/PEO (Polyethylene Oxide) composite (Park and Kim,

2006; Park *et al.*, 2008] is chosen as the example material. The MWCNTs were functionalized and well dispersed in the PEO matrix by stirring and sonication before the stretching. Therefore, we can assume that the CNTs are uniformly and well dispersed in the polymer matrix before the stretching. The length and the diameter of the CNTs range from 1μm to 5μm and 10 nm to 20 nm, respectively. The electrical conductivity of the polymer and the CNTs is taken as $\sigma_m = 1\times10^{-13}$ S/m and $\sigma_{CNT} = 100$ S/m (Deng and Zheng, 2008; Feng and Jiang, 2013). For the value of the Poisson's ratio of the composites, it should be noted that the true value naturally depends on both the CNT concentration and the CNT orientation, and it varies with the stretching. However, according to the evaluation method provided by Pan (1996), the effect of the orientation of fillers upon the Poisson's ratio of the composites is negligible. For example, for a CNT composite with volume fraction 3%, ν is approximately determined as 0.46 for a random CNT distribution while 0.45 for a perfectly aligned distribution. In addition, our previous work (Feng and Jiang, 2014) shows that the Poisson's ratio has limited effects on the electrical conductivity of the composites. Therefore, we choose the Poisson's ratio of the polymer, i.e., $\nu = 0.46$, as the value of the composite.

Figure 4.5 plots the variation of the electrical conductivity of the CNT-polymer composite in the three principal directions with the CNT concentration for different stretching strain ratios when the CNT size is fixed. From this figure, it can be seen that the electrical conductivity increases with the CNT volume fraction as expected. It is also observed that both uni-axial stretching and bi-axial stretching decrease the electrical conductivity of the composite, which is attributed to the stretching induced change in conductive networks, i.e., the increase in separation distance among CNTs and the decrease in percentage of percolated CNTs. However, it is found that for particularly low CNT volume fraction (below percolation threshold) and high enough CNT volume fraction (far away from percolation threshold), small discrepancy is observed between different scenarios. It can be explained by the fact that for the composite with low CNT volume fraction, no conductive networks are formed and the electrical conductivity is mainly attributed to the electron hopping, which slightly depends on the stretching. In contrast, for the composites with high enough CNT volume fraction, there exist a large

number of conductive networks in the composite. Thus any change in the conductive networks, stretching induced breakdown for example, will have relatively limited effect on the overall electrical conductivity of the composite as argued by Jiang *et al*. (2007). Furthermore, it is found that compared to the uni-axial stretching, bi-axial stretching decreases the electrical conductivity more significantly since the stretching in the X_2 direction enhances the re-orientation of CNTs in the stretching direction, resulting in more breakdowns of conductive networks. Such a bi-axial stretching enhanced decrease in the electrical conductivity was also experimentally observed by Mayoral *et al*.(2013).

(a) X_1-direction

$L = 3 \, \mu m$, $D = 15$ nm, $\varepsilon_1 = 5\%$, $\nu = 0.46$

——— no streching

- - - - uni-axial stretching

—·—· $\varepsilon_2 = 0.5\varepsilon_1$

········ $\varepsilon_2 = \varepsilon_1$

(b) X_2-direction

$L = 3 \, \mu m$, $D = 15$ nm, $\varepsilon_1 = 5\%$, $\nu = 0.46$

——— no streching

- - - - uni-axial stretching

—·—· $\varepsilon_2 = 0.5\varepsilon_1$

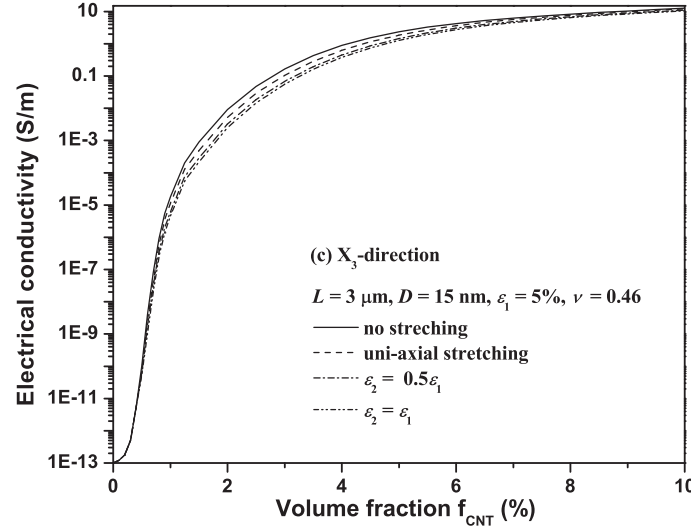········ $\varepsilon_2 = \varepsilon_1$

Figure 4.5 Variation of electrical conductivity with CNT volume fraction (a) X_1-direction; (b) X_2-direction; (c) X_3-direction.

As mentioned in Section 3, there are three major changes induced by the stretching, including volume expansion, re-orientation of fillers and breakdown of conductive networks (change in conductive networks). When the composite ($v = 0.46$) is under a maximum bi-axial stretching strain considered in the current work, i.e., $\varepsilon_1 = \varepsilon_2 = 5\%$, the volume expansion induces a relative decrease in the CNT concentration, which is calculated as less than 1.5% of the original CNT volume fraction. Therefore, such a small change in the CNT concentration is negligible under small deformation. It should be mentioned that although stretching overall decreases the electrical conductivity of the composite (Figure 4.5), the re-orientation itself is expected to increase the electrical conductivity along the stretching directions. To evaluate the relative effect of the other two stretching induced changes, Figure 4.6 demonstrates the variation of the normalized electrical conductivity with considering the individual effect of re-orientation and change in the conductive networks separately. From this figure, it can be seen that under the considered range of the volume fraction and the stretching strain, the decrease of the electrical conductivity induced by the change in the conductive networks is much more prominent than the re-orientation induced variation of the electrical conductivity, which indicates the dominate role of the change in the conductive networks.
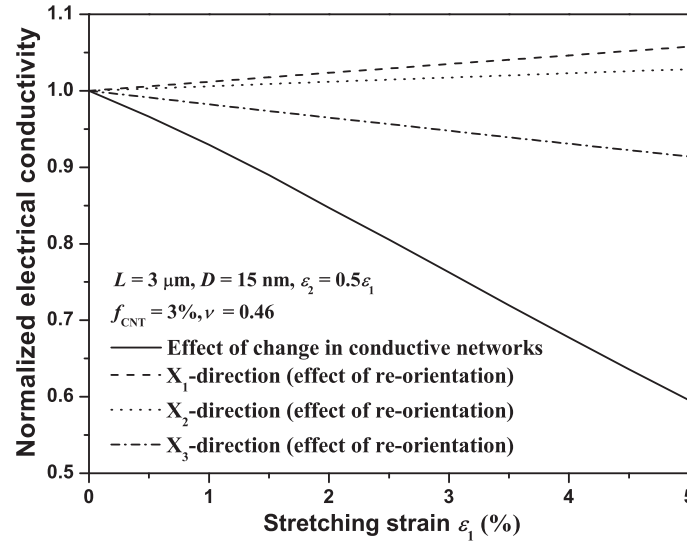
Figure 4.6 Effect of stretching induced re-orientation and change in conductive networks.

Figure 4.7 shows the variation of the normalized electrical conductivity with stretching strain ratio for the three principle directions, in which the electrical conductivity was normalized by the value before the stretching. As expected, under uni-axial stretching the electrical conductivity in the first principle stretching direction (X_1 direction) is higher than that in the other two transverse directions (X_2 and X_3 directions) due to the re-alignment of CNTs along the stretching direction X_1. With the increase of the stretching ratio, the electrical conductivity decreases in all the three directions while the electrical conductivity in the X_2 direction is approaching that in the X_1 direction until the equal bi-axial stretching condition is reached, indicating an increasing randomness of the CNT distribution in the bi-axial stretching plane (X_1-X_2 plane). This scenario was commented by Shen *et al.* (2012) that the second stretching enables CNTs to have less chance to be parallel, enhancing the randomness of the CNTs distribution in the bi-axial stretching plane.
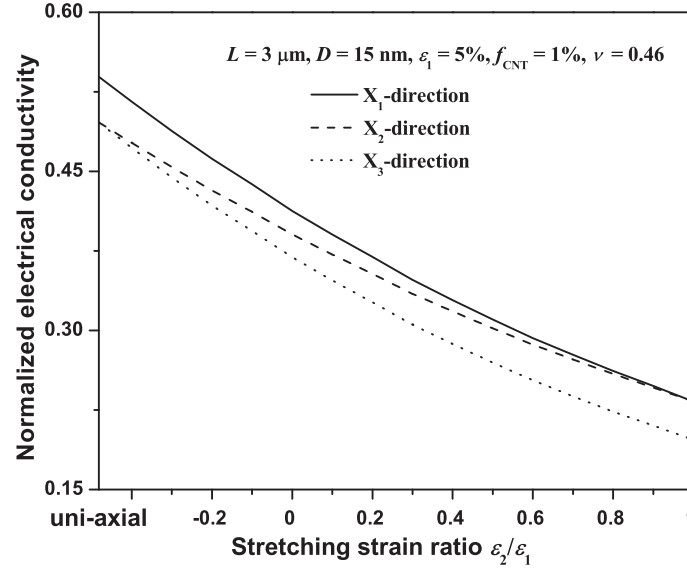
Figure 4.7 Variation of normalized electrical conductivity with stretching strain ratio.

Figure 4.8 investigates the variation of the electrical conductivity with stretching strain for different CNT volume fractions. It is observed that with a fixed stretching strain ratio ($\varepsilon_2/\varepsilon_1 = 0.5$), the electrical conductivity decreases with the stretching strain in the X_1 direction and the decreasing rate is enhanced for the composite with lower CNT volume fraction. This suggests that the electrical conductivity of the composite with lower CNT concentration is more sensitive to stretching. The reason behind such sensitivity relies on the combined dependency of the separation distance among CNTs and the percentage of percolated CNTs upon the CNT volume fraction as indicated by Eqs. (2.3) and (2.8). As argued by Jiang *et al.* (2007) that since only a few conductive networks exist in composites with lower CNT concentration, any small change in the networks, including stretching induced separation distance between CNTs, the percolation threshold and the percentage of percolated CNTs, will influence the electrical conductivity significantly. In contrast, any change in the conductive networks for composites with higher CNT concentration will have relatively limited effects on the electrical conductivity due to the existence of large amount of conductive networks.
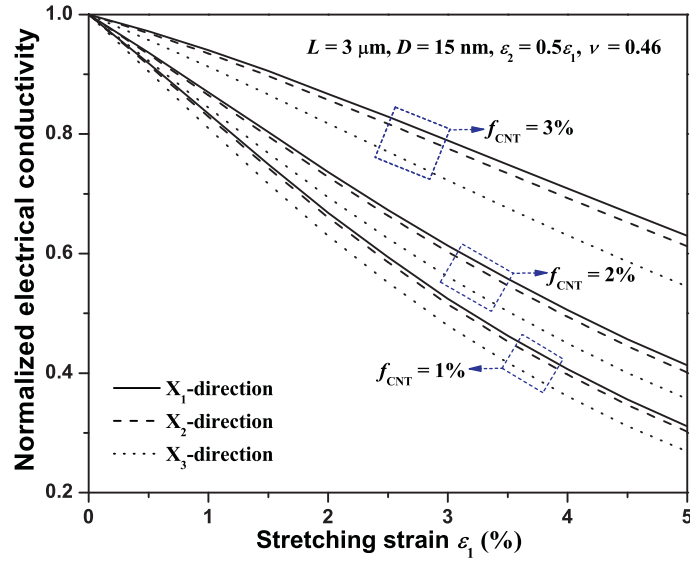
Figure 4.8 Variation of normalized electrical conductivity with stretching strain (a) X_1-direction; (b) X_2-direction; (c) X_3-direction.

Figure 4.9 demonstrates the effects of CNT size on the electrical conductivity of the composite under a bi-axial stretching. It is obvious that for the composite with a fixed CNT concentration (f_{CNT} = 1%) and fixed diameter of CNTs, the electrical conductivity of the composite with shorter CNTs decreases more significantly. It can be understood from the fact that the percolation threshold is highly dependent on the filler's aspect ratio, which results in the change of the separation distance among CNTs and the percentage of the percolated CNTs. As demonstrated in Figure 4.4, for the same CNT volume fraction the percentage of the percolated CNTs is reduced more significantly for the composite with shorter CNTs than that with longer CNTs. Therefore, it is concluded that the composite with shorter CNTs is more susceptible to decrease its electrical conductivity under stretching.
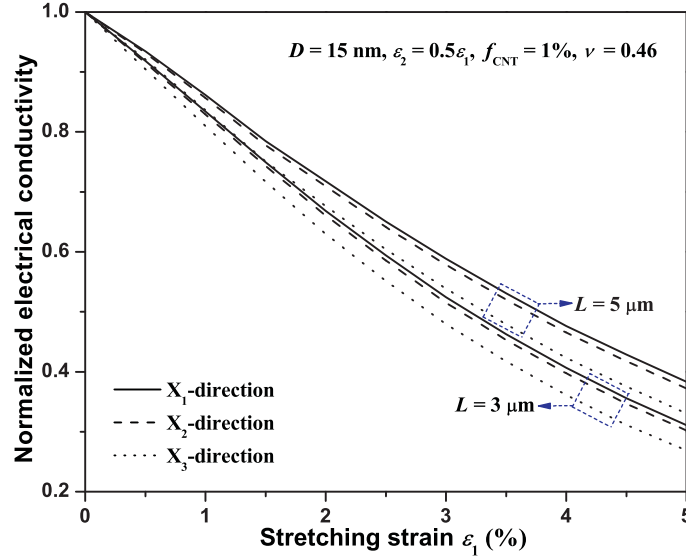
Figure 4.9 Variation of normalized electrical conductivity with stretching strain for different CNT lengths (a) X_1-direction; (b) X_2-direction; (c) X_3-direction.

It should be noted that in this current work we assume the CNTs dispersed in polymers are straight and randomly distributed in polymers before stretching. However, due to van der Waals forces among CNTs and low CNT bending stiffness, CNTs usually agglomerate and exist in a wavy state. Therefore, a more comprehensive model with the incorporation of the effects of agglomeration and waviness needs to be further developed.

4.5 Conclusions

In this work, stretching induced volume expansion, re-orientation of CNTs and change of conductive networks in the composite are incorporated into a mixed micromechanics model to study the bi-axial stretching effects upon the overall electrical conductivity of a CNT-polymer composite. Compared to a uni-axial stretching in which CNTs tend to re-align along the uni-stretching direction, bi-axial stretching increases the randomness of CNTs' distribution in the bi-axial stretching plane, while causes more breakdown of conductive networks. Therefore, the simulation results conclude that the bi-axial stretching decreases the electrical conductivity of the composite and the decreasing rate is enhanced by the increasing strain in the second principle stretching direction due to the dominant role of the change of the conductive networks. It is also observed that the

overall electrical conductivity of the CNT-polymer composite is more sensitive to stretching for the composites with lower CNT concentration and smaller CNT aspect ratio. The modeling in the current work is expected to provide an increased understanding on the stretching effects upon the electrical conductivity of CNT-polymer composites.

References

Allaoui, A., Hoa S. V. and Pugh M. D., 2008. The electronic transport properties and microstructure of carbon nanofiber/epoxy composites. Compos. Sci. Technol. **68**, 410–416.

Balberg, I. Binenbaum, N. and Wagner, N., 1984. Excluded Volume and Its Relation to the Onset of Percolation. Physical Review B **30**, 3933–3943.

Bao, S. P., Liang G. D. and Tjong S. C., 2011. Effect of mechanical stretching on electrical conductivity and positive temperature coefficient characteristics of poly(vinylidene fluoride)/carbon nanofiber composites prepared by non-solvent precipitation. Carbon **49**, 1758–1768.

Berson, S., de Bettignies, R., Bailly, S., Guillerez, S. and Jousselme, B., 2007. Elaboration of P3HT/CNT/PCBM composites for organic photovoltaic cells. Adv. Funct. Mater. **17**, 3363–3370.

Celzard, A., McRae, E., Deleuze, C., Dufort, M., Furdin, G. and Marêché, J. F., 1996. Critical concentration in percolating systems containing a high-aspect-ratio filler. Phys. Rev. B **53**, 6209–6214.

Chang, L., Friedrich, K., Ye, L. and Toro, P., 2009. Evaluation and visualization of the percolating networks in multi-wall carbon nanotube/epoxy composites, J. Mater. Sci. **44**, 4003–4012.

Deng, F. and Zheng, Q. S., 2008. An analytical model of effective electrical conductivity of carbon nanotube composites. Appl. Phys. Lett. **92**, 071902.

Entchev, P. B. and Lagoudas, D. C., 2002. Modeling porous shape memory alloys using micromechanical averaging techniques. Mech. Mater. **34**, 1–24.

Feng, C. and Jiang, L., 2013. Micromechanics modeling of the electrical conductivity of carbon nanotube (CNT)–polymer nanocomposites. Compos. Pt. A-Appl. Sci. Manuf. **47**, 143–149.

Feng, C. and Jiang, L., Investigation of uni-axial stretching effects on the electrical conductivity of CNT-polymer nanocomposites. Journal of Physics D: Applied Physics. Accepted.

Gojny, F. H., Wichmann, M. H. G., Fiedler, B. and Schulte, K., 2006. Evaluation and identification of electrical and thermal conduction mechanisms in carbon nanotube/epoxy composites. Polymer **47**, 2036–2045.

Gurp, M., 1995. The use of rotation matrices in the mathematical description of molecular orientations in polymers. Colloid Polym. Sci. **273**, 607–625.

Hu, N., Karube, Y., Arai, M., Watanabe, T., Yan, C., Li, Y., Liu, Y. L. and Fukunaga, H., 2010. Investigation on sensitivity of a polymer/carbon nanotube composite strain sensor. Carbon **48**, 680–687.

Jiang, M. J., Dang Z. M. and Xu, H. P., 2007. Giant dielectric constant and resistance-pressure sensitivity in carbon nanotubes/rubber nanocomposites with low percolation threshold. Appl. Phys. Lett. **90**, 042914.

Kim, Y. J., Shin, T. S., Choi, H. D., Kwon, J. H., Chung, Y. C. and Yoon, H. G., 2005. Electrical conductivity of chemically modified multiwalled carbon nanotube/epoxy composites. Carbon **43**, 23–30.

Kuhn, W. and Grün, F., 1942. Beziehungen zwischen elastischen Konstanten und Dehnungsdoppelbrechung hochelastischer Stoffe. Colloid Polym. Sci. **101**, 248–271.

Li, C. Y., Thostenson, E. T. and Chou, T. W., 2007. Dominant role of tunneling resistance in the electrical conductivity of carbon nanotube-based composites. Appl. Phys. Lett. **91**, 223114.

Lin, C. A., Wang, H. T. and Yang, Wei., 2010. Variable percolation threshold of composites with fiber fillers under compression. J. Appl. Phys. **108**, 013509.

Lu, W. B., Chou, T. W. and Thostenson, E. T., 2010. A three-dimensional model of electrical percolation thresholds in carbon nanotube-based composites. Appl. Phys. Lett. **96**, 223106.

Mayoral, B., Hornsby, P. R., McNally, T., Schiller T. L., Jack, K. and Marti, D. J., 2013. Quasi-solid state uniaxial and biaxial deformation of PET/MWCNT composites: structural evolution, electrical and mechanical properties. Rsc Adv. **3**, 5162–5183.

Mori, T. and Tanaka, K., 1973. Average Stress in Matrix and Average Elastic Energy of Materials with Misfitting Inclusions. Acta Metall. Sin. **21**, 571–574.

Nambiar, S. and Yeow, J. T. W., 2011. Conductive polymer-based sensors for biomedical applications. Biosens. Bioelectron. **26**, 1825–1832.

Odegard, G. M., Gates, T. S., Wise, K. E., Park, C. and Siochi, E. J., 2003. Constitutive modeling of nanotube-reinforced polymer composites. Compos. Sci. Technol. **63**, 1671–1687.

Ounaies, Z., Park, C., Wise, K. E., Siochi, E. J. and Harrison, J. S., 2003. Electrical properties of single wall carbon nanotube reinforced polyimide composites. Compos. Sci.Technol. **63**, 1637–1646.

Park, M. and Kim, H., 2006. Evaporation-based method for fabricating conductive MWCNT/PEO composite film and its application as strain sensor. Proc. 12th US-Japan Conf. Compos. Mater. Michigan, USA, pp. 78–86.

Park, M., Kim, H. and Youngblood, J. P., 2008. Strain-dependent electrical resistance of multi-walled carbon nanotube/polymer composite films. Nanotechnology **19**, 055705.

Pérez, R., Banda, S. and Qunaies, Z., 2008. Determination of the orientation distribution function in aligned single wall nanotube polymer nanocomposites by polarized Raman spectroscopy. J. Appl. Phys. **103**, 074302.

Seidel, G. D. and Lagoudas, D. C., 2009. A Micromechanics Model for the Electrical Conductivity of Nanotube-Polymer Nanocomposites. J. Compos. Mater. **43**, 917–941.

Shang, S. M., Zeng, W. and Tao, X. M., 2011. High stretchable MWNTs/polyurethane conductive nanocomposites. J. Mater. Chem. **21**, 7274–7280.

Shen, J. B., Champagne, M. F., Yang, Z., Yu, Q., Gendron, R. and Guo, S. Y., 2012. The development of a conductive carbon nanotube (CNT) network in CNT/polypropylene composite films during biaxial stretching. Compos. Pt. A- Appl. Sci. Manuf. **43**, 1448–1453.

Shiraishi, M. and Ata, M., 2001. Work function of carbon nanotubes. Carbon **39**, 1913–1917.

Simmons, J. G., 1963. Generalized Formula for the Electric Tunnel Effect between Similar Electrodes Separated by a Thin Insulating Film. J. Appl. Phys. **34**, 1793–1803.

Takeda, T., Shindo, Y., Kuronuma, Y. and Narita, F., 2011. Modeling and characterization of the electrical conductivity of carbon nanotube-based polymer composites. Polymer **52**, 3852–3856.

Tallman, T. and Wang, K. W., 2013. An arbitrary strains carbon nanotube composite piezoresistivity model for finite element integration. Appl. Phys. Lett. **102**, 011909.

Taya, M., 1995. Micromechanics modeling of electronic composites. J. Engineering Mater. Technol.-Trans. ASME **117**, 462–469.

Taya, M., 2005. Electronic composites: modeling, characterization, processing, and MEMS applications. Cambridge University Press, Cambridge.

Taya, M., Kim, W. J. and Ono, K., 1998. Piezoresistivity of a short fiber/elastomer matrix composite. Mech. Mater. **28**, 53–59.

Yan, K. Y., Xue, Q. Z., Zheng, Q. B. and Hao, L. Z., 2007. The interface effect of the effective electrical conductivity of carbon nanotube composites. Nanotechnology **18**, 255705.

Yang, Y., Gupta, M. C., Dudley, K. L. and Lawrence, W., 2005. Novel carbon nanotube-polystyrene foam composites for electromagnetic interference shielding. Nano Lett. **5**, 2131–2134.

Yu, C. J., Masarapu, C., Rong, J. P., Wei, B. Q. and Jiang, H. P., 2009. Stretchable Supercapacitors Based on Buckled Single-Walled Carbon Nanotube Macrofilms. Adv. Mater. **21**, 4793–4397.

Zhang, R., Dowden, A., Deng, H., Baxendale, M. and Peijs, T., 2009. Conductive network formation in the melt of carbon nanotube/thermoplastic polyurethane composite. Compos. Sci. Technol. 69, 1499–1504.

Chapter 5

5 Influence of CNT waviness upon the electrical conductivity of CNT-polymer composites under uni-axial stretching [4]

5.1 Introduction

Since the discovery of carbon nanotubes (CNTs) in 1991 (Iijima, 1991), their extraordinary electrical properties as well as high aspect ratio have made CNTs one of the most preferred conductive fillers to develop multi-functional conductive polymer composites. Compared to traditional conductive fillers, such as carbon black and metals, a very small amount of CNTs added into polymers, which are usually insulators, can significantly improve the electrical properties of the composites while still keep the beneficial features of the polymers, including flexibility, large deformation, easy processability, good chemical and biological compatibilities, etc (Yu *et al*., 2009; Nambiar and Yeow, 2011; Shang *et al*., 2011).

It has been experimentally and theoretically demonstrated that the electrical conductivity of CNT-polymer composites display a percolation-like behavior (Ounaies *et al*., 2003; Kim *et al*., 2005; Gojny *et al*., 2006; Yan *et al*., 2007; Feng and Jiang, 2013), i.e., the electrical conductivity increases abruptly when the CNT concentration is greater than a critical volume fraction, which is usually referred as percolation threshold. Such percolation-like behavior is attributed to two conductivity mechanisms: nanoscale electron hopping and microscale conductive networks (Deng and Zheng, 2008; Chang *et al*., 2009; Zhang *et al*., 2009; Lu *et al*., 2010; Feng and Jiang, 2013). It is well accepted that the contribution of these two mechanisms is highly dependent on CNT volume fraction. For example, when the CNT concentration is below the percolation threshold, CNTs in the polymer are electrically independent and only the nanoscale electron hopping contributes to the electrical conductivity. However, when the CNT concentration

---

[4] A version of this chapter is to be submitted for publication.

is above the percolation threshold, certain percent of CNTs will form microscale conductive networks, which will significantly contribute to the electrical conductivity in addition to the nanoscale electron hopping. The dependency of the overall electrical conductivity of the CNT-polymer composites upon the CNT concentration and the conductivity mechanisms has been extensively explored (Kim *et al.*, 2005; Gojny *et al.*, 2006; Li *et al.*, 2007; Chang *et al.*, 2009; Seidel and Lagoudas, 2009; Takeda *et al.*, 2011; Feng ang Jiang, 2013).

It should be mentioned that most of the existing theoretical studies of the electrical properties were focused on the composites with the assumption of straight conductive fillers. However, it is experimentally observed that CNTs dispersed in polymers are usually not straight but rather have a degree of waviness due to their large aspect ratio and low bending stiffness (Li *et al.*, 2008). The waviness of the CNTs was suggested to have considerable effects on the overall electrical properties of the composites (Yi *et al.*, 2004; Li *et al.*, 2008; Takeda *et al.*, 2011; Yu *et al.*, 2013). Therefore, the consideration of CNT waviness effects is necessary and essential for predicting the electrical conductivity of the CNT-polymer composites in realistic cases. In the literature, people have made some efforts in incorporating the CNT waviness effects to investigate the electrical properties of the composites. For example, assuming wavy CNTs with a simple sinusoidal shape, Yi *et al.* (2004), Berhan and Sastry (2007) and Fisher *et al.* (2003) investigated the effect of the waviness on the percolation onset of CNT-polymer composites. It was observed that the CNT waviness increases the percolation threshold of the composites. Approximating wavy CNTs as elongated polygons, Li *et al.'s* (2008) computational simulation on the CNT waviness effects showed that the waviness increases the percolation threshold and decreases the electrical conductivity and elastic stiffness of the composites. By introducing a length ratio into a simplified micromechanics model, Deng and Zheng (2008) and Takeda *et al.* (2011) investigated the effect of the non-straightness of the CNTs. It was found that the non-straightness of CNTs could significantly decrease the electrical conductivity of the composites. Nevertheless, these existing studies focused on the percolation behavior of the composites while did not combine any stretching effect, which is an important

consideration for the application of the composites as stretchable electronics. Therefore, the objective of the current work will focus on investigating the CNT waviness effect on the electrical conductivity of CNT-polymer composites under a uni-axial stretching through applying our previously developed micromechanics model.

5.2 Modeling and formulation

In this section, CNT waviness effects will be incorporated into the developed mixed micromechanics model (Feng and Jiang, 2013) by using straight CNTs with equivalent conductive performance. The iterations of the mixed micromechanics model with both nanoscale and microscale conductivity mechanisms, the stretching effects and the equivalence of wavy CNTs to straight CNTs are listed in the follows.

5.2.1 Nanoscale composite cylinder model

The nanoscale conductive mechanism of the CNT-polymer composites attributes to the electron hopping, which was captured by the introduction of an interphase outside the CNT to form an effective composite cylinder. Such a effective composite cylinder model has been widely adopted by researchers (Hashin, 1990; Yan et al., 2007; Seidel et al., 2009) as shown in Figure 5.1 in which the straight CNT is identified with length $L_{\mathrm{CNT}}^{\mathrm{str}}$ and diameter $D_{\mathrm{CNT}}^{\mathrm{str}}$ and the surrounding interphase is described with thickness t. By applying the law-of-mixture rule (Taya, 2005; Yan et al., 2007), the composite cylinder can be homogenized into an equivalent solid filler with effective longitudinal and transverse electrical conductivity determined as,
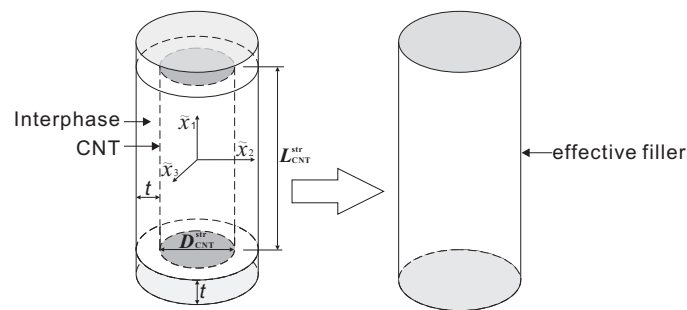

Figure 5.1 Sketch of a composite cylinder.

$$\tilde{\sigma}^{L} = \frac{\left(L_{CNT}^{str} + 2t\right)\sigma_{Int}\left[\sigma_{CNT}^{str}D_{CNT}^{str\ 2} + 4\sigma_{Int}\left(D_{CNT}^{str}t + t^{2}\right)\right]}{2\sigma_{CNT}^{str}D_{CNT}^{str\ 2}t + 8\sigma_{Int}\left(D_{CNT}^{str}t + t^{2}\right)t + \sigma_{Int}L_{CNT}^{str}\left(D_{CNT}^{str} + 2t\right)^{2}}$$

$$\tilde{\sigma}^{T} = \frac{\sigma_{Int}}{L_{CNT}^{str} + 2t}\left[L_{CNT}^{str}\frac{D_{CNT}^{str\ 2}\sigma_{CNT}^{str} + 2\left(\sigma_{CNT}^{str} + \sigma_{Int}\right)\left(t^{2} + D_{CNT}^{str}t\right)}{D_{CNT}^{str\ 2}\sigma_{Int} + 2\left(\sigma_{CNT}^{str} + \sigma_{Int}\right)\left(t^{2} + D_{CNT}^{str}t\right)} + 2t\right] \tag{5.1}$$

where the supscripts "L" and "T" denote the longitudinal and transverse directions, respectively; and σ_{CNT}^{str} and σ_{Int} are the electrical conductivity of the straight CNT and the interphase, respectively. Correspondingly, we can have the electrical conductivity tensor of the effective filler as $\tilde{\sigma} = \text{diag}\left(\tilde{\sigma}^{L},\ \tilde{\sigma}^{T},\ \tilde{\sigma}^{T}\right)$. With the equivalence of the CNTs to the effective solid fillers, the volume fraction of the fillers in the composite was expressed in terms of the original volume fraction of straight CNTs f_{CNT}^{str} (Yan *et al*., 2007; Seidel *et al*., 2009), i.e.,

$$f_{eff} = \frac{\left(D_{CNT}^{str} + 2t\right)^{2}\left(L_{CNT}^{str} + 2t\right)}{D_{CNT}^{str\ 2}L_{CNT}^{str}}L_{CNT}^{str}. \tag{5.2}$$

It is obvious from Eq. (5.1) that the interphase properties, i.e., the interphase electrical conductivity and the interphase thickness, are essential to determine the electrical properties of the composite cylinder. These interphase properties are naturally believed to correlate to the electrical conductivity mechanisms and vary with the CNT volume fraction. Some researchers have indicated that the average separation distance d_a between the adjacent CNTs forming conductive networks follows a power law relation (Allaoui *et al*., 2008; Deng *et al*., 2008; Takeda *et al*., 2011), i.e.,

$$d_{a} = \left(\frac{f_{c}^{str}}{f_{CNT}^{str}}\right)^{1/3} d_{c}, \tag{5.3}$$

where f_{c}^{str} is the percolation threshold of the composites with straight CNTs. Obviously, this separate distance decreases with the increase of the CNT volume fraction f_{c}^{str} after the percolation threshold. Existing experiments (Li *et al*., 2007; Takeda *et al*., 2011) and

simulations suggested that the critical separation distance for the formation of conductive networks is d_c = 1.8 nm. From the previous works (Simmons, 1963; Takeda *et al.*, 2011; Feng and Jiang, 2013), the thickness and the conductivity of the interphase for conductive networks were expressed as:

$$t = \frac{1}{2}\left(\frac{f_c^{str}}{f_{CNT}^{str}}\right)^{1/3} d_c \tag{5.4}$$

and

$$\sigma_{Int} = \frac{d_a}{aR_{Int}(d_a)}, \tag{5.5}$$

where $R_{Int}(d_a) = \dfrac{d_a \hbar^2}{ae^2(2m\lambda)^{1/2}}\exp\left(\dfrac{4\pi d_a}{\hbar}(2m\lambda)^{1/2}\right)$ is the tunneling-type contact resistance between two CNTs. λ = 5.0 eV is the potential barrier height for CNTs dispersed in most polymers. m = 9.10938291×10^{-31} kg and e = −1.602176565×10^{-19} C are mass and electric charge of an electron, respectively. a is the contact area of CNTs and $\hbar$ = 6.626068×10^{-34} m^2·kg·s^{-1} is the Planck constant. In contrast, for the CNTs without forming conductive network, the separation distance is larger than the critical distance 1.8 nm. However, this distance was assumed as a constant for the CNTs without forming conductive networks. Therefore, the thickness and the electrical conductivity of the interphase for CNTs without forming conductive networks can be approximated as (Feng and Jiang, 2013):

$$t = \frac{1}{2}d_c \text{ and } \sigma_{Int} = \frac{d_c}{aR_{Int}(d_c)}. \tag{5.6}$$

5.2.2 Micromechanics model

Based on the composite cylinder model, the CNT-polymer composite becomes a composite filled with effective solid fillers with effective electrical conductivity $\tilde{\sigma}$ and

effective volume fraction *f*. For the two-phase composite with uniformly and randomly distributed fillers, the overall electrical conductivity can be predicted by applying a micromechanics model with selecting a representative volume element (RVE) containing enough fillers (shown in Figure 5.2). In the RVE, ($\tilde{x}_1, \tilde{x}_2, \tilde{x}_3$) and ($X_1$, X_2, X_3) are the local and global coordinate systems to describe the position of the fibers, respectively. The orientation of any individual filler is identified by two Euler angles, φ and θ. By averaging the contribution of the fillers from all possible orientations in the RVE, the overall electrical conductivity of the two-phase composite can be determined as (Taya, 1995; Entchev and Lagoudas, 2002; Odegard *et al.*, 2003; Taya, 2005; Seidel *et al.*, 2009):
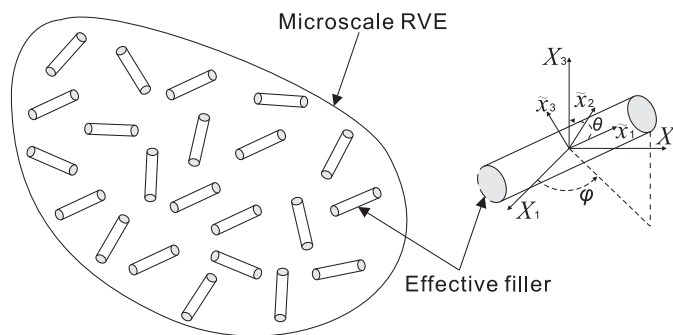

Figure 5.2 Sketch of a microscale RVE containing conductive fillers.

$$\sigma_{\text{eff}} = \sigma_{\text{m}} + \frac{\int_0^{2\pi} \int_0^{\pi} \rho(\varphi,\theta) f_{\text{eff}} (\sigma - \sigma_{\text{m}}) A \sin\theta \mathrm{d}\theta \mathrm{d}\varphi}{\int_0^{2\pi} \int_0^{\pi} \rho(\varphi,\theta) \sin\theta \mathrm{d}\theta \mathrm{d}\varphi}$$

(5.7)

where $\rho(\varphi,\theta)$ is the orientation distribution function (ODF), which denotes the probability of the distribution of the fillers with a given orientation; *A* is the electric field concentration tensor; σ_{m} is the electrical conductivity tensor of the polymer and σ is the electrical conductivity tensor of the effective filler in the global coordinate system, which can be transformed from the electrical conductivity tensor in the local coordinate system as:

$$\sigma = Q^T \tilde{\sigma} Q$$

(5.8)

where Q is the transformation matrix given as (Entchev *et al.*, 2002):

$$Q = \begin{bmatrix} \sin\theta\cos\varphi & -\cos\theta\cos\varphi & \sin\varphi \\ \sin\theta\sin\varphi & -\cos\theta\sin\varphi & -\cos\varphi \\ \cos\theta & \sin\theta & 0 \end{bmatrix} \qquad (5.9)$$

Applying Mori-Tanaka method (Mori and Tanaka, 1973), the concentration tensor A in Eq. (5.7) can be defined as (Taya, 2005; Seidel and Lagoudas, 2009; Feng and Jiang, 2013):

$$A = QA^{\mathrm{dil}}Q^{\mathrm{T}}\left\{(1-f_{\mathrm{eff}})\delta + f_{\mathrm{eff}}\frac{\int_0^{2\pi}\int_0^{\pi} f_{\mathrm{eff}}\left\{QA^{\mathrm{dil}}Q^{\mathrm{T}}\right\}\rho(\varphi,\theta)\sin\theta\,\mathrm{d}\theta\,\mathrm{d}\varphi}{\int_0^{2\pi}\int_0^{\pi}\rho(\varphi,\theta)\sin\theta\,\mathrm{d}\theta\,\mathrm{d}\varphi}\right\}^{-1}, \qquad (5.10)$$

where A^{dil} is defined as:

$$A^{\mathrm{dil}} = \left\{\delta + S\left(\sigma_{\mathrm{m}}\right)^{-1}\left(\tilde{\sigma} - \sigma_{\mathrm{m}}\right)\right\}^{-1} \qquad (5.11)$$

with δ being the Kronecker delta tensor. S is the Eshelby tensor of the effective filler, which is given by:

$$S = \begin{bmatrix} S_{11} & 0 & 0 \\ 0 & S_{22} & 0 \\ 0 & 0 & S_{33} \end{bmatrix}, \qquad (5.12)$$

where

$$S_{22} = S_{33} = \frac{A_{\mathrm{re}}}{2\left(A_{\mathrm{re}}^2 - 1\right)^{3/2}}\left[A_{\mathrm{re}}\left(A_{\mathrm{re}}^2 - 1\right)^{1/2} - \cosh^{-1}A_{\mathrm{re}}\right] \qquad (5.13)$$

with A_{re} being the aspect ratio of the effective filler, i.e., $A_{\mathrm{re}} = \left(L_{\mathrm{CNT}}^{\mathrm{str}} + 2t\right)\left(D_{\mathrm{CNT}}^{\mathrm{str}} + 2t\right)$, and $S_{11} = 1 - 2S_{22}$.

According to Deng and Zheng's (2008) argument, conductive networks start to contribute to the electrical conductivity after the percolation and the percentage of CNTs forming conductive networks can be estimated as:

$$\xi = \frac{\left(f_{\mathrm{CNT}}^{\mathrm{str}}\right)^{1/3} - \left(f_{\mathrm{c}}^{\mathrm{str}}\right)^{1/3}}{1 - \left(f_{\mathrm{c}}^{\mathrm{str}}\right)^{1/3}} \quad \left(f_{\mathrm{CNT}}^{\mathrm{str}} \geq f_{\mathrm{c}}^{\mathrm{str}}\right) \tag{5.14}$$

Considering the percolation process of CNT-polymer composites, i.e., both electron hopping and conductive networks contribute to the electrical conductivity of the composite after the percolation, while only electron hopping is responsible for the electrical conductivity before the percolation, the overall electrical conductivity can be determined by a mixed micromechanics model as (Feng andg Jiang, 2013):

$$\sigma_{\mathrm{eff}} = \begin{cases} \sigma_{\mathrm{m}} + \dfrac{\int_{0}^{2\pi}\int_{0}^{\pi}\left\{f_{\mathrm{eff}}\left(\sigma_{\mathrm{EH}} - \sigma_{\mathrm{m}}\right)A_{\mathrm{EH}}\right\}\rho(\varphi,\theta)\sin\theta\,\mathrm{d}\theta\,\mathrm{d}\varphi}{\int_{0}^{2\pi}\int_{0}^{\pi}\rho(\varphi,\theta)\sin\theta\,\mathrm{d}\theta\,\mathrm{d}\varphi}, \quad f_{\mathrm{CNT}}^{\mathrm{str}} < f_{\mathrm{c}}^{\mathrm{str}} \\[2em] \sigma_{\mathrm{m}} + \left(1-\xi\right)\dfrac{\int_{0}^{2\pi}\int_{0}^{\pi}\left\{f_{\mathrm{eff}}\left(\sigma_{\mathrm{EH}} - \sigma_{\mathrm{m}}\right)A_{\mathrm{EH}}\right\}\rho(\varphi,\theta)\sin\theta\,\mathrm{d}\theta\,\mathrm{d}\varphi}{\int_{0}^{2\pi}\int_{0}^{\pi}\rho(\varphi,\theta)\sin\theta\,\mathrm{d}\theta\,\mathrm{d}\varphi} \\[2em] + \xi\dfrac{\int_{0}^{2\pi}\int_{0}^{\pi}\left\{f_{\mathrm{eff}}\left(\sigma_{\mathrm{CN}} - \sigma_{\mathrm{m}}\right)A_{\mathrm{CN}}\right\}\rho(\varphi,\theta)\sin\theta\,\mathrm{d}\theta\,\mathrm{d}\varphi}{\int_{0}^{2\pi}\int_{0}^{\pi}\rho(\varphi,\theta)\sin\theta\,\mathrm{d}\theta\,\mathrm{d}\varphi}, \quad f_{\mathrm{CNT}}^{\mathrm{str}} \geq f_{\mathrm{c}}^{\mathrm{str}} \end{cases}, \tag{5.15}$$

where the superscripts "EH" and "CN" denote the terms contributed by the electron hopping and the conductive networks, respectively. When conductive networks are formed, several CNTs will be electrically connected to each other while not in physical contact due to van der Waals forces between CNTs. Thus, the effective aspect ratio of the formed networks can be taken as infinite due to the large aspect ratio of CNTs. However, quantities associated with the electron hopping correspond to the real effective filler aspect ratio as defined. Correspondingly, A_{EH} and A_{CN} in Eq. (5.15) can be determined from Eq. (5.10) by using different aspect ratios for CNTs.

5.2.3 Equivalence of wavy carbon nanotubes

As mentioned, CNTs dispersed in polymers usually exist in a wavy state. The basic idea of considering waviness effects is to convert wavy CNTs into equivalent straight fillers as adopted by previous studies (Deng and Zheng, 2008; Takeda *et al*., 2011). In the current work, we assume the wavy CNT with length of L_{CNT}^{wavy} and diameter of D_{CNT}^{wavy} has a sinusoidal shape as illustrated in Figure 5.3. The sinusoidal shape is described by two parameters, amplitude a_w and wavelength λ_w, as:
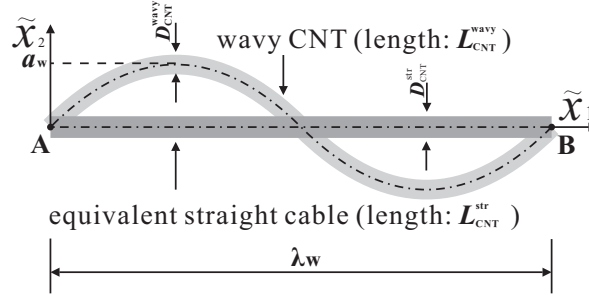

Figure 5.3 Sketch of a wavy CNT and its equivalent straight counterpart.

$$\tilde{x}_2 = a_w \sin(\frac{2\pi\tilde{x}_1}{\lambda_w}) . \tag{5.16}$$

To characterize the waviness of the CNT, a parameter referred as waviness ratio is defined as following (Fisher *et al*., 2003)

$$\chi = \frac{a_w}{\lambda_w} . \tag{5.17}$$

Combining Eqs. (5.16)–(5.17), the length of the wavy CNT can be correlated to the amplitude and the wavelength as:

$$L_{CNT}^{wavy} = \int_0^{\lambda_w} \sqrt{1+\left(\frac{d\tilde{x}_2}{d\tilde{x}_1}\right)^2} \, d\tilde{x}_1 = \lambda_w \int_0^1 \sqrt{1+\left(2\pi\chi\cos\left(2\pi u\right)\right)^2} \, du , \tag{5.18}$$

where $u = \tilde{x}_1 / \lambda_\mathrm{w}$.

The equivalence of the wavy CNTs into straight fillers is carried out according to the rules from the perspective of electrical conduction mechanisms. When the wavy CNT as shown in Figure 5.3 is subjected to a two-ends potential difference, $\Delta V = V_2 - V_1$, the CNT can be taken as an electrical CNT cable and the electrical flux J through the CNT can be approximated (Deng and Zheng, 2008)

$$J = \sigma_\mathrm{CNT}^\mathrm{wavy} \frac{\Delta V}{L_\mathrm{CNT}^\mathrm{wavy}} . \qquad (5.19)$$

On the other side, the wavy CNT can be regarded as an equivalent straight CNT with the capability of conducting the same electrical flux J between the two ends of the CNT with a minimum distance $L_\mathrm{CNT}^\mathrm{str}$ which equals to the wavelength λ_w of the wavy CNT. Such an analysis can produce the effective electrical conductivity of the equivalent straight CNT as:

$$\sigma_\mathrm{CNT}^\mathrm{str} = \alpha \sigma_\mathrm{CNT}^\mathrm{wavy} , \qquad (5.20)$$

where $\alpha = L_\mathrm{CNT}^\mathrm{str} / L_\mathrm{CNT}^\mathrm{wavy}$ is the length ratio. It is suggested that the length ratio α usually ranges from 0.5 to 1.0 (Fisher *et al*., 2003; Takeda *et al*., 2011) for composites with wavy CNTs. Particularly, α equals unity for straight CNTs. To fully convert the wavy CNT into an equivalent straight CNT, in addition to conducting the same electrical flux, the equivalent straight CNT should have the capability of transporting the same amount of electrical charges from end A to end B as that for the wavy CNT within a certain time interval, from which we can have the following relationship

$$R_\mathrm{CNT}^\mathrm{str} = R_\mathrm{CNT}^\mathrm{wavy} , \qquad (5.21)$$

where $R_\mathrm{CNT}^\mathrm{wavy}$ and $R_\mathrm{CNT}^\mathrm{str}$ are the resistance of the wavy CNT and the equivalent straight CNT respectively. Combining Eqs. (5.20) and (5.21), it can be easily obtained that the

diameter of the equivalent CNT is the same as that of the wavy CNT, i.e., $D_{\mathrm{CNT}}^{\mathrm{str}} = D_{\mathrm{CNT}}^{\mathrm{wavy}}$, which was also adopted by Deng and Zheng (2008). Due to the reduced equivalent length, the volume fraction of the equivalent straight CNT in the composites reduces to $f_{\mathrm{CNT}}^{\mathrm{str}} = \alpha f_{\mathrm{CNT}}^{\mathrm{wavy}}$, where $f_{\mathrm{CNT}}^{\mathrm{wavy}}$ is the volume fraction of the wavy CNTs.

Replacing wavy CNTs with equivalent straight CNTs, the electrical conductivity and the geometric property of the CNTs in the formulation of the previous sections take the values for the equivalent straight CNTs.

5.2.4 Uni-axial stretching induced changes

When composites with fillers are under stretching, it has been accepted that stretching induces three changes in the composites, including volume expansion of the composites, re-orientation of the fillers and change in conductive networks (Taya *et al*., 1998; Taya, 2005; Feng and Jiang, 2014). In the following, the stretching effects on the electrical conductivity of the composites will be investigated by characterizing these three changes and incorporating them into the micromechanics model.

Figure 5.4 shows a cell containing an effective filler under a uni-axial stretching with stretching strain ε in the X_3 direction. After stretching, the dimensions of the beam become (Feng and Jiang, 2014):
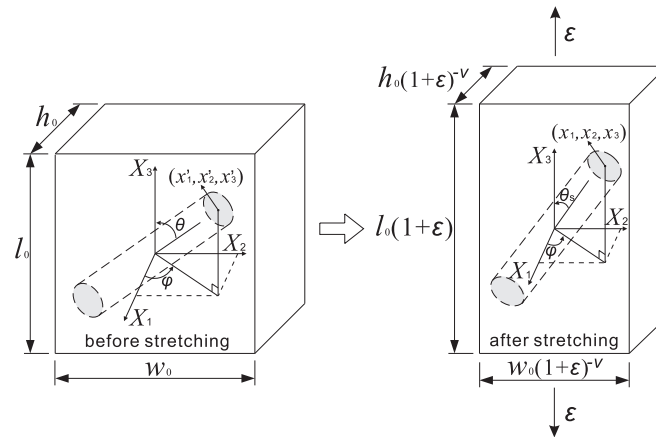

Figure 5.4. Orientation description of a conductive filler in a cell.

$$l = l_0 (1+\varepsilon), \ w = w_0 (1+\varepsilon)^{-\nu} \text{ and } h = h_0 (1+\varepsilon)^{-\nu}, \tag{5.22}$$

where l_0, w_0 and h_0 are the initial length, width and height of the cell, respectively, and v is the Poisson's ratio of the composites. Due to the expansion of the composites, the volume fraction of the effective filler after stretching reduces to (Feng and Jiang, 2014)

$$f_{update} = f_{eff} / (1+\varepsilon)^{1-2\nu}. \tag{5.23}$$

In addition to volume expansion, the fillers in the cell are also re-oriented, resulting in the change of the polar angel, i.e.,

$$\theta_s = \arctan \left[(1+\varepsilon_3)^{-1-\nu} \cdot \tan \theta \right]. \tag{5.24}$$

The change of the other Euler angle, φ, can be neglected here under the uni-axial stretching condition (Kuhn and Grün, 1942; Feng $et\ al.$, 2014). Such a re-orientation will disrupt the random distribution of fillers before the stretching, i.e., the ODF in Eq. (5.7) changes from unity to the following expression (Feng and Jiang, 2014)

$$\rho(\varphi, \theta_s) = \frac{(1+\varepsilon)^{\frac{1+\nu}{2}}}{\left[(1+\varepsilon)^{-(1+\nu)} \cos^2 \theta_s + (1+\varepsilon)^{1+\nu} \sin^2 \theta_s \right]^{3/2}}. \tag{5.25}$$

Our previous work demonstrated that after the uni-axial stretching, fillers in the polymer tend to re-align along the stretching direction and the increase of the Poisson's ratio can enhance such a re-alignment (Feng and Jiang, 2014a and 2014b).

In addition, stretching also induces change in conductive networks, including the increase of the percolation threshold and the separation distance between CNTs (Taya $et\ al.$, 1998; Lin $et\ al.$, 2010; Tallman and Wang, 2013). Based on the excluded volume method (Balberg $et\ al.$, 1984; Celzard $et\ al.$, 1996; Tallman $et\ al.$, 2013), the percolation threshold can be determined as:

$$f_c^{str} = 1 - \exp\left(-\frac{\langle V_{ex} \rangle V_{CNT}^{str}}{\langle V_e \rangle}\right)$$ (5.26)

where $\langle V_{ex} \rangle$ is the total average excluded volume of equivalent straight CNT, V_{CNT}^{str} is the volume of the equivalent straight CNT and $\langle V_e \rangle = \frac{4\pi}{3}\left(D_{CNT}^{str}\right)^3 + 2\pi\left(D_{CNT}^{str}\right)^2 L_{CNT}^{str} + 2D_{CNT}^{str}\left(L_{CNT}^{str}\right)^2 \langle \sin\gamma \rangle$ is the average excluded volume of the equivalent straight CNT with D_{str} and L_{str} being the diameter and the length, respectively, and γ being the angle between two CNTs. Fitting from Monte Carlo simulation, Tallman and Wang (2013) proposed an approximate expression for $\langle \sin\gamma \rangle_\mu$, i.e.,

$$\langle \sin\gamma \rangle_\mu = 0.018\theta_\mu^5 + 0.021\theta_\mu^4 - 0.234\theta_\mu^3 - 0.015\theta_\mu^2 + 0.909\theta_\mu$$ (5.27)

where $\theta_\mu = \arcsin[(1+\varepsilon)^{-1-\nu}]$ is a critical polar angle representing the randomness of the filler distribution. From Eqs. (5.26) and (5.27), it can be seen that the stretching will change the percolation threshold due to the variation of the θ_μ with the stretching strain. To further consider the stretching effect on the percolation threshold, Tallman and his co-worker (2013) proposed a linear expression for the total average excluded volume, i.e.,

$$\langle V_{ex} \rangle = 2.8 - 5.6\frac{\langle \sin\gamma \rangle_\mu}{\pi} .$$ (5.28)

Combining Eqs. (5.26)-(5.28), the percolation threshold is cast as:

$$f_c^{str} = 1 - \exp\left[-\frac{\left(2.1\pi - 4.2\langle \sin\gamma \rangle_\mu\right)p}{4\pi + 6\pi p + 6p^2\langle \sin\gamma \rangle_\mu}\right]$$ (5.29)

where $p = L_{CNT}^{str}/D_{CNT}^{str}$ is the aspect ratio of the equivalent straight CNT. Figure 5.5 presents the variation of the percolation threshold with the waviness ratio. From this figure, it can be seen that the percolation threshold increases with the waviness ratio,

which was also observed by researchers applying Monte Carlo simulations (Yi *et al*., 2004; Li *et al*., 2008; Yu *et al*., 2013). In addition, the uni-axial stretching increases the percolation threshold as well.
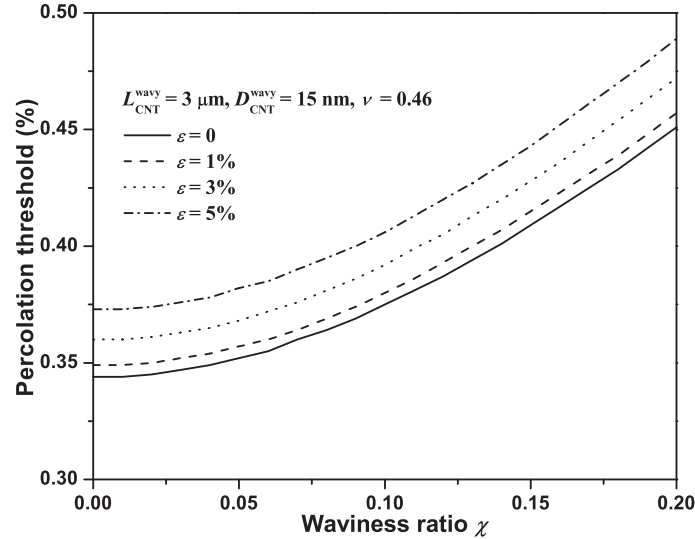

Figure 5.5 Variation of percolation threshold with waviness ratio.

5.3   Results and discussion

To study the CNT waviness effects on the electrical conductivity of the composites under a uni-axial stretching, we take the MWCNT/PEO (Polyethylene Oxide) composite in references (Park and Kim, 2006; Park *et al*., 2008) as the example material. The length and the diameter of the CNTs are taken as $L_{\mathrm{CNT}}^{\mathrm{wavy}} = 3$ μm and $D_{\mathrm{CNT}}^{\mathrm{str}} = 15$ nm, respectively. We adopt $\sigma_{\mathrm{m}} = 1 \times 10^{-13}$ S/m and $\sigma_{\mathrm{CNT}}^{\mathrm{wavy}} = 100$ S/m as the electrical conductivity of the polymer and the wavy CNTs, respectively (Deng *et al*., 2008; Feng and Jiang, 2013). The Poisson's ratio of the composite is set as $v = 0.46$. In Park and co-workers' experiments (Park *et al*., 2006; Park *et al*., 2008), it was observed that MWCNTs with functionalized surface were well dispersed in the PEO matrix before the stretching.

To investigate the waviness effects on the percentage of percolated CNTs, Figure 5.6 plots the variations of the normalized percentage of the percolated CNTs, $\xi_{\mathrm{N}} = \xi_{\mathrm{w}}/\xi_{0}$, for a composite under a uni-axial stretching for different CNT volume fractions and different

stretching strains, where ξ_0 and ξ_w denote the percentages of percolated CNTs for the composite with straight and wavy CNTs, respectively. From the figure, it is found that the percentage decreases with the increase of the waviness ratio. It is also suggested in the figures that the percentage is more sensitive to the waviness for the composites with lower CNT volume fraction and larger stretching strain.
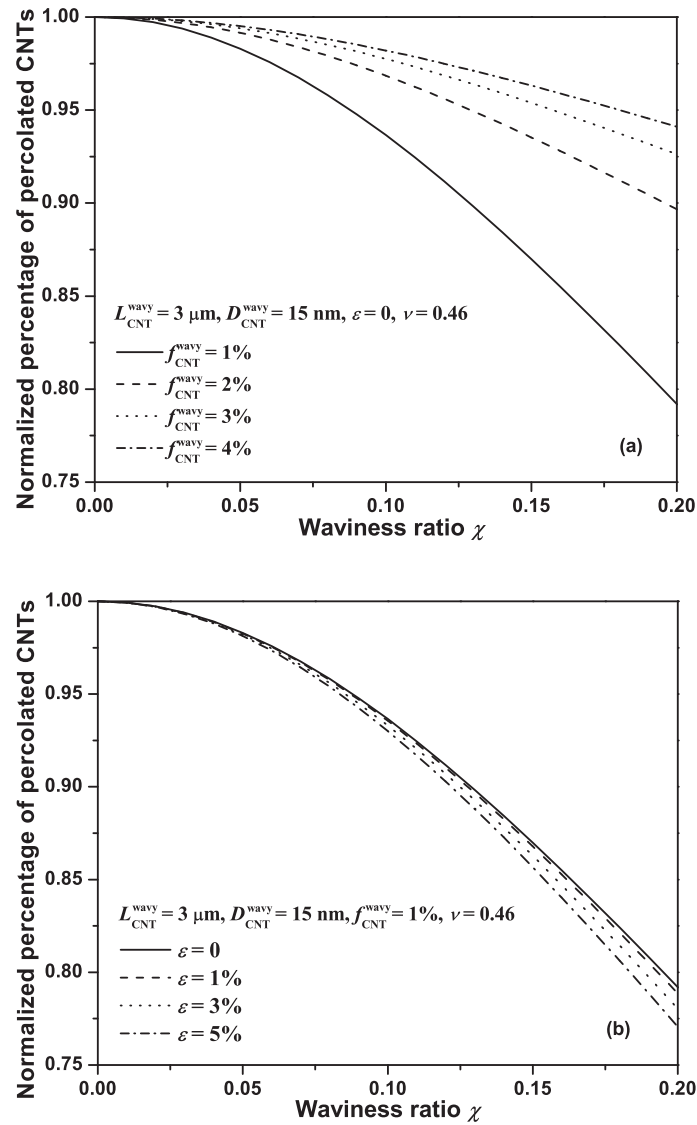

Figure 5.6 Variation of normalized percentage of percolated CNTs with waviness ratio (a) Different CNT volume fractions; (b) Different stretching strains.

Figure 5.7 plots the variation of the electrical conductivity of the composite with CNT volume fraction for different waviness ratios. From this figure, it can be seen that the

electrical conductivity of the composite increases with the increase of CNT volume fraction as expected. However, it is noticed that for the same CNT volume fraction, the electrical conductivity of the composite with wavy CNTs is much lower than that of the composite with straight CNTs. Such decrease in the electrical conductivity can be attributed to the waviness induced decrease in the effective electrical conductivity of the equivalent straight CNT and the change of the conductive networks.
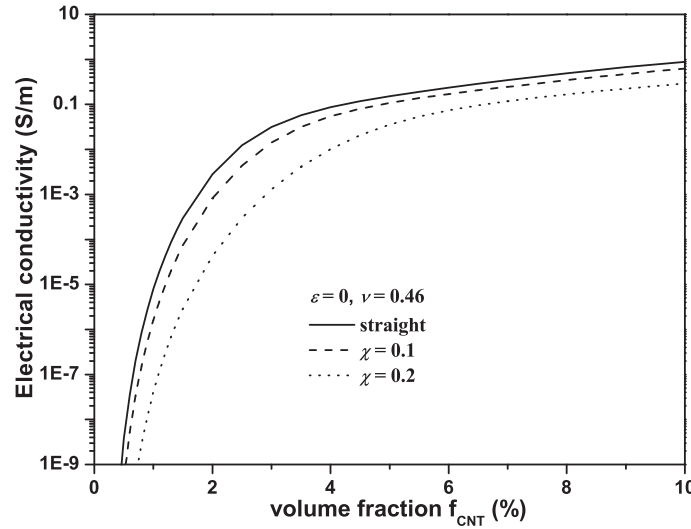

Figure 5.7. Variation of electrical conductivity with CNT volume fraction for different waviness ratios.

Figure 5.8 demonstrates the variation of the normalized electrical conductivity, $\sigma_N = \sigma_{eff}^{wavy} / \sigma_{eff}^{str}$, with the waviness ratio for different CNT volume fractions, where σ_{eff}^{wavy} and σ_{eff}^{str} denote the electrical conductivity of the composite with wavy CNTs and straight CNTs, respectively. It can be observed that the electrical conductivity decreases with the increase of the waviness ratio. In addition, it is found that with the same waviness ratio, the electrical conductivity decreases with the waviness ratio more significantly for the composite with lower CNT concentration. The sensitivity of the electrical conductivity to the CNT concentration can be explained by the variations of the normalized percentage with the waviness ratio as demonstrated in Figure 5.6a. For lower CNT volume fraction, since only a few conductive networks exist in the composite, any small change, such as

CNT waviness, will have relatively more significant effect on the conductive networks, which results in more decrease in the overall electrical conductivity of the composites.
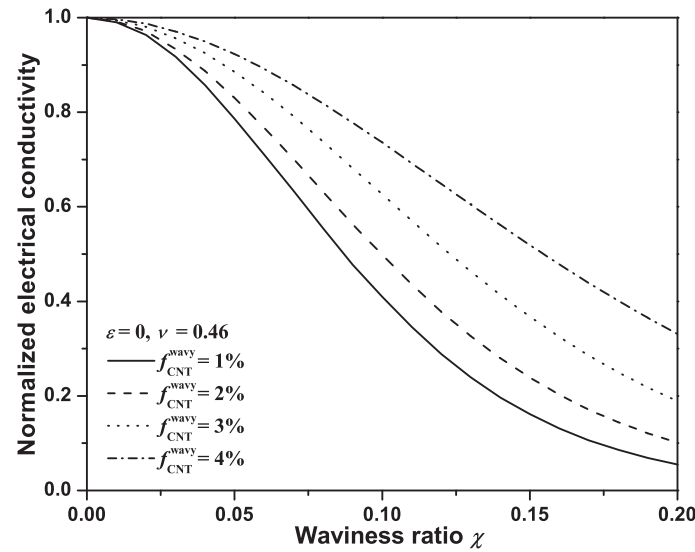

Figure 5.8 Variation of normalized electrical conductivity with waviness ratio for different volume fractions.

Figure 5.9 shows the dependency of the normalized electrical conductivity on the waviness ratio for different stretching strains. From this figure, it can be seen that similar to Figure 5.7 and Figure 5.8, the electrical conductivity decreases with the CNT waviness ratio for both the longitudinal and the transverse directions. Furthermore, it is demonstrated that for a fixed CNT volume fraction the electrical conductivity is more sensitive to the waviness ratio for the composite under a larger uni-axial stretching strain. The stretching effects on the sensitivity of the electrical conductivity to the waviness can be interpreted by the demonstration in Figure 5.6b, in which the normalized percentage of percolated CNTs decreases more significantly with the waviness ratio for the composites with larger stretching strain.
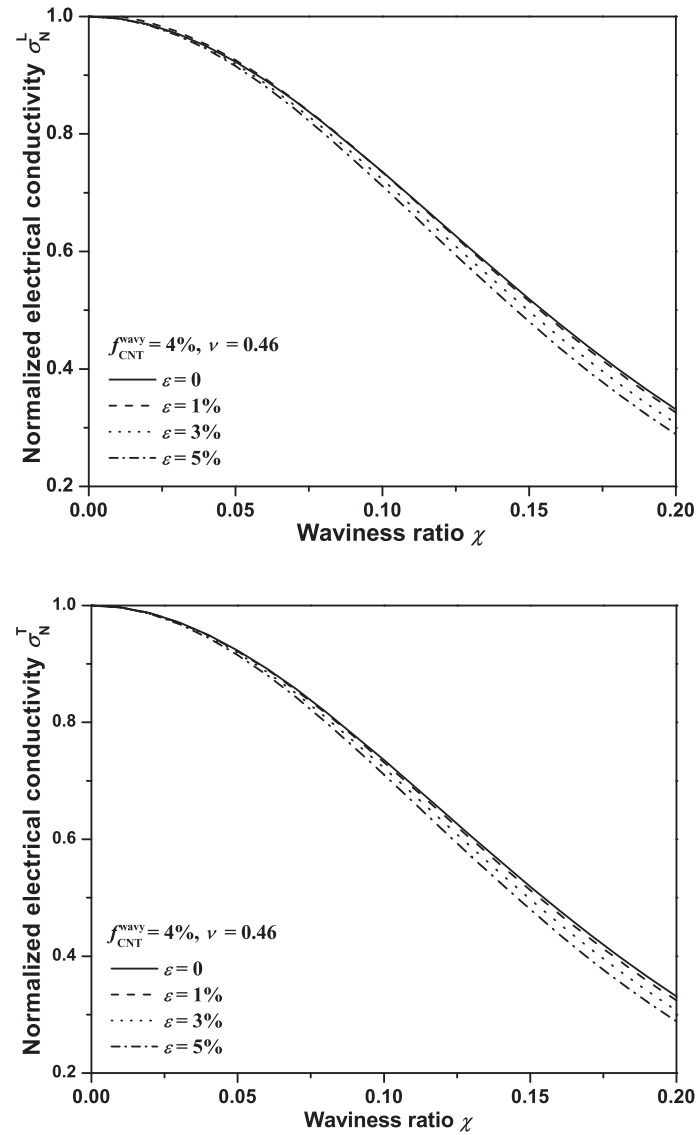
Figure 5.9 Variation of normalized electrical conductivity with waviness ratio for different stretching strains (a) Longitudinal direction; (b) Transverse direction.

5.4 Conclusions

Based on electrical conduction mechanisms, wavy CNTs characterized by a sinusoidal function are converted into equivalent straight CNTs with effective electrical conductivity and dimensions. Then CNT waviness effects on the electrical behaviors of CNT-polymer composites under a uni-axial stretching are studied through applying our previously developed mixed micromechanics model. The modeling results show that the electrical conductivity of the composites with wavy CNTs is much lower than that with

straight CNTs. It is observed that the increasing waviness of CNTs enhances the stretching induced decrease of the electrical conductivity of the composites. It is also found that the electrical conductivity decreases with the increase of CNT waviness more significantly for the composites with lower CNT volume fraction and under larger stretching strain. The investigation in the current work is expected to provide qualitative predictions on the CNT waviness effects on the electrical conductivity of CNT-polymer composites.

References

Allaoui, A., Hoa, S. V. and Pugh, M. D., 2008. The electronic transport properties and microstructure of carbon nanofiber/epoxy composites. Compos. Sci. Technol. **68**, 410–416.

Balberg, I., Binenbaum, N. and Wagner, N., 1984. Percolation thresholds in the three-dimensional sticks system. Phys. Rev. Lett. **52**, 1465–1468.

Berhan, L. and Sastry, A. M., 2007. Modeling percolation in high-aspect-ratio fiber systems. II. The effect of waviness on the percolation onset. Phys. Rev. E **75**, 041121.

Celzard, A., McRae, E., Deleuze, C., Dufort, M., Furdin, G. and Marêché, J., 1996. Critical concentration in percolating systems containing a high-aspect-ratio filler. Phys. Rev. B **53**, 6209–6214.

Chang, L., Friedrich, K., Ye, L. and Toro, P., 2009. Evaluation and visualization of the percolating networks in multi-wall carbon nanotube/epoxy composites. J. Mater. Sci. **44**, 4003–4012.

Dastgerdi, J. N., Marquis, G. and Salimi, M., 2013. The effect of nanotubes waviness on mechanical properties of CNT/SMP composites. Compos. Sci. Technol. **86**, 164–169.

Deng, F. and Zheng, Q. S., 2008. An analytical model of effective electrical conductivity of carbon nanotube composites. Appl. Phys. Lett. **92**, 071902.

Entchev, P. B. and Lagoudas, D. C. 2002. Modeling porous shape memory alloys using micromechanical averaging techniques. Mech. Mater. **34**, 1–24.

Feng, C. and Jiang, L., 2013. Micromechanics modeling of the electrical conductivity of carbon nanotube (CNT)–polymer nanocomposites. Compos. Pt. A-Appl. Sci. Manuf. **47**, 143–149.

Feng, C. and Jiang, L., 2014. Investigation of uni-axial stretching effects on the electrical conductivity of CNT-polymer nanocomposites. Submitted.

Feng, C. and Jiang, L., 2014. Micromechanics modeling of bi-axial stretching effects on the electrical conductivity of CNT-polymer composites. Submitted.

Fisher, F. T., Bradshaw, R. D. and Brinson, L. C., 2003. Fiber waviness in nanotube-reinforced polymer composites-1: Modulus predictions using effective nanotube properties. Compos. Sci. Technol. **63**, 1689–1703.

Gojny, F. H., Wichmann, M. H. G., Fiedler, B., Kinloch, I. A., Bauhofer, W., Windle, A. H. and Schulte, K. 2006. Evaluation and identification of electrical and thermal conduction mechanisms in carbon nanotube/epoxy composites. Polymer **47**, 2036–2045.

Hashin, Z., 1990. Thermoelastic Properties and Conductivity of Carbon Carbon-Fiber Composites. Mech. Mater. **8**, 293–308.

Iijima, S., 1991. Helical microtubules of graphitic carbon. Nature **354**, 56–58.

Kim, Y. J., Shin, T. S., Choi, H. D., Kwon, J. H., Chung, Y. C. and Yoon, H. G., 2005. Electrical conductivity of chemically modified multiwalled carbon nanotube/epoxy composites. Carbon **43**, 23–30.

Kuhn, W. and Grün, F., 1942. Beziehungen zwischen elastischen Konstanten und Dehnungsdoppelbrechung hochelastischer Stoffe. Kolloid-Zeitschrift **101**, 248–271.

Li, C., Thostenson, E. T. and Chou, T. W., 2008. Effect of nanotube waviness on the electrical conductivity of carbon nanotube-based composites. Compos. Sci. Technol. **68**, 1445–1452.

Li, C. Y., Thostenson, E. T. and Chou, T. W., 2007. Dominant role of tunneling resistance in the electrical conductivity of carbon nanotube-based composites. Appl. Phys. Lett. **91**, 223114.

Li, J., Ma, P. C., Chow, W. S., To, C. K., Tang, B. Z. and Kim, J. K., 2007. Correlations between Percolation Threshold, Dispersion State, and Aspect Ratio of Carbon Nanotubes. Adv. Funct. Mater. **17**, 3207–3215.

Lin, C., Wang, H. and Yang, W., 2010. Variable percolation threshold of composites with fiber fillers under compression. J. Appl. Phys. **108**, 013509.

Lu, W. B., Chou, T. W. and Thostenson, E. T., 2010. A three-dimensional model of electrical percolation thresholds in carbon nanotube-based composites. Appl. Phys. Lett. **96**, 223106.

Mori, T. and Tanaka, K., 1973. Average Stress in Matrix and Average Elastic Energy of Materials with Misfitting Inclusions. Acta Metall. Mater. **21**, 571–574.

Nambiar, S. and Yeow, J. T. W., 2011. Conductive polymer-based sensors for biomedical applications. Biosens. Bioelectron. **26**, 1825–1832.

Odegard, G. M., Gates, T. S., Wise, K. E., Park, C. and Siochi, E. J., 2003. Constitutive modeling of nanotube-reinforced polymer composites. Compos. Sci. Technol. **63**, 1671–1687.

Ounaies, Z., Park, C., Wise, K. E., Siochi, E. J. and Harrison, J. S., 2003. Electrical properties of single wall carbon nanotube reinforced polyimide composites. Compos. Sci. Technol. **63**, 1637–1646.

Park, M. and Kim, H., 2006. Evaporation-based method for fabricating conductive MWCNT/PEO composite film and its application as strain sensor. Proc. 12th US-Japan Conf. Compos. Mater. Michigan: University of Michigan, pp 78–86.

Park, M., Kim, H. and Youngblood, J. P., 2008. Strain-dependent electrical resistance of multi-walled carbon nanotube/polymer composite films. Nanotechnology **19**, 055705.

Seidel, G. D. and Lagoudas, D. C., 2009. A Micromechanics Model for the Electrical Conductivity of Nanotube-Polymer Nanocomposites. J. Compos. Mater. **43**, 917–941.

Shang, S. M., Zeng, W. and Tao, X. M., 2011. High stretchable MWNTs/polyurethane conductive nanocomposites. J. Mater. Chem. **21**, 7274–7280.

Shi, D. L., Feng, X. Q., Huang, Y. G. Y., Hwang, K. C. and Gao, H. J., 2004. The effect of nanotube waviness and agglomeration on the elastic property of carbon nanotube-reinforced composites. J. Eng. Mater.-Tran. ASME **126**, 250–257.

Takeda, T., Shindo, Y., Kuronuma, Y. and Narita, F., 2011. Modeling and characterization of the electrical conductivity of carbon nanotube-based polymer composites. Polymer **52**, 3852–3856.

Tallman, T. and Wang, K. W., 2013. An arbitrary strains carbon nanotube composite piezoresistivity model for finite element integration. Appl. Phys. Lett. **102**, 011909.

Taya, M., 1995. Micromechanics modeling of electronic composites. J. Eng. Mater.-Tran. ASME **117**, 462–469.

Taya, M., 2005. Electronic composites: modeling, characterization, processing, and MEMS applications, Cambridge University Press, Cambirdge.

Taya, M., Kim, W. and Ono, K., 1998. Piezoresistivity of a short fiber/elastomer matrix composite. Mech. Mater. **28**, 53–59.

Yan, K. Y., Xue, Q. Z., Zheng, Q. B. and Hao, L. Z., 2007. The interface effect of the effective electrical conductivity of carbon nanotube composites. Nanotechnology **18,** 255705.

Yanase, K., Moriyama, S. and Ju, J. W., 2013. Effects of CNT waviness on the effective elastic responses of CNT-reinforced polymer composites. Acta Mech. **224**, 1351–1364.

Yi, Y., Berhan, L. and Sastry, A., 2004. Statistical geometry of random fibrous networks, revisited: Waviness, dimensionality, and percolation. J. Appl. Phys. **96**, 1318–1327.

Yi, Y. B., Berhan, L. and Sastry, A. M., 2004. Statistical geometry of random fibrous networks, revisited: Waviness, dimensionality, and percolation. J. Appl. Phys. **96**, 1318–1327.

Yu, C. J., Masarapu, C., Rong, J. P., Wei, B. Q. and Jiang, H. Q., 2009. Stretchable Supercapacitors Based on Buckled Single-Walled Carbon Nanotube Macrofilms. Adv. Mater. **21**, 4793–4797.

Yu, Y., Song, S., Bu, Z., Gu, X., Song, G. and Sun, L., 2013. Influence of filler waviness and aspect ratio on the percolation threshold of carbon nanomaterials reinforced polymer nanocomposites. J. Mater. Sci. **48**, 5727–5732.

Yu, Y., Song, S. Q., Bu, Z. X., Gu, X. F., Song, G. B. and Sun, L., 2013. Influence of filler waviness and aspect ratio on the percolation threshold of carbon nanomaterials reinforced polymer nanocomposites. J. Mater. Sci. **48**, 5727–5732.

Zhang, R., Dowden, A., Deng, H., Baxendale, M. and Peijs, T., 2009. Conductive network formation in the melt of carbon nanotube/thermoplastic polyurethane composite. Compos. Sci. Technol. **69**, 1499–1504.

Chapter 6

6   Conclusions and future work

6.1   Conclusions

Compared to conductive polymer composites with traditional fillers, such as carbon black and metals, the electrical conductivity of CNT-polymer composites demonstrates a significant percolation-like behavior. For engineering application, understanding of the mechanisms that underpin the macroscopic behaviors is essential for accurate prediction of the electrical behaviors of the composites. In addition, for the application of the composites as stretchable electronics, stretching and CNT waviness have significant effects upon the electrical conductivity of the composites. In this work, a mixed micromechanics model with the incorporation of the electrical conductivity mechanisms, stretching effects and CNT waviness is developed to settle the as-mentioned challenges. The contributions of the thesis include:

1. Based on percolation process of the CNT-polymer composites, the work is the first to develop a mixed form of micromechanics model, in which nanoscale electron hopping and microscale conductive networks are incorporated. Also instead of fixing the properties of the interphase surrounding the CNTs, such as the thickness and the electrical conductivity, the properties of the interphase vary with the CNT volume fraction.

2. We incorporate the stretching induced three changes, including volume expansion of composites, re-orientation of fillers and change in conductive networks, into our developed micromechanics model to investigate the uni-axial and bi-axial stretching effects on the electrical conductivity of the composites. Theoretical modeling work on the stretching effects upon the electrical properties of CNT-polymer composites through incorporating the stretching induced changes has not been reported thus far in the literature.

3. We investigate the CNT waviness effects on the electrical conductivity of the composites under uni-axial stretching through converting wavy CNTs into equivalent straight fillers and the developed micromechanics model. There exists some work on considering CNT waviness effects on mechanical properties of the composites. However, limited theoretical work has been found on study the CNT waviness effects on the electrical conductivity of the composites.

Based on the developed model and the work done, we have some conclusions, which are listed in the following:

1. The developed micromechanics model is validated by comparing modeling results with experimental data. It was found that both electron hopping and conductive networks contribute to the electrical conductivity of the nanocomposite, while conductive networks become dominant after the percolation. Meanwhile, it was observed that both CNT length and diameter significantly affect the percolation concentration of nanocomposites, while having moderate effects on the overall electrical conductivity of the nanocomposites after the percolation.

2. Modeling results show that uni-axial stretching decreases the electrical conductivity in both the longitudinal and transverse directions. The electrical conductivity is more sensitive to the stretching for composites with lower CNT concentration than those with higher CNT concentration. It is also indicate that the stretching induced change in conductive networks plays a dominant role for the variation of the electrical conductivity along the stretching direction.

3. The investigation found that the bi-axial stretching decreases the electrical conductivity of the composites and the decreasing rate is enhanced by the increasing strain in the second principle stretching direction due to the dominant role of stretching induced change in conductive networks. Compared to uni-axial stretching, in which CNTs tend to be re-aligned along the one stretching direction, bi-axial stretching enables CNTs to be re-oriented in the two stretching directions and increases the randomness of CNTs' distribution in the stretching plane. It is also

observed that the composites under bi-axial stretching are more sensitive to stretching with lower CNT concentration and smaller aspect ratio.

4.   It concludes that the electrical conductivity of the composites increases with the CNT concentration while the electrical conductivity of the composites with wavy CNTs is much lower than that with straight CNTs. The waviness decreases the electrical conductivity of the composites in both the stretching and the transverse direction. It is also found that the electrical conductivity is more sensitive to CNT waviness for the composites with lower CNT volume fraction and larger stretching strain.

6.2   Future work

The current work developed a mix micromechanics model to investigate the overall electrical conductivity of the CNT-polymer composites. The work is expected to provide theoretical predictions and better understanding on the electrical conductivity of the composites and useful guidelines for the design and optimization of conductive polymer nanocomposites. However, there exist limitations for the developed model in the current work, which include:

1.   The micromechanics model developed in this current work is based on small strain formulation, which used linear kinematics for the traditional micromechanics theory. Therefore, the model is not applicable for composites under finite deformation.

2.   It is assumed that the intrinsic electrical conductivity of CNTs does not change under small stretching strain. However, it is argued that the intrinsic electrical conductivity of CNTs would vary due to CNT's elongation when the composite is under stretching. The assumption may cause inaccuracy on the model's prediction, particularly for the composites under large stretching.

Based on the existing limitations, the following work is proposed:

1. For certain CNT–polymer composites with the capability of undergoing large deformation, such as CNT–rubber composites, linear kinematics assumed for traditional micromechanics theory may be violated. Therefore, a more comprehensive micromechanics model based on finite deformation formulation needs to be developed.

2. When the composites are under large deformation, the elongation of the CNTs will become obvious resulting in the variation of the intrinsic electrical conductivity of the CNTs, which may become a significant contribution to the variation of the electrical conductivity of the composites. Such intrinsic variation of the electrical conductivity of the CNTs needs to be taken into account.

3. As materials are required to sustain more and more extreme loading conditions, in addition to the mechanisms of the translation of CNTs' extraordinary performance into the bulk composites, the effects of bonding/debonding between CNTs and the polymer molecules at the nanoscale and the failure of the composites under large deformation, are still unanswered due to the multiscale nature of the problems. Therefore, a multiscale model with the combination of continuum modeling and atomistic simulation needs to be developed in the future.

Curriculum Vitae

Name:	Chuang Feng
Post-secondary Education and Degrees:	Chang'an University Xi'an, Shaanxi, China 2000–2004 B.A. University of Science and Technology Beijing Beijing, China 2004–2007 M.A. The University of Western Ontario London, Ontario, Canada 2010–2014 Ph.D.
Honors and Awards:	Western Graduate Thesis Research Fund Award 2012 Chinese Government Award for Outstanding Graduates 2014 Academic Achievement Scholarship 2014
Related Work Experience	Lecturer Northwest University of Agriculture and Forestry 2007–2010 Research Assistant/Teaching Assistant The University of Western Ontario 2010–2014

Publications:

Feng, C. and Jiang, L. Y., 2014. CNT waviness effects on the electrical conductivity of CNT-polymer nanocomposites. To be submitted.

Feng, C. and Jiang, L. Y., 2014. Bi-axial stretching effects on the electrical conductivity of CNT-polymer composites. Under review.

Feng, C. and Jiang, L. Y., 2014. Investigation of uni-axial stretching effects on the electrical conductivity of CNT–polymer composites. Journal of Physics D: Applied Physics. Accepted.

Feng, C. and Jiang, L. Y., 2014. Multi-scale modeling of CNT waviness effects on the electrical conductivity of CNT-polymer composites. Proceedings of CSME International Congress 2014, June 1–4, 2014, Toronto, Canada

Feng, C. and Jiang, L. Y., 2013. Micromechanics modeling of the electrical conductivity of carbon nanotube (CNT)-polymer nanocomposites. Composites Part: Applied Science and Manufacturing **47**, 143–149.

Feng, C. and Jiang, L. Y., 2012. Dynamic performance of a dielectric elastomer-based nanobeam resonator. Proceedings of the 3rd International Conference on Nanotechnology: Fundamentals and Applications August 7–9, Montreal, Canada

Feng, C. and Jiang, L. Y. and Lau, W. M., 2011. Dynamic characteristics of a dielectric elastomer based microbeam resonator with small vibration amplitude. J. Micromechanics and Microengineering **21**, 095002, selected for IOPSelect

Feng, C. and Jiang, L. Y., 2011. Molecular dynamics simulation of squeeze-film damping effect on nano resonators in the free molecular regime. Physica E-Low Dimensional Systems and Nanostructures **43**, 1605–1609.